Neoproterozoic glaciated basins: a critical review of the Snowball Earth hypothesis by comparison with Phanerozoic glaciations

J.L. ETIENNE*, P.A. ALLEN*†, R. RIEU* *and* E. LE GUERROUÉ*

**Geological Institute, Department of Earth Sciences, ETH-Zentrum, Haldenbachstrasse 44, CH-8092 Zürich, Switzerland (e-mail: james.etienne@erdw.ethz.ch)*

†Department of Earth Science and Engineering, Imperial College London, South Kensington Campus, London SW7 2AS, UK

ABSTRACT

The Neoproterozoic is widely considered to have experienced some of the most severe climatic perturbations recorded in Earth history, with extensive glaciations often referred to as 'Snowball Earth' events. The Snowball Earth and competing hypotheses seek to explain a wide range of geological data on Neoproterozoic pre-, syn- and post-glacial successions including glacial sedimentology, chemostratigraphy, palaeoceanography, geochronology, palaeomagnetism and palaeogeography, geodynamics, tectonics, palaeontology and palaeobiogeochemistry. However, our understanding of the Phanerozoic and particularly the Cenozoic and contemporary glacial geological record is often relatively neglected when evaluating the evidence for apparent severe and prolonged periods of globally synchronous glaciation. This paper presents a review of the available geological data for Neoproterozoic glacial successions in the light of what we know about the Cenozoic and recent glacial record. Most Neoproterozoic successions are shown to exhibit spatial and temporal variability, with sediment stacking patterns and facies associations indicative of dynamic ice masses. These characteristics are typical of sedimentary sequences deposited along glaciated continental margins throughout Earth history, without the need for global synchroneity or necessarily severe climatic excursions. Although recurrent very widespread glaciation is envisaged in the Neoproterozoic, the presence of analogous glacigenic and interglacial successions in the Neoproterozoic and Cenozoic suggest the operation of a similar set of processes across a similar range of depositional environments. Consequently, an unambiguous sedimentary record of hydrological shutdown during a prolonged global glaciation appears to be lacking. This indicates either a preservational bias in Neoproterozoic successions of the advance and recessional stages of glacial epochs, or the occurrence of dynamic, non-global glaciations during the Neoproterozoic.

Keywords Glacial sedimentation, Neoproterozoic, Snowball Earth

INTRODUCTION

Earth's Neoproterozoic glacial record retains a number of features that are apparently contradictory to our understanding of Phanerozoic glaciation, the foremost of which are palaeomagnetic data suggesting marine-terminating glaciers at low latitudes and the association of ^{13}C-depleted carbonates above and locally below glacigenic successions across the globe (Sumner *et al.*, 1987; Schmidt *et al.*, 1991; Schmidt & Williams, 1995; Williams, 1996; Hoffman *et al.*, 1998a, b; Sohl *et al.*, 1999; Schrag *et al.*, 2002; Halverson *et al.*, 2004; Fig. 1a). Several radical models have been proposed in order to explain these observations, including long-lived, but rapidly terminated (10^4 to 10^6 years) global glaciations (the Snowball Earth hypothesis; Kirschvink, 1992; Hoffman *et al.*, 1998a, b; Hoffman & Schrag, 2002), high obliquity (Williams & Schmidt, 2004) and progressive rifting

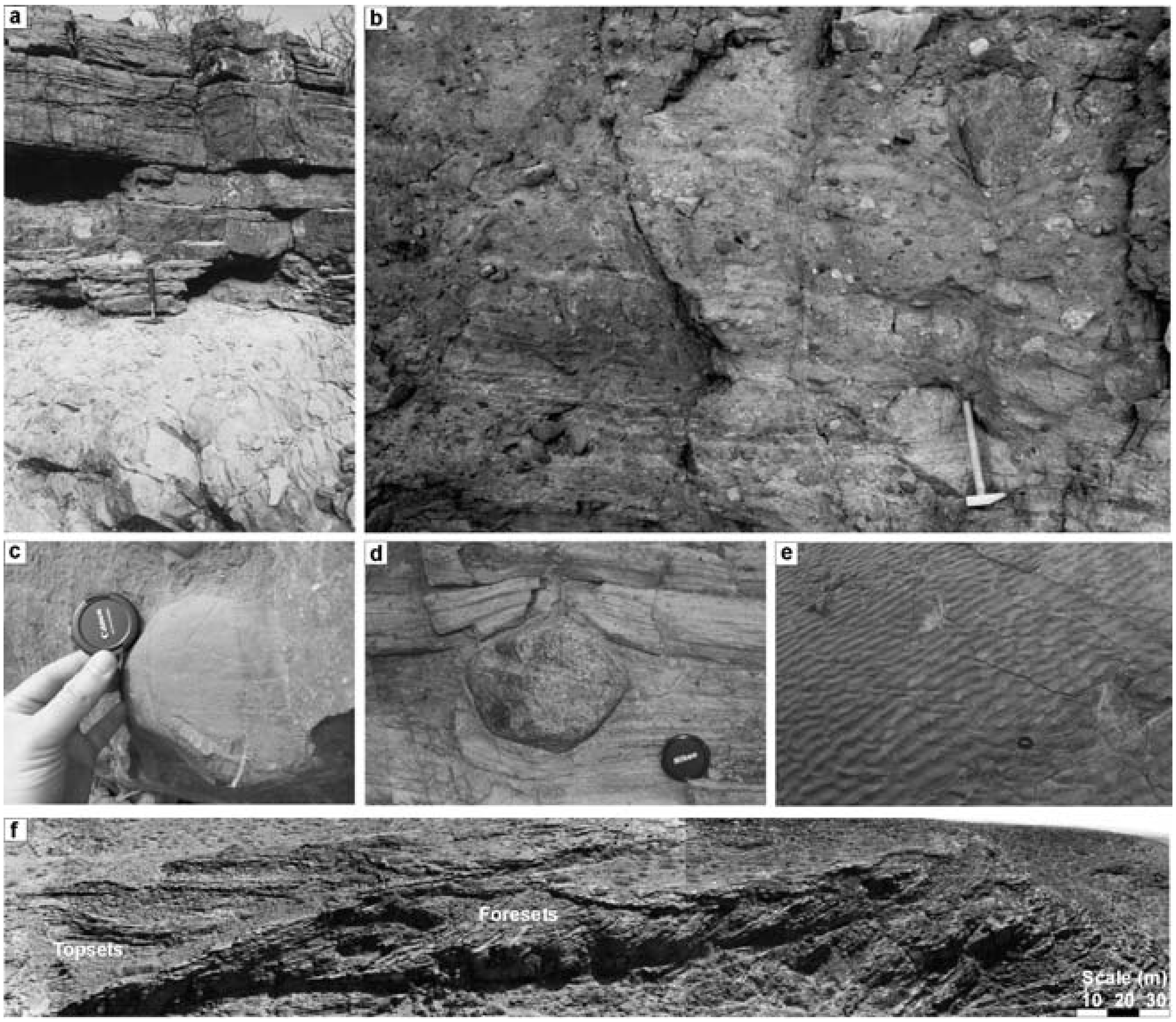

Fig. 1 Glacially influenced Neoproterozoic deposits: (a) contact between Fiq diamictite and Hadash cap carbonate, Wadi Bhani Kharus, Jabal Akhdar, (b) stratified diamictite lithofacies, Ayn Fm. (formerly Mirbat Sandstone Fm., Lower member), Dhofar; (c) glacially striated clast in diamictite lithofacies of the Blaini Fm. near Dadahu; (d) dropstone in glaciolacustrine deposits, Ayn Fm., Dhofar; (e) wave-rippled deposits in the Fiq member, Ghadir Manqil Fm., Wadi Sahtan, Jabal Akhdar; (f) Gilbert-type delta foresets in the Ayn Fm. in Wadi Anushar, Dhofar. All photographs Sultanate of Oman, except (c) from the Lesser Himalaya, northern India. Hammer for scale in (a) and (b) is 30 cm in length. Lens cap in (c) 3.5 cm diameter; lens cap in (d) to (f), 5 cm diameter.

during the breakup of the Rodinia super-continent (the 'Zipper Rift' model of Eyles and Januszczak, 2004). The high obliquity theory suffers since a mechanism is required in order to reduce obliquity (Williams & Schmidt, 2004), while the Snowball Earth and Zipper Rift models argue the genetic nature of diamictite facies and their palaeoclimatic significance. Although the Zipper Rift model concedes that low solar luminosity may have allowed glaciation at lower latitudes than during the Phanerozoic, the quality of the palaeomagnetic evidence for tropical or equatorial glaciation at low altitudes is seriously questioned (Eyles & Januszczak, 2004). Despite their differences,

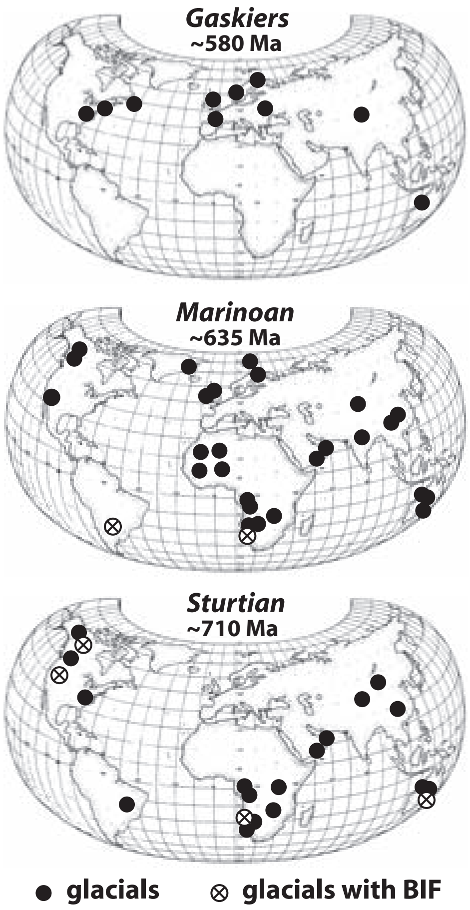

Fig. 2 Modern distribution of Sturtian (~710 Ma), Marinoan (~635 Ma) and Gaskiers (~580 Ma) successions. Crossed circles indicate association of Banded Iron Formations (BIF). Reproduced from Hoffman (2005) with permission of the Geological Society of South Africa. Copyright (2005) Geological Society of South Africa.

all models agree on at least local glacial activity, typically subdivided temporally into the Sturtian (c. 700 Ma), Marinoan (c. 635 Ma) and Gaskiers (c. 580 Ma) glacial epochs (Fig. 2). Historical reviews on the development of Proterozoic climate models can be found in Hoffman and Schrag (2002) and Eyles and Januszczak (2004).

While advances have been made in geochronology and the chemostratigraphic characteristics of overlying 'cap' carbonate sequences, relatively little detailed work has been undertaken on the glacial facies assemblages in the context of the Snowball Earth hypothesis (with notable exceptions; Arnaud & Eyles, 2002a, b; Allen *et al.*, 2004; Benn & Prave, 2006; Dobrzinski & Bahlburg, *In Press*; Rieu *et al.*, unpublished data). Since the style of Neoproterozoic glaciation remains to be rigorously tested, our understanding of the Phanerozoic, and particularly the Cenozoic glacial record, provides the most appropriate means by which to test depositional models and identify the dominant glaciological processes which operated in Neoproterozoic basins. This paper aims to review sedimentological data that provide insights into the palaeoglaciological characteristics of Neoproterozoic glaciation. A better understanding of climatic variability during this time is highly desirable, since it is here that the first fossil evidence for metazoan life is recorded (Narbonne *et al.*, 1994), and because the Snowball hypothesis challenges our knowledge of the boundary conditions of Earth climate.

The Palaeomagnetic Record

While most Neoproterozoic glacial successions lack reliable palaeomagnetic constraints, the predominance of low-latitude palaeopoles is notable (Evans, 2000) and is atypical by Phanerozoic standards (Evans, 2003). However, relatively few samples have conclusively passed syn-sedimentary fold tests to demonstrate natural remanent magnetization (NRM), and the age of magnetization acquisition is often open to debate. The issue is complicated further given the evidence for a significant (~30%) octopole component in the Proterozoic Earth's magnetic field (e.g. Kent & Smethurst, 1998), although Williams and Schmidt (2004) argue that this would be insufficient to make moderate latitude palaeopoles appear equatorial. Our understanding of Neoproterozoic palaeogeography is limited for the time between 720 Ma and 600 Ma (Meert & Powell, 2001), and competing high and low latitude models for Laurentia have different implications for testing both the high obliquity and Snowball Earth hypotheses (Meert & Torsvik, 2004). Nevertheless, good palaeogeographical models have been developed for 750 Ma and 580 Ma which may provide palaeolatitudinal constraints on some of the older Neoproterozoic basins, and those that are equivalent to the Gaskiers epoch (Fig. 3). Given the problems in resolving the timing of 'Sturtian' glacial events (Halverson, 2005; see below), a detailed palaeogeographical model for the end of the Marinoan glacial epoch at

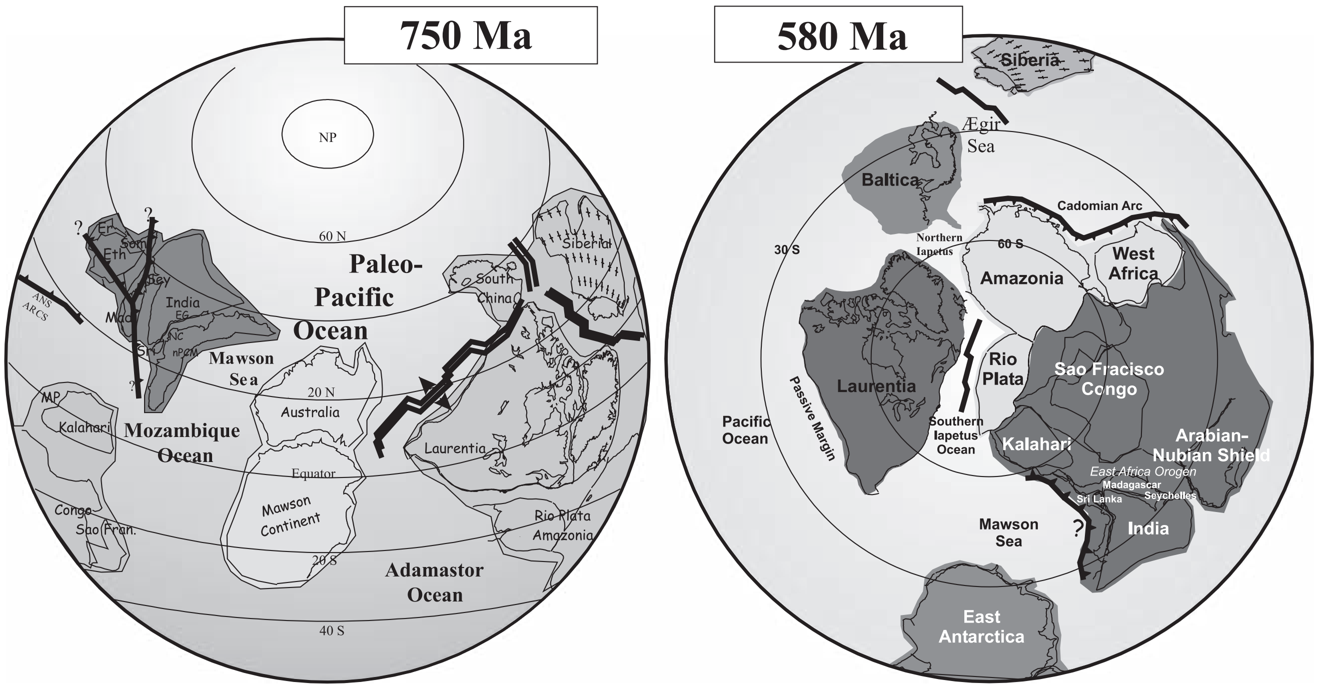

Fig. 3 Palaeogeographical reconstructions for 750 Ma and 580 Ma. Reproduced from Meert and Torsvik (2003) with permission of Elsevier.

635 Ma (Hoffmann *et al.*, 2004; Condon *et al.*, 2005) is now much required. A comprehensive review of Neoproterozoic palaeomagnetic data may be found in Evans (2000).

Chemostratigraphy

One of the key characteristics of Proterozoic glacial successions is their association with ^{13}C depleted carbonates. However, the exact nature of the relationship between ^{13}C depleted carbonates and glaciation is a subject of debate. Negative $\delta^{13}C$ anomalies occur in preglacial stratigraphic units in Svalbard (Halverson *et al.*, 2004), Namibia (Halverson *et al.*, 2002), Ethiopia (Miller *et al.*, 2003), Canada (Hoffman & Schrag, 2002), Australia (McKirdy *et al.*, 2001) and Scotland (Brasier & Shields, 2000). Schrag *et al.* (2002) proposed that the low-latitude position of continental landmasses during this time would have led to more efficient burial of organic carbon and the development of large methane reservoirs, the slow release of which resulted in the negative $\delta^{13}C$ anomalies observed in preglacial carbonates. Negative $\delta^{13}C$ values observed in postglacial cap carbonates are interpreted differently, and are considered to be a result of low organic productivity during long-lived global glaciations (4–30 Myrs; Hoffman *et al.*, 1998a) and an alkalinity flux driven by post-glacial weathering. High partial pressures of atmospheric carbon dioxide are required to initiate deglaciation in the Snowball Earth model, and are achieved by volcanic outgassing of CO_2 (Hoffman *et al.*, 1998a; Hoffman & Schrag, 2002). Some geochemical evidence in support of elevated pCO_2 has been presented for the Marinoan glacial succession in Namibia, although the associated $\delta^{13}C$ excursion may not be fully accounted for (Kasemann *et al.*, 2005).

Overall the linkage between Proterozoic glaciation and carbon cycling remains unclear. For example, geochemical analysis of the Ediacaran Shuram Formation of the Nafun Group in Oman shows a pronounced negative (–12‰ $\delta^{13}C_{carb}$) excursion which persists through hundreds of metres of stratigraphy (Le Guerroué *et al.*, 2006; Fig. 4). This perturbation is greater in magnitude and more long lived than those recorded in cap carbonate sequences, and highlights that large negative $\delta^{13}C$ shifts do not require glaciation as a precursory condition. However, it is interesting

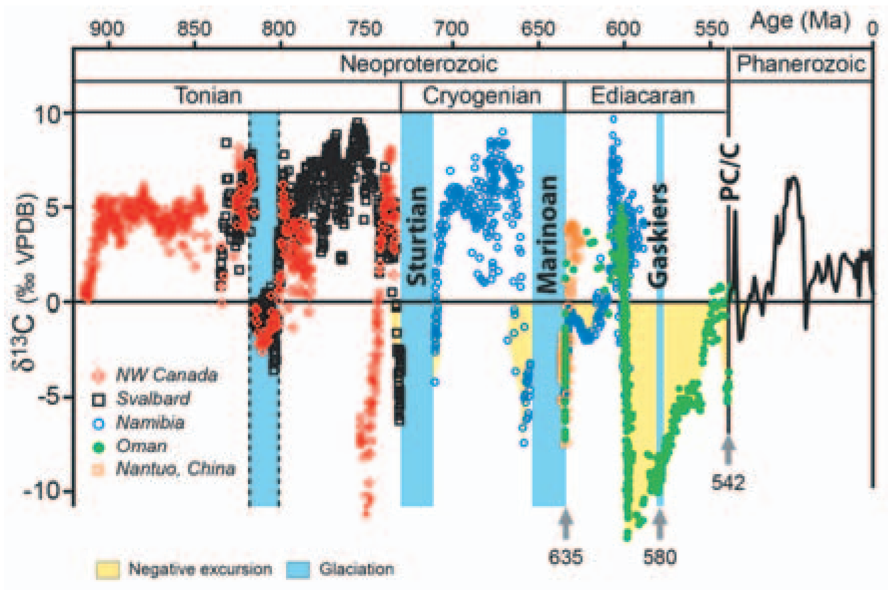

Fig. 4 Composite $\delta^{13}C$ record for the Neoproterozoic modified from the Halverson (2005) version 2 reconstruction (calibrated by lithostratigraphic correlation of the Petrovbreen Member diamictites (Svalbard) with the Chuos Fm. in Namibia), with revised calibration for the Ediacaran period following Le Guerroué *et al.* (2006a, b). A simplified Phanerozoic $\delta^{13}C$ record is included for comparison after Jacobsen and Kaufman (1997) and Hayes *et al.* (1999). Note the difference in scale between Proterozoic and Phanerozoic composite records. Data for Canada, Svalbard and Namibia after Halverson (2005), Oman (Le Guerroué *et al.*, 2006a, b; Burns & Matter, 1993; McCarron, 2000; Cozzi and Al-Siyabi, 2004), and China (Condon *et al.*, 2005).

to note that as with cap carbonates, the Shuram excursion is associated with a transgressive cycle. Although local extreme (−41‰ $\delta^{13}C_{carb}$) isotope values occur within some cap carbonate sequences, such values have been interpreted as a result of methane clathrate release (e.g. Jiang *et al.*, 2003; see also Kennedy *et al.*, 2001). Studies of geologically recent submarine continental slope failures (past 45 ka) are co-incident with ice-core records of elevated atmospheric methane, and highlight the linkage between submarine mass movement processes and release of methane hydrates over glacial-interglacial transitions (Maslin *et al.*, 2004). Since the Phanerozoic record illustrates a relationship between deglaciation and gas hydrate release, similar mechanisms are likely to have caused local, short-lived perturbations of the carbon cycle in the Neoproterozoic.

PALAEOENVIRONMENTAL DISCRIMINATION OF DIAMICTITE FACIES

In order to critically evaluate and interpret sediments of glacigenic origin in the geological record, an understanding of contemporary processes of glacial and glacially influenced sedimentation is required. Knowledge of the range and distinctiveness of depositional systems, processes, resulting lithofacies assemblages and sediment-landform associations is essential for accurate palaeoenvironmental reconstruction. However, glacial deposystems tend to be complex and in some cases, even basic tasks such as distinguishing marine from terrestrial glacigenic sediments can be challenging (e.g. Lowe *et al.*, 2001, and references therein). This is particularly the case in the absence of palaeoclimatologically significant faunal assemblages. Perhaps one of the key issues in many Neoproterozoic successions is determining to what degree the evidence favours a glacial origin. Eyles and Januszczak (2004) argued that many 'tillites' of former workers are in fact tectonically induced mass flow deposits, many of which do not contain a demonstrable glaciclastic debris content (but see Table 1). Similar arguments have been provoked over many Neoproterozoic diamictite-bearing formations (e.g. Schermerhorn, 1974; Bhatia & Kanwar, 1975; Eyles, 1992; Eyles & Januszczak, 2004, and references therein), which is unsurprising since sediment gravity flows are a common component of glacimarine environments (e.g. Benn & Evans, 1998; Eyles *et al.*, 2001; Laberg & Vorren, 2000; Elverhøi *et al.*, 2002; Taylor *et al.*, 2002; Nygård *et al.*, 2002; Ó Cofaigh *et al.*, 2004). Indeed, stacked debris flows are thought to be the principal building blocks of large glacial fan systems in the polar North Atlantic (Dowdeswell *et al.*,

Table 19.1 Sedimentological characteristics of some Neoproterozoic diamictite-bearing successions. Note that a significant literature is represented in the Hambrey and Harland (1981) volume on Earth's Pre-Pleistocene glacial history; the reader is referred to this for age constraints (including biostratigraphy) at the time of publication, and interpretations for the genesis of individual successions. This volume is freely available in PDF format at http://www.aber.ac.uk/glaciology. Some examples are provided of formation thicknesses, but it should be noted that many successions show considerable lateral thickness variations

Stratigraphic unit		Characteristics	References
AUSTRALIA			
Louisa Downs Gp. 4000 m	Egan Fm. 80 m	Diamictite, dolomite, limestone, sandstone, arkose, conglomerate, shale and siltstone. Well preserved striated pavement occurs in the Mount Ramsay area. Striations indicate ice flow from the North. Capped by a laminated flaggy pink dolomite with red shale interbeds	Coats & Preiss (1980) Corkeron *et al.* (2001) Griffin *et al.* (1998)
Kuniandi Gp. 210 m	Landrigan Tillite	2 polished and striated pavements occur beneath the Landrigan tillite; east-west oriented striae; pluck marks indicate ice flow from the east; polished and striated boulders; diamictites are poorly sorted and lack stratification; clasts mainly extra-basinal	Roberts *et al.* (1972) Coats & Preiss (1980) Yeats & Muhling (1977)
Duerdin Gp. (E. Kimberleys)	Moonlight Valley Tillite 200 m	Diamictites with massive red siltstone matrix; contain abundant striated and faceted clasts; overlain by lonestone-bearing shales. Diamictites in the Osmond Range overlie a striated pavement with crescentic structures – ice flow from the northeast. Capped by a pink finely laminated dolomite with red shale partings and passes gradationally upwards into the Ranford Fm.	Coats & Preiss (1980) Dow & Gemuts (1967) Blake *et al.* (1998) Dunster *et al.* (2000)
	Fargoo Tillite >100 m	Diamictites contain abundant polished, striated and faceted clasts	
Mount House Gp. (Kimberleys)	Walsh Tillite	Abundant striated clasts, erosively based (unconformable), clast imbrication possibly indicative of lodgement till	Coats & Preiss (1980)
Umberatana Gp., Yudnamutana Subgroup (Adelaide Rift Basin)	Bolla Bollana Tillite 204 m	Massive diamictite; shale, siltstone, mudstone, pebbly calcareous diamictite, quartzite and arkose. Rare striated and faceted clasts, including extra-basinal errratics	Coats (1981) Preiss (2000) Krieg *et al.* (1991)
	Wilyerpa Fm. 584 m	Laminated mudstone, siltstones, arenites, grits and minor diamictites; gradationally overlies and local intertongues with the Appila Tillite	Preiss (2000) McKirdy *et al.* (2001) Krieg *et al.* (1991)
	Pualco Tillite <3300 m	Calcitic diamictite, orthoquartzite, siltstone, sandstone and limestone. Rare faceted and striated clasts, but locally abundant in the Central Flinders Ranges (Daily & Forbes, 1969)	Daily & Forbes (1969) Coats (1981) Young & Gostin (1991)

	Elatina Fm. (100–500 m)	Sandstone with local lenses of diamictite, interpreted as glacifluvial outwash; some evidence of ice-contact deformation. Abundant faceted and striated clasts (Mawson, 1949; Dalgarno & Johnson, 1964)	Mawson (1949) Dalgarno & Johnson (1964) Preiss *et al.* (1998) Preiss (2000) Lemon & Reid (1998) Lemon & Williams (1998) Schmidt & Williams (1995) Krieg *et al.* (1991) Coats (1973) Parkin (1969)
	Sturt (300 m)/ Appila Tillite Bibliando, Hanborough, Merinjina (650–1500 m) and Calthorinna tillites (650 m)	Muddy and sandy diamictites. The Appila Tillite (~170 m thick) consists of pebbly diamictite and conglomerate with a disconformable base and contains abundant striated and faceted clasts. The Sturt Tillite contains rare faceted clasts (Sprigg, 1942). A number of other diamictite units occur at similar stratigraphic levels including the Bibliando, Hanborough, Merinjina and Calthorinna tillites. The Hansborough tillite contains rare faceted clasts; the Merinjina Tillite contains abundant striated clasts. Further details on these may be found in Coats (1981)	Coats (1981) and references therein Dunn *et al.* (1971) Sprigg (1942) http://www.ga.gov.au/oracle /stratnames_info.jsp
Umberatana Gp., Yerelina Subgroup	Pepuarta ~280 m Mount Curtis Tillite ~90 m	Pepuarta: massive pebbly-cobble siltstone with lenticular sandstone bodies. Mount Curtis: predominantly dolomitic silty diamictite. Both units contain abundant faceted and striated clasts (Coats, 1981 and references therein).	Coats (1981) and references therein Preiss (2000)
	Olympic Fm. 36 m (Halls Creek Gp.)	Cross-bedded arkosic sandstone with conglomerate lenses; poorly sorted sandstones with shale interbeds, conglomerates, diamictites and carbonate beds. Considerable lateral variation in facies associations; diamictites interpreted by Lindsay (1989) as mass flow deposits; channelised conglomerates; striated and faceted clasts common (Wells, 1981)	Wells *et al.* (1967) Wells (1981) Lindsay (1989) Freeman *et al.* (1991)
Amadeus Basin	Areyonga Fm. (230 m)	Diamictites, with intercalated sandstone, conglomerate and carbonate interbeds, shales and siltstones; diamictites are 1–40 m thick; diamictites towards the top of the formation show weak stratification and contain conglomerate pellets, abundant sandstone lenses; intra- and extra-basinal clast lithologies; boulder pavements widely distributed throughout the formation; rare (<1%) striated and faceted clasts. Other units of diamictite containing striated and faceted clasts are known from elsewhere in the Amadeus Basin, and occur in the Boord Fm. and the Inindia beds (Wells, 1981)	Wells (1981) Lindsay (1989) Prichard & Quinlan (1962) redefined at http://www.ga.gov.au/oracle /stratnames_info.jsp
	Boord Fm.	Sandstone, siltstone, carbonate, diamictite and calcilutite, calcarenite; faceted clasts are common, with occasional examples of striated clasts	Wells (1981)

Table 19.1 (*cont'd*)

Stratigraphic unit		Characteristics	References
Ngalia Basin	Naburula Fm. (8 m)	Shale, siltstone, diamictite and dolomite. Common striated and faceted clasts	Wells (1981) http://www.ga.gov.au/oracle/stratnames_info.jsp
	Mount Doreen Fm. (340 m)	Shale, diamictite and dolomite. Striated and faceted quartzite clasts	Wells (1976) Wells (1981)
Georgina Basin	Mount Cornish Fm. (680 m), Yardida Tillite (650–2900 m) and Mount Stuart Fm.	Siltstone, shale, diamictite associated with arkose and dolomite. Frequent faceted and striated clasts are known from diamictites in both the Mount Cornish Fm. and the Yardida Tillite; lensoid bodies of diamictite are also known from the Mount Stuart Formation which crops out in the Georgina Basin, and locally in outliers between the Ngalia and Georgina basins.	Walter (1981) Wells (1981) Kruse *et al.* (2002)
Grassy Gp. (**Tasmania**)	Cottons Brecca	Diamictite, volcaniclastic sandstones; till pellets and dropstones in interbedded laminites, wide range of clast lithologies; capped by a pale pinkish-grey laminated Cumberland Creek Dolostone	Jago (1974) Calver & Walter (2000) Calver *et al.* (2004)
Togaria Gp. (NW **Tasmania**)	Croles Hill Diamictite <250 m	Diamictite, rare laminated mudstone and siltstone interbeds containing dropstones; no known cap carbonate unit	Calver *et al.* (2004)
AFRICA			
Morocco, Anti-Atlas; Siroua Series	Tiddiline Fm. Anzi Fm.	Conglomerates, turbiditic greywackes, laminated siltstone, diamictite and feldspathic sandstones. Greywackes contain possible dropstones; no faceted or striated clasts observed	Leblanc (1981)
Central **Sierra Leone**; Rokel River Gp.	Tibai Mbr., Tabe Fm.	Diamictites (including paraconglomerates and orthoconglomeratic facies), medium-coarse sandstones, laminated siltstone, fine sandstone. Slump folds and contorted bedding indicate mass-movement processes. Bedded facies contain lonestones	Tucker & Reid (1981)
Algeria, western Hoggar	Série Pourprée	Conglomerates, diamictites, lonestone-bearing claystones, arkosic sandstones, pelites, siltstones, greywackes and breccias. Clasts in the Adafar glacigenic beds are striated, faceted and bear pressure marks; glacifluvial facies in the Ouallen-In Semmen Gp. also contain striated clasts; 'varved' claystones at Ouallen contain small dropstones.	Caby & Fabre (1981)
W. **Uganda**	Bunyoro Series	Rare faceted, 'scratched' exotic pebbles in diamictites, associated with rhythmically laminated argillites interpreted as varvites	Davies (1939) Bjørlykke (1981)
Northern **Zaïre**	Lower Lenda Tillite, Itari district	Poorly sorted pebbly mudstone containing striated cobbles	Cahen (1954)
Lower **Zaïre**	Niari Tillite	Striated and faceted clasts in diamictites locally abundant	Cahen & Lepersonne (1967) Cahen & Lepersonne (1981)

Lower **Zaïre**	Bamba Mt. tillite	Rhythmically laminated ('varvite') containing sparsely distributed pebbles. Faceted clasts and clasts bearing percussion marks have been reported from equivalent strata in Angola (Schermerhorn & Stanton, 1963; Kröner & Correia, 1973), but are interpreted as non-glacial.	Cahen & Lepersonne (1967) Cahen & Lepersonne (1981)
NW **Angola,** Schisto-calcaire Gp	'Upper Tilloid Formation' <200 m	Lithofacies: diamictite, mudstone, greywacke, conglomerate, breccia, quartzite and limestones; striated clasts reported, but their significance debated	Schermerhorn & Stanton (1963) Schermerhorn (1981)
NW **Angola**, Haut Shiloango Gp	'Lower Tilloid Formation' <500 m	Lithofacies: diamictites, conglomerate, breccia, arkosic and calcareous quartzite, greywacke, mudstone, limestone. Exotic (extra-basinal clasts) reported from tilloids (diamictites?).	Schermerhorn & Stanton (1963) Schermerhorn (1981)
Urungwe District, **Zimbabwe**	Msukwi River tillite ~105 m	Diamictites overlain by laminated shales; clasts in the diamictite are faceted and bear striae	Bond (1981)
Namibia; Otavi Gp.	Chuos southwestern congo	Dropstone intervals in laminated hemipelagic sediment. Dropstones interpreted by Hoffman *et al*., 1998 and Condon *et al*., (2002) as rafted by glacier ice; Eyles & Januszczak (2004) contest the presence of convincing dropstone structures, and interpret lonestone-bearing units as debrites and highlight previous sedimentological investigations which identify predominantly mass flow facies, with no indication of glaciclastic debris (Schermerhorn, (1974, 1975; Martin *et al*., 1985)	Schermerhorn (1974, 1975) Martin *et al.* (1985) Hoffman *et al.* (1998) Condon *et al.* (2002) Eyles & Januszczak (2004)
Namibia; Swakop Gp.	Ghaub congo	Dropstone intervals in laminated hemipelagic sediment. Dropstones interpreted by Hoffman *et al*., 1998 and Condon *et al*., (2002) as rafted by glacier ice; Eyles & Januszczak (2004) contest the presence of convincing dropstone structures, and interpret lonestone-bearing units as debrites.	Condon *et al.* (2002) Eyles & Januszczak (2004)
Namibia; Kuibis sub-group	Blaubeker Fm. >500 m	Diamictite, conglomerate, quartzite, shale; diamictites contain abundant striated and faceted clasts	Kröner (1981)
SW Namibia; Gariep Basin	Numees	Massive diamictite; rhythmically laminated pelites with erratic dropstones; thin iron formation. Numerous faceted and striated clasts reported (De Villers & Söhnge, 1959), although Kröner, (1981) argues many are probably tectonic features, a glaciclastic debris component is accepted.	Rogers (1916) Martin (1965) Kröner (1981)
	Kaigas	Diamictite, arkose, greywackes; dropstones, striated and faceted clasts. Sorting, graded bedding and conglomerate channel-fills led Kröner (1975) to suggest a fluviatile origin.	Kröner (1981) Von Veh (1993)
NW Zambia; Kundelungu Basin	Grand Conglomerat <500 m	Diamictites containing striated and faceted clasts; associated facies variably interpreted as ground moraine, glacilacustrine, glacifluvial sediments and glacially influenced marine deposits dominated by mass flow facies.	Gray (1930) Cahen (1954) Robert (1956) Cahen & Lepersonne (1967) Binda & Van Eden (1972) Cahen & Lepersonne (1981)
	Petit Conglomerat	Striated pebble-sized clasts in diamictites	Cahen (1954)

Table 19.1 *(cont'd)*

Stratigraphic unit		Characteristics	References
Mauritania, Mali, E. Senegal, Guinea	Jbéliat Fm./'Triad'	Facies: terrestrial glacigenic tillites, deltaic, lacustrine (or marine), and fluviatile facies. Tillites contain striated clasts, lenticular pockets of sandstone and conglomerate which are folded and fractured; rare stratified tillites. Striated pavements, roches moutonnées, glacitectonic structures including step fractures and folds and breccias in preglacial substrate. Polygonal structures associated with sandstone wedges occur at the top of the glacial sequence, always beneath the cap dolostones. These are interpreted as periglacial features. 3–5% striated clasts	Trompette (1973) Deynoux (1978) Deynoux & Trompette (1981) Deynoux (1982) Deynoux (1985)
N. Ethiopia; Tambien Gp.	Matheos Fm. ~1000 m	Carbonate, slate and pebbly slate ('diamictite'). The pebbly slate contains striated and polished cobble-sized clasts	Miller *et al.* (2003)
NORTH AMERICA			
Canada; Newfoundland; Conception Gp. (4 km thick)	Gaskiers Fm.	Massive and crudely stratified tabular units of diamictite, interbedded with and overlain by turbidites. Striated and faceted clasts occur. Associated volcanics suggest glaciation on a volcanic cone of a complex island arc (Eyles, 1990).	Eyles (1990)
Canada; Windermere Supergroup	Mount Vreeland <1200 m	Massive to crudely bedded diamictite and sandstones; dropstones provide evidence for iceberg rafting. Overlain by a thin laminated grey cap dolostone.	Hein & McMechan (1994) Ross *et al.* (1995)
	Toby Fm. <2500 m	Diamictite, conglomerate, breccia, pelite, carbonate and sandstones	Aalto (1971, 1981) Eisbacher (1981) Ross *et al.* (1995)
Canada; NW Territories; Rapitan Gp.	Sayunei (>500 m) Shezal (<300 m)	Diamictites (<250 m thick) associated with turbidites bearing dropstones. Stratified diamictite occurs with mudstone interbeds. Scoured and polished pavement beneath lowermost diamictite units. Rare striated clasts. Extrabasinal (erratic) clasts in laminated siltstones, till pellets and dropstones. The Sayunei Formation is predominantly siliclastic rhythmite; where well developed, the Shezal Formation contains reasonably abundant striated clasts, with thin diamictite sheets separated by shale, siltstone and sandstone beds. Clusters of outsize clasts locally occur which may represent iceberg dump-features.	Yeo (1981) Eisbacher (1985) Young (1995)
NW Canada; McKenzie Mountains	Icebrook Formation, Stelfox Member	Dropstones, till pellets, angular quartz grains, rare striated clasts. Diamictites interpreted as glacimarine, interbedded with laminated mudstone and siltstones and associated with slope deposits and olistostromes (Aitken, 1991).	Aitken, (1991)
U.S.A.; Kingston Peak Fm.	Surprise Mbr. Wildrose Mbr.	Argillite, diamictite, siltstone, sandstone, conglomerates. Small proportion of striated and faceted clasts occurs. Dropstone intervals in laminated hemipelagic sediment	Miller *et al.* (1981) Condon *et al.* (2002)
U.S.A.; Idaho; Windermere Supergroup	Edwardsburg Fm. 700–1200 m	Quartzite, diamictites with deformed subangular to subrounded clasts (no dropstones or faceted clasts recorded), volcaniclastics including sandstones and conglomerates. Link *et al.*, (1994) interpret a proximal to distal glacimarine succession, but no definitive evidence presented of glaciclastic debris	Lund *et al.* (2003) Link *et al.* (1994)

U.S.A.; SE Idaho; Pocatello Fm.	Scout Mountain Mbr.,	Diamictites containing striated clasts; local iron-rich laminites. The succession is capped by a pink dolomite.	Link *et al.* (1994) Fanning & Link (2004)
U.S.A.; Virginia	Mechum River Fm. (>400 m)	Mudstones, boulder conglomerates, rhythmites, diamictites; discontinuous lenses of arkose sandstones (possible meltwater channel-fills). Rare striated clasts, but apparent lack of dropstones.	Bailey & Peters (1998)
U.S.A.; Southwest Virginia	Konnarock Fm. (formerly Mount Rogers Fm.)	Diamictite, laminated pebbly mudstone; dropstones; striated and faceted clasts 'exceedingly' rare, but do occur	Schwab (1981)
U.S.A.; N. Carolina	Grandfather Mountain Fm.	Laminated pebbly mudstone; widely dispersed dropstones	Schwab (1981)
U.S.A.; Roxbury Conglomerate, Boston Basin	Squantum Tillite Mbr. ~215 m	Diamictite, conglomerate, feldspathic sandstone, laminated (rhythmically) mudstone and siltstones. Rare striated and faceted clasts have been reported, but are considered by some to be of tectonic origin. Rip-up clasts support a mass flow origin for at least part of the succession. Further literature may be found in Rehmer (1961) and Eyles & Januszczak (2004).	Dott (1961) Rehmer (1981) Eyles & Januszczak (2004)
U.S.A.; Utah	Mineral Fork Fm. ~900 m	Conglomerate, sandstone, siltstone, shale, diamictites; diamictites contain rip-up clasts, silty lenses and irregular slumped tops, thought to represent mass flow or ice contact phenomena, however, striated, polished pavement on the underlying Big Cottonwood Fm., and associated whaleback forms, rare faceted and striated clasts reported from diamictites, till pellets; little evidence for major uplift or tectonism during deposition. Interpreted as continental to marine or fully marine glacially-influenced succession	Ojakangas & Matsch (1980) Christie-Blick (1982) Young (2002)
Greenland; Tillite Gp.	Storeelv Fm.	Clast fabrics in diamictites consistent with lodgement till characteristics. Striated clasts in diamictites; Two striated levels, one at base of Storeelv, and 52 m above base of the formation. Facies include basal tillites, waterlain tillites, debris flow facies, ice-proximal and distal glacimarine deposits, rhythmites (proximal and distal facies). Till pellets locally occur. Far-travelled erratics from extra-basinal sources. Lithologies: diamictite, sandstone and conglomerates. Rare sandstone wedges and downfolds interpreted as periglacial features. Capped by laminated orange dolostone associated with grey shaly dolomitic mudstones of the Canyon Fm.	Hambrey (1988) Moncrieff (1989a, b) Moncrieff & Hambrey (1988, 1990) Hambrey *et al.* (1989) Hambrey & Spencer (1987) Fairchild & Hambrey (1995)
	Arena Fm.	Lithologies: sandstone and dolomitic mudstones; wave ripples towards base indicate open marine conditions; local dropstones.	
	Ulvesø Fm.	Possible Aeolian sandstone facies at base of formation; periglacial thermal contraction and load structures above the youngest diamictite; evaporitic facies include non-ferroan dolomite pseudomorphs after gypsum including alabastrine gypsum and gypsum laths; cubic halite pseudomorphs also occur – 30 m above the base of the formation and at the top of the Arena Fm. which divides the Ulvesø and Storeelv Fms. Lithologies: diamictite, sandstone, conglomerate and mudstone. Sandstone wedges and downfolds with polygonal arrangement in plan view at the top of the formation, interpreted as periglacial features. Interpreted as transitional low level terrestrial to glacimarine depositional environments.	

Table 19.1 (*cont'd*)

Stratigraphic unit		Characteristics	References
SOUTH AMERICA			
Brazil São Francisco Supergroup	Jequitaí Fm. (Macaubus Gp)	Massive diamictites dominant in the western part of the Macaubas Gp., but in the east are associated with quartzites, phyllites, siltstones, greenschists and laminites. Faceted and striated clasts are locally abundant. Overlain by the Bebedouro cap carbonate	Rocha-Campos & Hasui (1981)
Brazil; Jaganda Gp. (1400 m thick)	Puga Fm.	Diamictite, conglomerate, shale and sandstone. Diamictites contain 1–2% faceted clasts and occasional striated clasts interpreted as terrestrial glacial deposits which grade laterally into more distal glacimarine facies in the Paraguay-Araguaia geosyncline Overlain by cap carbonate of the Araras Fm. Diamictites are also known of the Jacadigo Group where they are associated with banded iron formations similar to those of the Rapitan Group (Gaucher *et al.*, 2003).	Rocha-Campos & Hasui (1981) de Almeida (1964a) de Almeida (1964b) Alvarenga *et al.* (2004) Nogueira *et al.* (2003) Gaucher *et al.* (2003)
EUROPE			
Scotland; Dalradian Supergroup	Port Askaig Formation	Diamictites, conglomerates, sandstones, siltstones. Faceted clasts occur, but no striated clasts have been reported. A mass flow origin is indicated for many of the diamictite sheets that occur in the formation (Arnaud & Eyles, 2002b)	Spencer (1985) Arnaud & Eyles (2002b)
Scotland	Kinlochlaggan boulder bed	'Boulder bed' associated with feldspathic quartzite and massive and bedded quartzitic psammites. Dropstones reported, but no striated clasts.	Treagus (1981)
Scotland, Southern Highland Group	Loch na Cille boulder bed	Interpretations differ considerably from volcanic hyaloclastic breccia (Gower, 1977) to glacial (Prave, 1999). The beds contain extra-basinal clasts which may support a glacial influence.	Condon & Prave (2000); Prave (1999)
France; Upper Brioverian Supergroup	Granville Fm.	Pebbly mud diamictites associated with thick sequences of Brioverian turbidites and volcaniclastics. Interpreted as non-glacial debris flows.	Eyles (1990)
Norway; Vestertana Gp.	Mortensnes Fm. 10–60 m	Laminated mudstones bearing dropstones, structureless tillite (?diamictite) contains extra-basinal erratic clasts and rare striated and faceted clasts.	Edwards & Føyn (1981)
	Smalfjord Fm.	Rare striated and faceted clasts, a single striated pavement at Bigganjargga; diamictites interpreted as subaqueous mass flow deposits.	Edwards & Føyn (1981) Arnaud & Eyles (2002a)
S. **Norway**, Hedmark Group	Moelv Fm.	Massive and stratified diamictites occur in association with conglomerates, sandstones, laminated mudstones containing dropstones and rare striated and faceted clasts. Interpreted as basal tillite transitional with glacimarine sediments with iceberg rafting.	Bjørlykke & Nystuen (1981)

Sweden; Swedish Caledonides	Sito Tillite	Diamictite associated with siltstone and dolomite. No striated clasts have been reported from this unit, and a non-glacial origin is favoured in the absence of dropstones.	Strømberg (1981)
	Långmarkberg Fm.	Laminated siltstones bearing abundant lonestones, massive and stratified (with siltstone and sandstone interbeds) sandy diamictite facies bearing striated clasts.	Thelander (1981)
	Lillfjället Fm.	Massive diamictite, laminated siltstones, dolomitic sandstone and weakly stratified diamictite. No striated or faceted clasts have been reported, but rare dropstones occur.	Kumpulainen (1981)
Southern **Sweden**	Lilla Hals Boulder Bed ~240 m	Bedded diamictites associated with feldspathic and arkosic sandstone, laminated shales and mudstones. Faceted clasts occur, but no striated examples reported. Interpreted as submarine debris flows by Vidal & Bylund (1981).	Vidal & Bylund (1981)
Russia; Rybachiy Peninsula	Motka tilloids	Sandstone, conglomerate, tilloids (?diamictites), breccia, mudstones interpreted as mass flow (slump, slide, turbidites) deposits deposited in a non-glacial setting.	Chumakov (1981)
Russia; S. and Middle Urals	Tolparovo Fm. 600–650 m	Sandstones interbedded with mixtite, gritstone, conglomerate and argillite.	Maslov (2000)
	Kurgashlya Fm. 160–200 m	Mixtites intercalated with sandstone, massive and thinly-bedded siltstones, gritstone, conglomerate, breccia and dolomite interpreted as distal glacimarine sediments reworked by density currents. Mixtites contain very rare striated and faceted clasts.	Chumakov (1981) Chumakov (1998)
	Koiva Fm.	Shale, siltstone, carbonates with localised mixtites and volcanics	Maslov (2000)
	Tany Fm. 360–800 m	Mixtite, sandstones and shales with subordinate carbonate and volcanics. Mixtites contain extra-basinal clasts and dropstones in laminated hemipelagic sediments (Chumakov, 1996). Possible lateral equivalents include the Vil'va Fm. which comprises weakly stratified mixtites (Maslov, 2000), although metamorphism and tectonism are regarded to have destroyed original clast surface features, such that striae have not been observed (Chumakov, 1981).	Chumakov (1981) Chumakov (1996) Maslov (2000)
Belarus	Vilchitsy Fm.	Sandstone, diamictite, rhythmically laminated siltstones containing lonestones, sandy diamictites containing striated clasts.	Chumakov (1981)
Russia; N. Urals; Polyudov Ridge	Churochnaya tillite	Shale, sandstone, brecciated dolomite, diamictite, chert. Diamictites contain extra-basinal clasts and striated clasts.	Chumakov (1981)
Svalbard; Polarisbreen Gp. (1075 m thick)	Wilsonbreen Fm. >200 m	Dolomitic diamictite, discontinuous sandstone and conglomerate bodies, dolostone, limestone, dolomitic shale and rhythmites. Dolostone underlying the Wilsonbreen Formation is frost-wedged. The Gropbreen Mbr. (73 m) diamictites contain <15% striated clasts. Overlain by cap carbonate of the Dracoisen Fm. Sequence interpreted as temperate glacimarine and terrestrial environment.	Hambrey (1988, 1989) Hambrey *et al.* (1981) Fairchild *et al.* (1989) Harland *et al.* (1993) Fairchild & Hambrey (1984, 1995) Harland (1997) Halverson *et al.* (2004)
	Elbobreen Fm. >400 m	Dolomitic diamictite, dolomitic conglomerate, rhythmites, shale and silty homogenous dolostone. The Petrovbreen Mbr. diamictites contain <15% striated clasts and shows considerable lateral thickness variations.	

Table 19.1 (*cont'd*)

Stratigraphic unit		Characteristics	References
ASIA			
Oman; Abu Mahara Gp.	Fiq Mbr. (Ghadir Manquil Fm.)	Striated clasts, rare dropstones, massive diamictite sheets; overlain by cap dolostone of the Hadash Fm.	Rabu (1988) Kellerhals & Matter (2003) Allen *et al.* (2005) Leather *et al.* (2002) Rieu *et al.* (*In Review*) This study
	Ghubrah Fm.	Massive diamictites with mixed clast composition; occasional striated clasts.	
Oman; Mirbat Gp. (formerly Mirbat Sandstone Fm.)	Shareef Fm.	Diamictites and laminated lonestone-bearing muds; abundant polished and striated clasts.	
	Ayn Fm.	Abundant striated and faceted clasts, dropstones in stratified diamictite facies. Glacifluvial facies in Gilbert-type deltas.	
India; Baliana Gp.	Blaini Fm. <300 m	Abundant striated and faceted clasts; massive and weakly stratified diamictite sheets and rhythmically laminated mudstones and siltstones; rare sandstones. Overlain by a laminated pink or grey microcrystalline dolomite with red shale interbeds.	Bhatia & Kanwar (1975) and references therein Jain & Varadaraj (1978) Bhatia & Prasad (1981) Brookfield (1987) This study
China; Yangtze Platform, South China	Nantuo Fm. ~210 m	Major facies types include lodgement tillites, glacifluvial and proglacial subaqueous deposits. Lithofacies: stratified and massive clast-rich (30–50% clasts) diamictites, laminated siltstones bearing lonestones and argillo-arenaceous rocks containing <10% clasts. Discontinuous sandstone and conglomerate channel fills occur in the diamictites. Abundant dropstones, striated and faceted clasts.	Songnian *et al.* (1985) Songnian & Lesheng (1987) Dobrzinski *et al.* (2004) Dobrzinski & Bahlburg (*In Press*)
	Chang'an Fm. <3700 m	Argillaceous pebbly sandstone, slate, sandstone and pebbly sandy mudstone. Striated clasts also occur.	Yuelun *et al.* (1981)
Central **China**; E. Qinling Range, Henan Province,	Luoquan Fm. (204 m)	Massive, bedded and weakly bedded diamictites, conglomerates, pebbly sandstones and rhythmites containing up to 15% dropstones. Diamictites contain abundant striated clasts, and locally overlie striated pavements with p-forms and friction cracks.	Baode *et al.* (1986)
Northwest **China**; Tarim Block,	Beiyixi Fm. Altungal Fm. Tereeken Fm. Hangelchaok Fm.	Diamictites, sandstones, conglomerates, rhythmically laminated slates (varvites?) containing dropstones. A number of different facies types are recognised including tillites, turbidites, glacilacustrine, glacimarine and glacifluvial facies associations (Zhenjia & Jianxin, 1985). General indications in favour of glaciation include glacially polished bedrock surfaces, pebbles bearing striations, grooves, abrasion pits and cracks, dropstones in laminated hemipelagic sediment. Permafrost features also occur.	Zhenjia & Jianxin (1985)

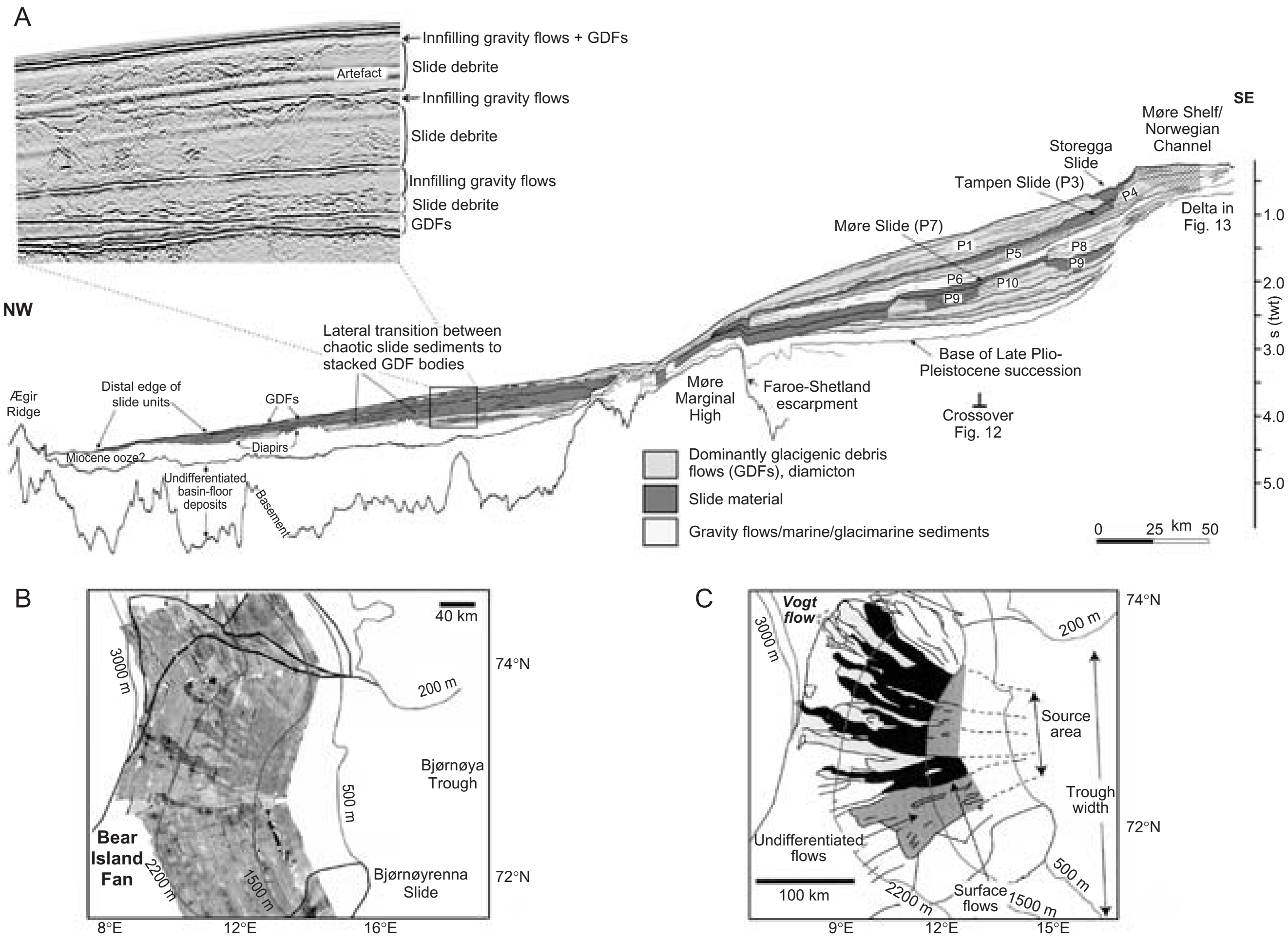

Fig. 5 Submarine glacial fan systems in the polar North Atlantic. (A) Geoseismic section across the North Sea Fan. P1 to P10 are Late Plio–Pleistocene seismic sequences. GDFs: Glacigenic debris flows. Reprinted from Sejrup *et al.* (2004) with permission from Elsevier. (B) GLORIA side-scar sonar imagery of the Bear Island Fan, Barents Sea, and (C) location of subsurface (light grey), surface (black) and undifferentiated (dark grey) glacigenic debris flows. Reproduced from Taylor *et al.* (2002) with permission of the Geological Society, London.

1996; Fig. 5). Examples include the Storfjorden and Isfjorden fans on the continental margin of the Barents Sea and to the west of Svalbard, the Scoresby Sund Fan off the east coast of Greenland and the massive (~350,000 km^3) Bear Island Fan, which covers much of the western part of the Barents Sea (Dowdeswell *et al.*, 1996). Redistribution of glacigenic sediment is also a characteristic feature of grounding-line fan assemblages developed on continental shelves (e.g. Lønne, 1995; Powell & Cooper, 2002; Figs 6, 7). In order to derive some palaeoglaciological data for Neoproterozoic successions, it is relevant therefore to examine some basic characteristics of glacial debris entrainment, transport and sedimentation processes as a means for palaeoenvironmental discrimination.

Subglacial debris entrainment

The entrainment of subglacial debris is dependent on a number of factors, principally the nature of the geological substrate and glacier thermal regime (Kirkbride, 1995; Table 2). Polythermal glaciers (for example on Brøggerhalvøya, Svalbard) tend to be effective erosional agents (e.g. Boulton, 1970; Sugden, 1978), as these ice masses have considerable areas where basal melting and re-freezing of meltwater occurs. Such areas are dependent on the

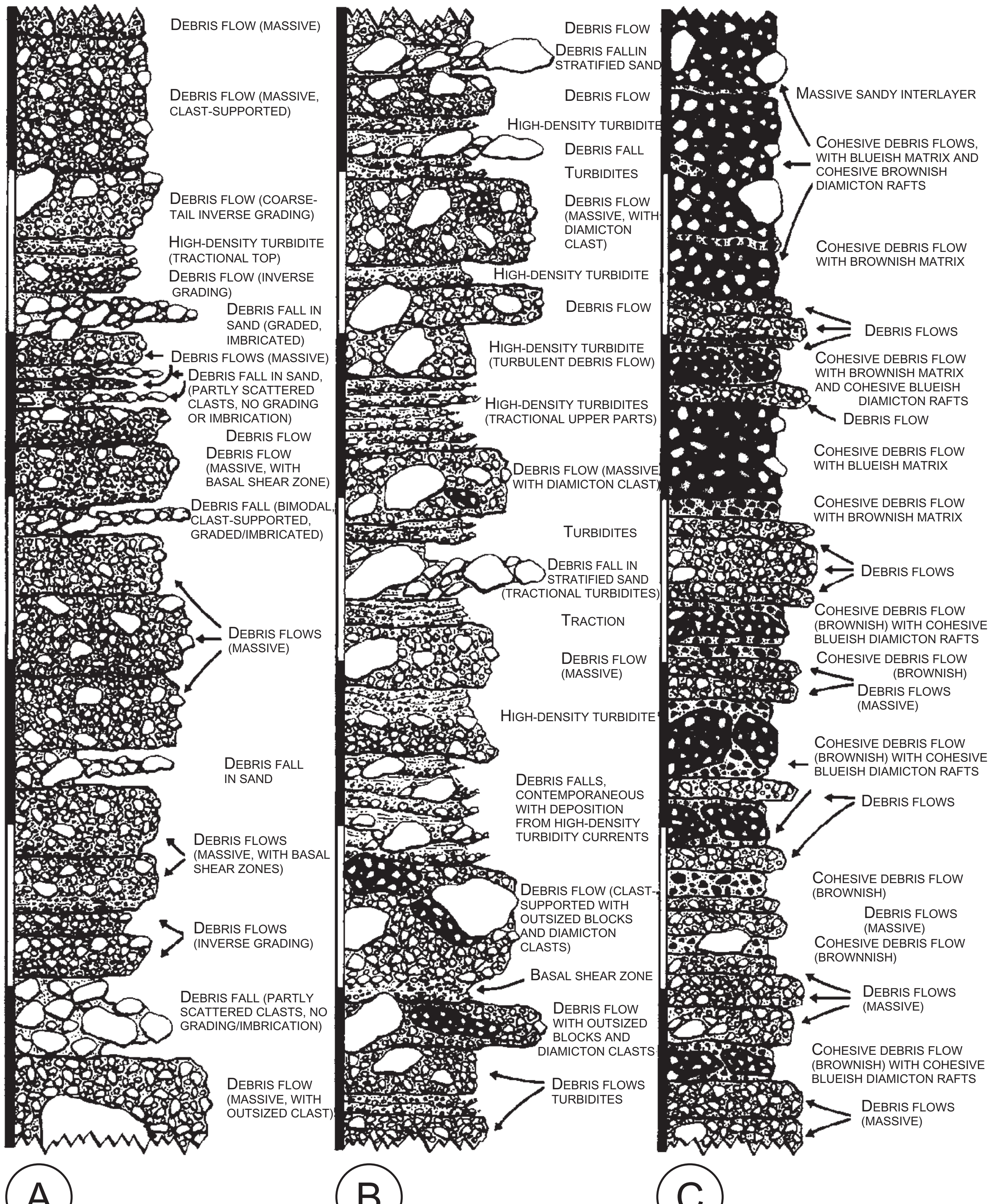

Fig. 6 Stratigraphic logs from the mid-upper part of an ice-contact submarine fan system at Storsand, Oslofjorden, southern Norway. (A) Cohesionless debrites interbedded with turbidites and debris-fall gravel; (B) debrites containing blocks of ice-rafted diamicton; (C) cohesive debrites. Vertical scale bars are metres. Reprinted from Lønne (1995) with permission from Elsevier.

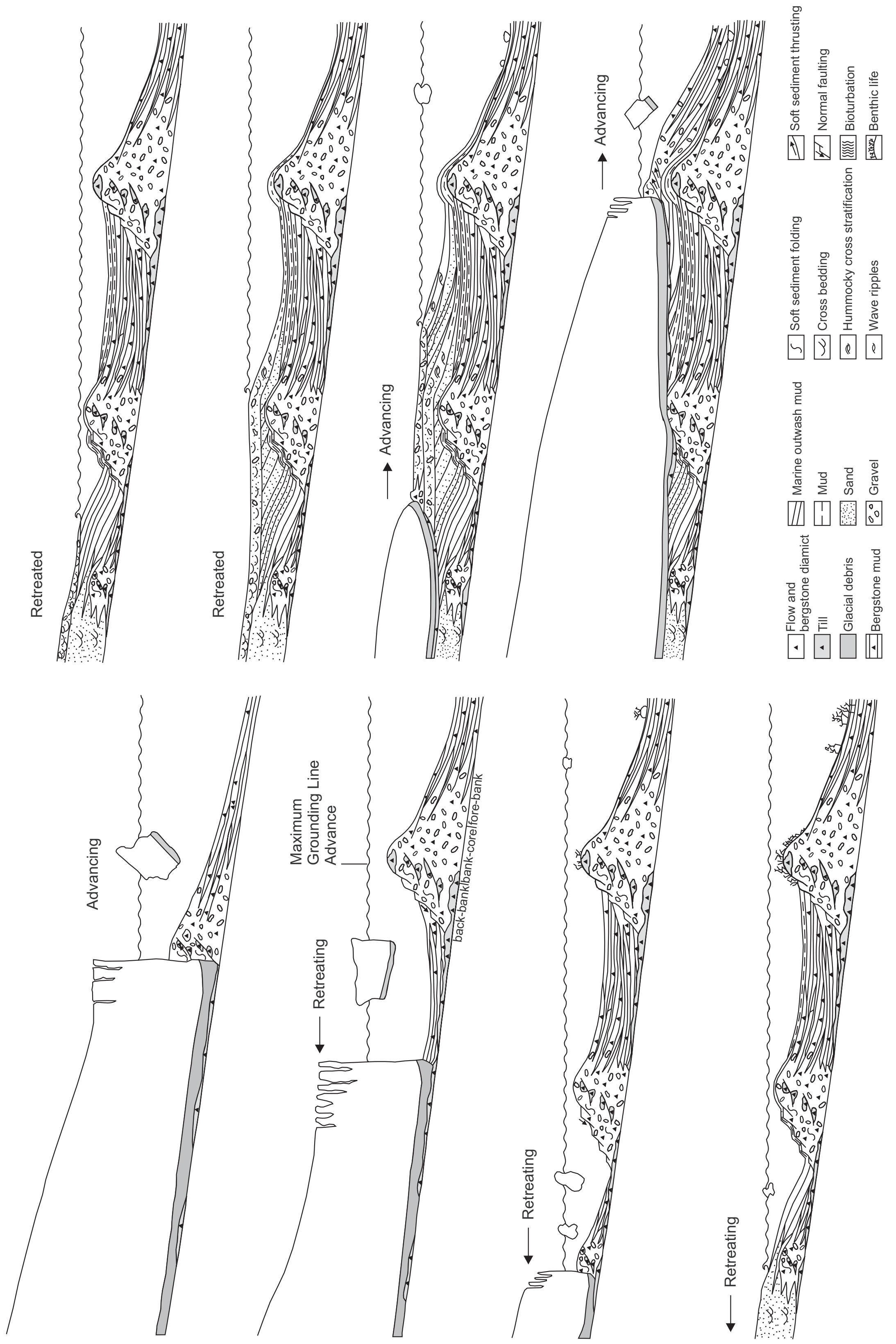

Fig. 7 Sequence stratigraphic models for glaciomarine depositional successions. Reproduced from Powell and Cooper (2002) with permission of the Geological Society, London.

Table 19.2 Glacier characteristics under different thermal regimes

Glacier thermal regime	Characteristics	Modern distribution
Warm/wet-based (Temperate glaciers)	Ice is at or above the pressure melting point. Melting and re-freezing of basal ice keeps subglacial debris loads close to the glacier bed. Meltwater at the bed allows basal sliding processes, thus temperate glaciers typically have greater flow velocities than cold-based glaciers.	Mid-latitudes, Alpine environments, e.g. European Alps, Iceland.
Polythermal (Subpolar glaciers)	Variable distribution of cold ice (below pressure melting point) and warm basal ice (at or above the pressure melting point). Polythermal glaciers are typically frozen in their terminal zones with temperate interiors. Both ice temperatures and water content vary throughout polythermal glaciers. Net adfreezing of subglacial debris often leads to thick basal debris loads. The presence of subglacial meltwater and deformable bed means that polythermal glaciers can attain greater flow velocities than polar glaciers which are frozen at the bed.	Widespread in Arctic and high Alpine environments, e.g. Brøggerhalvøya in Svalbard; Kebnekaise massif, northern Sweden.
Cold-based (Polar glaciers)	Ice is below the pressure melting point. Although cold-based glaciers can entrain, transport and deposit sediment debris, basal debris loads are typically very low, unless the debris was entrained during a different thermal stage in glacier evolution. Polar glaciers typically move by internal deformation and have relatively low flow velocities with respect to temperate and polythermal glaciers.	Polar environments e.g. Dry Valleys, Antarctica.

subglacial bed topography and local ice thickness; where the ice is thin, it is typically cold-based and promotes entrainment by downstream re-freezing and regelation of sediment into basal ice (Boulton, 1979; Hutter & Olunloyo, 1981; Menzies, 1981; see below). Polythermal and temperate glacial masses are generally considered the most powerful erosive agents, whilst the lack of basal meltwater associated with cold-based glaciers (being frozen to the substrate; Boulton, 1972) inhibits basal sliding, erosion, deformation and debris entrainment. Cold-based glaciers thus move principally as a result of slow internal deformation of glacier ice (Paterson, 1994). Nevertheless, a growing number of research papers have illustrated that cold-based ice masses *are* capable of entraining, transporting, deforming and depositing sediment debris (e.g. Holdsworth, 1974; Koerner & Fisher, 1979; Chinn & Dillon, 1987; Echelmeyer & Wang, 1987; Fitzsimons *et al.*, 1999; Cuffey *et al.*, 2000; Atkins *et al.*, 2002). Mechanisms involving entrainment by basal ice include re-freezing of subglacial meltwater (Weertman regelation), regelation into the bed, and net adfreezing which includes processes of freeze-on by conductive cooling and glaciohydraulic supercooling of subglacial meltwater.

Regelation involves pressure-related melting of basal ice around obstacles at the bed (Weertman, 1957, 1964). Melting occurs on the stoss face, where the pressure is highest, while pressure shadows in the lee allow re-freezing of subglacial meltwater. This mechanism effectively allows ice to 'pluck' sediment and rock from the bed, but is thought to be capable of producing only thin (<0.1 m) basal debris layers, with low sediment concentrations (Alley *et al.*, 1997). Repetitive regelation, typical under temperate glacier thermal regimes, limits the thickness of basal debris layers (Kirkbride, 1995). Regelation can also occur *downwards* into pore spaces in subglacial sediment, and is considered a much more effective entrainment mechanism, capable of generating thick basal debris layers (e.g. Alley *et al.*, 1997; Iverson, 2000). Debris contents vary depending on the substrate, but can be very high (Boulton, 1970; Harris & Bothamley, 1984). This mechanism is similar to the basal freeze-on model of Christoffersen and Tulaczyk (2003), which involves the formation of a segregated ice layer as pore water accretes to the glacier sole. The freezing front then migrates downwards into the substrate, allowing effective entrainment of large volumes of debris (Christoffersen, 2003).

Net adfreezing occurs where freezing dominates over melting at the bed, allowing considerable volumes of debris-rich basal ice to form. This is particularly effective when meltwater flows into areas of the bed that are cold-based (Weertman, 1961; Hubbard & Sharp, 1989; Hubbard, 1991), and thus explains why polythermal glaciers are important transporters of large volumes of sediment debris (Elverhøi *et al.*, 1998). Freeze-on by conductive cooling occurs as a result of changing basal thermal conditions (Alley *et al.*, 1997). The thick ice-sheets envisaged in Snowball Earth models are likely to have been effective at insulating the bed, and thus resisted cold-based glacial conditions; however, where ice was thin over highs in the subglacial topography (typical of dispersal centres) cold-based conditions probably existed (*cf*. Kleman *et al.*, 1997; Kleman & Hättestrand, 1999). Changes in basal thermal conditions may be initiated over time by surface cooling, or increased accumulation leading to downward advection of cold surface ice (Alley *et al.*, 1997). This mechanism is likely to be very important in the long-term evolution of ice sheets, because of the resulting changes in dynamics. Indeed, Christoffersen (2003) has suggested that basal freeze-on is a viable mechanism for the shutdown of ice streams observed in West Antarctica. Changes in basal thermal conditions over time can therefore radically affect the overall flow dynamics of ice masses. Dependent on the duration of glaciation, surface temperature conditions and degree of precipitation, it is likely that these processes would operate in a Snowball Earth glaciation. Given the important role played by sea ice dynamics in numerical climate models that simulate Snowball Earth conditions (e.g. Warren *et al.*, 2002; Goodman & Pierrehumbert, 2003; Lewis *et al.*, 2003), a consideration of terrestrial ice sheet dynamics is also required.

Net freeze-on by glaciohydraulic supercooling occurs when subglacial meltwater is supercooled as it rises from overdeepenings at the bed. Thick debris-rich layers can be accreted on to the glacier sole (e.g. Lawson *et al.*, 1996; Strasser *et al.*, 1996). This mechanism of entrainment is likely to be important over a range of spatial scales, for temperate glaciers and ice sheets that have complex basal topography, and particularly in Snowball Earth scenarios.

Particle roundness and other shape parameters

Numerous different processes operate in the transfer of sediment debris through the glacier system, and, in some cases involve large-scale reorganisation of debris between supraglacial, englacial and subglacial transport zones. Active *versus* passive transport (Boulton, 1978) relates to the relative histories of material in subglacial transport compared with supraglacial and englacially transported debris. Supraglacial material is considered to be passively transported, with little modification to particle shape by physical processes other than local reworking by surface meltwater, freeze-fracturing, and, in some instances, aeolian ventifact formation. Since the majority of supraglacial debris is derived from rockfall and talus, the debris is often very angular or angular in clast roundness. Glaciers with considerable supraglacial debris loads are most common in areas of high relief (e.g. in the Himalaya; Benn *et al.*, 2001; Benn & Owen, 2002; the Southern Alps, New Zealand; Hambrey & Ehrmann, 2004), particularly where there is a strong coupling between mountain slope and glacier transport systems (Kirkbride, 1995), although supraglacial debris can also accumulate on ice shelves which fringe mountainous terrain (Evans & Ó Cofaigh, 2003). By contrast, debris incorporated in subglacial transport displays a wide variety of particle sizes and shapes, with surface features resulting from abrasive wear. This material is said to be *actively* transported and is significantly modified during subglacial transport.

Actively and passively transported debris are often analysed in terms of their constituent particle roundness (following Powers, 1953) and other aspects of particle shape. One of the more recent

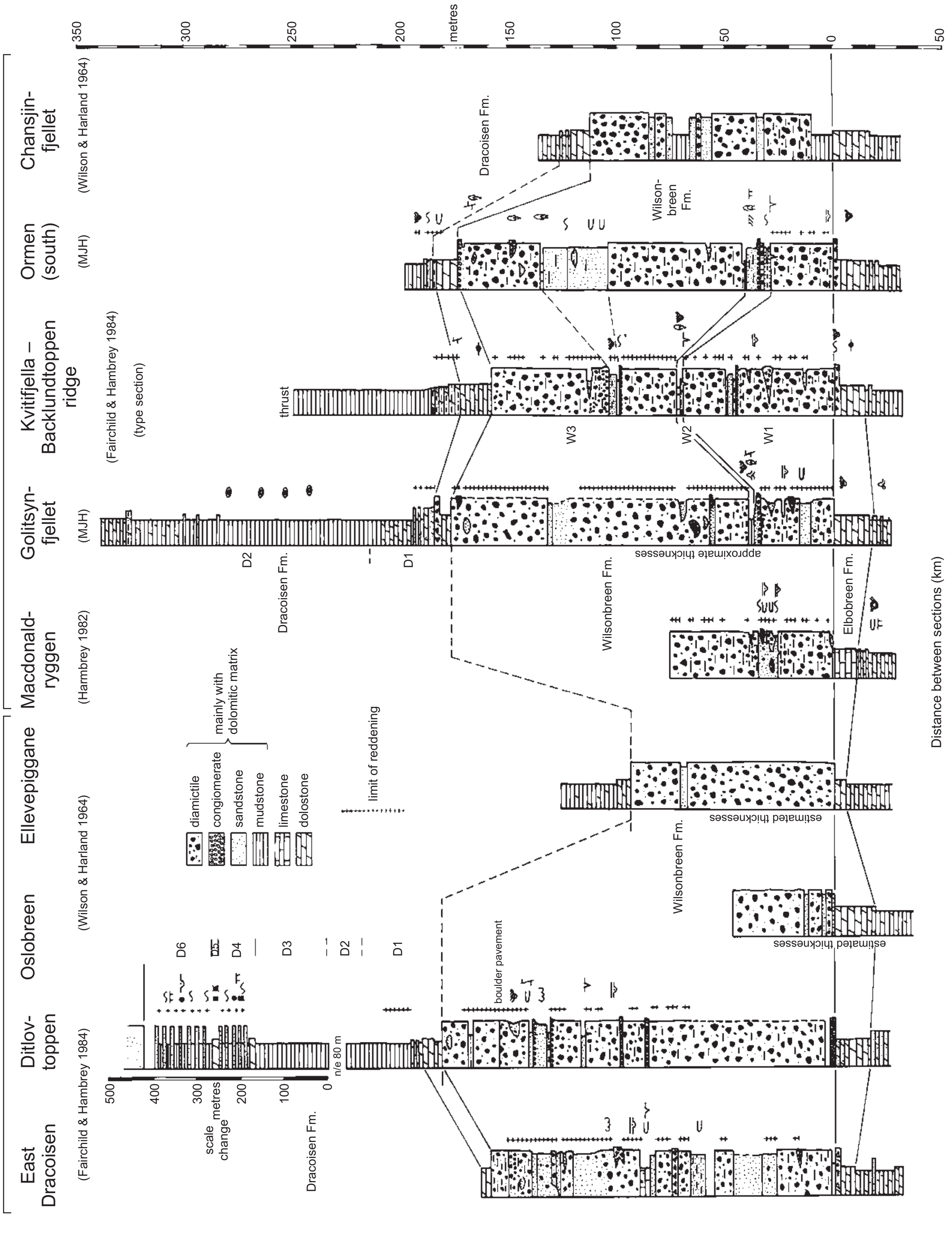

Fig. 8 Lithostratigraphic logs and correlation panel for the Neoproterozoic Wilsonbreen Fm., Olav V Land and Ny Friesland, Svalbard. Reproduced from Harland *et al*., 1993 with permission of Norsk Polarinstitutt.

approaches employed involves the use of the RA/C_{40} index (the percentage of angular and very angular clasts plotted against the percentage of clasts with a c/a axial ratio ≤0.4), following the methods outlined by Benn and Ballantyne (1993, 1994). This technique can provide good discrimination between different glacigenic lithofacies in Arctic environments (Bennett *et al.*, 1997), and is particularly effective in separating supraglacial (passively transported) from subglacial (actively transported) debris. Other techniques for evaluating clast shape such as the use of maximum projection sphericity and oblate-prolate indices formerly used to distinguish beach and fluvial gravels (e.g. Dobkins & Folk, 1970; Stratten, 1974; Gale, 1990) have limited applicability since modern glaciofluvial gravels have similar values to beach sediments (Etienne, 2004).

From a palaeoenvironmental perspective, the presence or absence of supraglacially derived angular debris is significant, as it provides a means to evaluate whether or not nunataks existed, although supraglacial debris buried by primary stratification may remain in englacial transport for a considerable length of time. Supraglacial debris is most likely to be deposited during glacier recession, since surface ablation leads to melt-out of sediment buried in primary stratification (e.g. Glasser & Hambrey, 2001), and mechanical weathering of freshly exposed rock is likely to increase the flux of supraglacial debris. The dominance of subangular to subrounded clasts (typical of many subglacial tills) in the Neoproterozoic Wilsonbreen and Petrovbreen diamictites (Svalbard; Fig. 8) indicates that nunataks were not important debris sources, although angular debris has been reported locally from the former (e.g. Hambrey, 1983; Fairchild & Hambrey, 1984). Diamictites containing angular gravel-sized clasts are also known from many other Neoproterozoic successions (Hambrey & Harland, 1981 and references therein), including those in Oman (Ayn Formation), North India (Blaini Formation), Brazil (Puga Formation; Gaucher *et al.*, 2003) and Africa (Kundelungu Basin; Cahen, 1963).

Subglacial facies

Subglacial deposits (tills) are typically poorly sorted (often diamicton lithofacies), with polymodal particle-size distributions (Boulton, 1978) and include a wide variety of particle sizes and shapes. Diamicton, and its equivalent term for lithified rocks 'diamictite' are non-genetic terms introduced by Flint *et al.* (1960a, b) for poorly sorted deposits comprising sand and/or larger (gravel-sized) particles in a muddy matrix. Since this time, the terminology for poorly sorted sediments has moved towards quantitative classifications for diamicts which provide more specific textural information (e.g. Moncrieff 1989; Hambrey, 1994; Table 3). The Udden-Wentworth particle-size scale has also been expanded allowing better description of very coarse grained deposits (Blair & McPherson, 1999). Gravel clast lithologies and heavy mineral fractions reflect the geology of the glacierised catchment (e.g. Dewez & Geurts, 1996; Lee *et al.*, 2002), and clasts which are faceted or bear striations, crescentic gouges or chattermarks are characteristic of subglacial transportation (e.g. Agassiz, 1838; Chamberlin, 1888; Hambrey, 1994; Miller, 1996; Benn & Evans, 1998; Fig. 1c). Glacial striae are easily distinguished from tectonic features such as slickenlines which tend to be more regular and are often associated with mineralization. Fine-grained calcareous precipitates may occur on large clasts as a result of solute precipitation from subglacial water films in response to localised variations in basal ice-contact pressures (Weertman, 1957; Hallet, 1979; Hubbard & Sharp 1993), although such features may be difficult to distinguish in carbonate-cemented diamictites typical of many Neoproterozoic successions (e.g. in Namibia, Scotland). It is worth noting that some studies have indicated that modern subglacially precipitated carbonates are isotopically depleted in $\delta^{13}C$ (Souchez & Lemmens, 1985; Aharon, 1988).

Alignment of gravel clast a-axes in tills can reflect glacier palaeoflow; and, as such, three-dimensional clast macrofabrics are commonly used for palaeoenvironmental reconstruction. Well developed a-axial clast macrofabrics are often supportive of till deposition by either lodgement or meltout processes (Boulton, 1970; Dreimanis, 1988; Hambrey, 1994; Ham & Mickelson, 1994; Menzies & Shilts, 1996); however, fast-flowing debris, flow- or 'deformation' tills can produce similar fabrics. Clast orientation data may be analysed using principal direction analysis, or in terms of overall fabric shape, based on ratios between eigenvalues for the measured population (Dowdeswell *et al.*, 1985). Fabrics which

<table>
<tr><th>Sand/mud ratio of matrix (Mud <0.06mm; Sand 2.0–0.06 mm)</th><th colspan="6">Percent gravel (<2mm) in whole sediment</th><th>Percent sand in matrix</th></tr>
<tr><th></th><th>Trace (<0.01)</th><th><1%</th><th>1–5%</th><th>5–50%</th><th>50–95%</th><th>>95%</th><th></th></tr>
<tr><td>Mud – 0.11</td><td>MUD(STONE)</td><td>MUD(STONE) with dispersed clasts</td><td rowspan="2">clast-poor muddy DIAMICT(ON/ITE)</td><td rowspan="2">clast-poor muddy DIAMICT(ON/ITE)</td><td>Muddy GRAVEL/BRECCIA/ CONGLOMERATE</td><td></td><td>0</td></tr>
<tr><td>0.11 – 1</td><td rowspan="2">Sandy MUD(STONE)</td><td rowspan="2">Sandy MUD(STONE) with dispersed clasts</td><td colspan="2" rowspan="4">GRAVEL/ BRECCIA/ CONGLOMERATE</td><td>20; 33</td></tr>
<tr><td></td><td rowspan="2">clast-poor intermediate DIAMICT(ON/TE)</td><td rowspan="2">clast-rich intermediate DIAMICT(ON/TE)</td><td>40; 50</td></tr>
<tr><td>1 – 9</td><td rowspan="2">Muddy SAND(STONE)</td><td rowspan="2">Muddy SAND(STONE) with dispersed clasts</td><td>60; 66</td></tr>
<tr><td></td><td>clast-poor sandy DIAMICT(ON/TE)</td><td>clast-poor sandy DIAMICT(ON/TE)</td><td>80</td></tr>
<tr><td>9 – Sand</td><td>SAND(STONE)</td><td>SAND(STONE) with dispersed clasts</td><td colspan="2">Gravelly SAND(STONE)</td><td>Sandy GRAVEL/BRECCIA/ CONGLOMERATE</td><td></td><td>100</td></tr>
<tr><td></td><td></td><td></td><td></td><td></td><td>50% gravel</td><td></td><td></td></tr>
</table>

Table 19.3 Classification for poorly sorted sediments, based on Moncrieff (1989) and modified by Hambrey and Glasser (2003)

have low isotropy and moderate to high elongation values are thought to be characteristic of lodgement till (Dowdeswell *et al.*, 1985; Benn & Evans, 1998), and shallow upglacier clast imbrications develop in some lodgement tills (Dowdeswell & Sharp, 1986; Krüger, 1994). However, genetic discrimination between massive till facies is often difficult and interpretations based *solely* on macrofabric analyses are considered tenuous (e.g. Bennett *et al.*, 1999). Doubts have also been raised regarding the reliability of fabric strength in determining depositional process, with problems attributed to sampling effects (Benn & Ringrose, 2001). In the Neoproterozoic record, additional factors have to be considered in clast fabric and shape analyses including post-depositional compaction, growth of diagenetic cements and, in tectonically deformed terrain (particularly orogenic belts), metamorphism, flattening, stretching or clast re-orientation resulting from shearing and pressure solution. These factors inhibit the use of clast fabric analyses in many successions, including (but not limited to) the Blaini Formation in North India, the Tambien Group in NE Africa (Beyth *et al.*, 2003), the Toby and Edwardsburg Formations in Idaho, U.S.A. (Aalto, 1981; Lund *et al.*, 2003) and parts of the Port Askaig Formation in the U.K. This technique has been applied to the little-deformed Petrovbreen diamictites in Svalbard, East Greenland and those of the Jbéliat Formation in Mauritania where clast fabrics are similar to waterlain and lodgement tills (Deynoux, 1985; Harland *et al.*, 1993).

Given complications in clast fabric analyses, other factors need to be taken into account. Association with other lithofacies, particularly with regard to their structural deformation features, is important. For example, tills deposited as a result of lodgement or meltout often overlie deformed sediments, as large shear stresses can be generated by the overriding ice mass (Boulton, 1996). Conversely, deformation concentrated *within* subglacial till may act as a buffer, reducing the intensity of substrate deformation. Layered or stratified deformation tills may develop (as described from Breiðamerkurjökull in Iceland; Boulton, 1979; Boulton & Hindmarsh, 1987; Benn & Evans, 1996), which overlie non-deformed soft-sediment. The character of these subglacial deposits reflects variations in incremental strain (Boulton, 1996), and is inherently related to subglacial porewater pressure (e.g. Hiemstra & van der Meer, 1997). The gross-scale architecture of basal till sheets, particularly thickness and spatial distribution, is also considered to be closely linked to subglacial drainage conditions, and is partly dependent on the character of pre-existing substrate (e.g. Kjaer *et al.*, 2003). However, it is likely that mechanisms such as deformation and melt-out are part of a continuum of basal processes that vary over spatial and temporal scales. Features traditionally thought to be diagnostic of deformation at the bed, such as clast pavements and high porosity, are also thought to develop during passive melt-out (e.g. Mickelson *et al.*, 1992; Ronnert & Mickelson, 1992), although examples of pavements with planed-off tops are unlikely to develop by this process. Discrimination between deformation and melt-out till is considerable importance, since they imply different subglacial conditions at the time of sedimentation and the resultant dynamics of the ice mass in question (Benn, 1995).

Gross-scale stratigraphic architecture, associated lithofacies or subglacial erosional features such as striated pavements, meltwater channels (including Nye channels and p-forms) and glacial lineations including flutes, drumlins and roches moutonnées all provide additional information on the likely depositional setting of diamictite facies. For example, striated pavements are known beneath numerous successions in Australia (e.g. Egan, Landrigan and Moonlight Valley tillites; Coats & Preiss, 1980), Greenland (beneath the Storeelv Formation; Hambrey & Spencer, 1987), Mauritania (Jbéliat Formation; Deynoux & Trompette, 1981), Norway (Smalfjord Formation; Arnaud & Eyles, 2002a), Brazil (Macaubas Megasequence; Isotta *et al.*, 1969) and India (Blaini Formation; this study) where they provide solid evidence for grounded ice. Roches moutonnées and other whaleback forms are also known from the Jbéliat (Deynoux & Trompette, 1981) and Mineral Fork Formations (Ojakangas & Matsch, 1980), and may indicate relatively thin ice, since subglacial quarrying tends to be enhanced by cavities at the bed (Benn & Evans, 1998).

Glacitectonic structures

Much recent research on modern and Pleistocene glacigenic sediments has highlighted the importance of using soft sediment (glacitectonic) or thermal contraction deformation structures to provide additional information for determining sediment transport mode and deposition (Fig. 9). These studies have improved our understanding of processes of moraine formation (Bennett *et al.*, 1996a, b, 1998; Hambrey *et al.*, 1997), sediment stacking patterns in proglacial environments (Hambrey & Huddart, 1995; Hart & Boulton, 1991) and palaeoenvironmental interpretations of diamicton and diamictite lithofacies (e.g. Menzies & Maltman, 1992; Rijsdijk *et al.*, 1999, 2001; Maltman *et al.*, 2000; Menzies, 2000; van der Wateren *et al.*, 2000; Khatwa & Tulaczyk, 2001; Lachniet *et al.*, 2001; van der Meer *et al.*, 2003). Such structures are only occasionally recognized or utilized for palaeoenvironmental reconstruction in older geological terrains (e.g. Le Heron *et al.*, 2005), where they are often overprinted by diagenetic, metamorphic or regional tectonic events. Those working on microstructures in diamicton lithofacies have been primarily concerned with the identification of features which act as clues towards sediment genesis, and the ability to differentiate deposits resulting from primary subglacial deposition, re-distribution of sediment by subaerial debris flows or accumulation of periglacial slope deposits (e.g. Harris, 1998; Lachniet *et al.*, 2001). However, few diagnostic criteria can be presented since terrestrial debris flow deposits commonly display similar microstructural features to subglacially deformed till (Khatwa & Tulaczyk, 2001). The presence of fractured grains (observed in thin-sections) is considered by some as evidence of glacitectonism (Hiemstra & van der Meer, 1997), although terrestrially deposited tills can be reworked by paraglacial slope processes with little or no modification of gravel clast shapes, imbrication, texture, consolidation or granulometry (Curry & Ballantyne, 1999). Thus structurally similar deposits can form as a result of different depositional processes. Differentiating subglacial deposits from other poorly sorted facies types is problematic, particularly with regard to mass flow deposits such as debris flows, or massive sediments containing 'outsized' gravel lonestones, such as glacimarine or glacilacustrine sediments. Overcompaction or stratification are not considered sufficiently critical for discounting a subglacial origin, and Kluiving *et al.*, (1999) advocate sorting and the presence of dropstones as key criteria. Dropstones are defined as outsized clasts in finely stratified or laminated sediment, which deform and truncate underlying laminae (Hambrey & Harland, 1981). Isolated clasts are probably the best

Code	Description
P	**Pure shear**
PDH	Horizontal dilation (psa vertical)
PDI	Inclined dilation (psa not vertical)
PCC	Crushed clasts
PMC	Matrix and clast re-alignment
PCF	Compressional fractures
S	**Simple shear**
SHZ	Shear zone comprising sheared (inclined, isoclinal) folds, boudins, tectonic laminae
SSP	Simple shear profiles
STW	Shear thrust wedges
SFD	Shear thrust fractures and dykes
SHY	Shear hydrofractures
SEC	Extensional clastic dykes
SPB	Sheared and plucked pre-glacial breccia
SPR	Sheared and plucked bedrock
C	**Compressional**
CNA	Nappes
CAS	Anticlinal and synclinal folding (longitudinal compression)
CFR	Compressional fractures
CDK	Compressional dykes
CHY	Compressional hydrofractures
V	**Vertical**
VDS	Descending clast stringers
VLO	Loadcasts
VDI	Diapirs
VFL	Flexures
VCO	Collapse structures
VEX	Extensional fractures
VPO	Pods, rafts and pseudonodules
VCS	Cone-shaped clast clusters
VSY	Synforms (no longitudinal compression)
VHF	High-angle unimodal fabrics
U	**Undeformed**
UHS	Horizontal bedding
ULA	Lamination (graded)
UCR	Cross bedding
UON	Onlaps and drapes
UGR	Gradational contacts

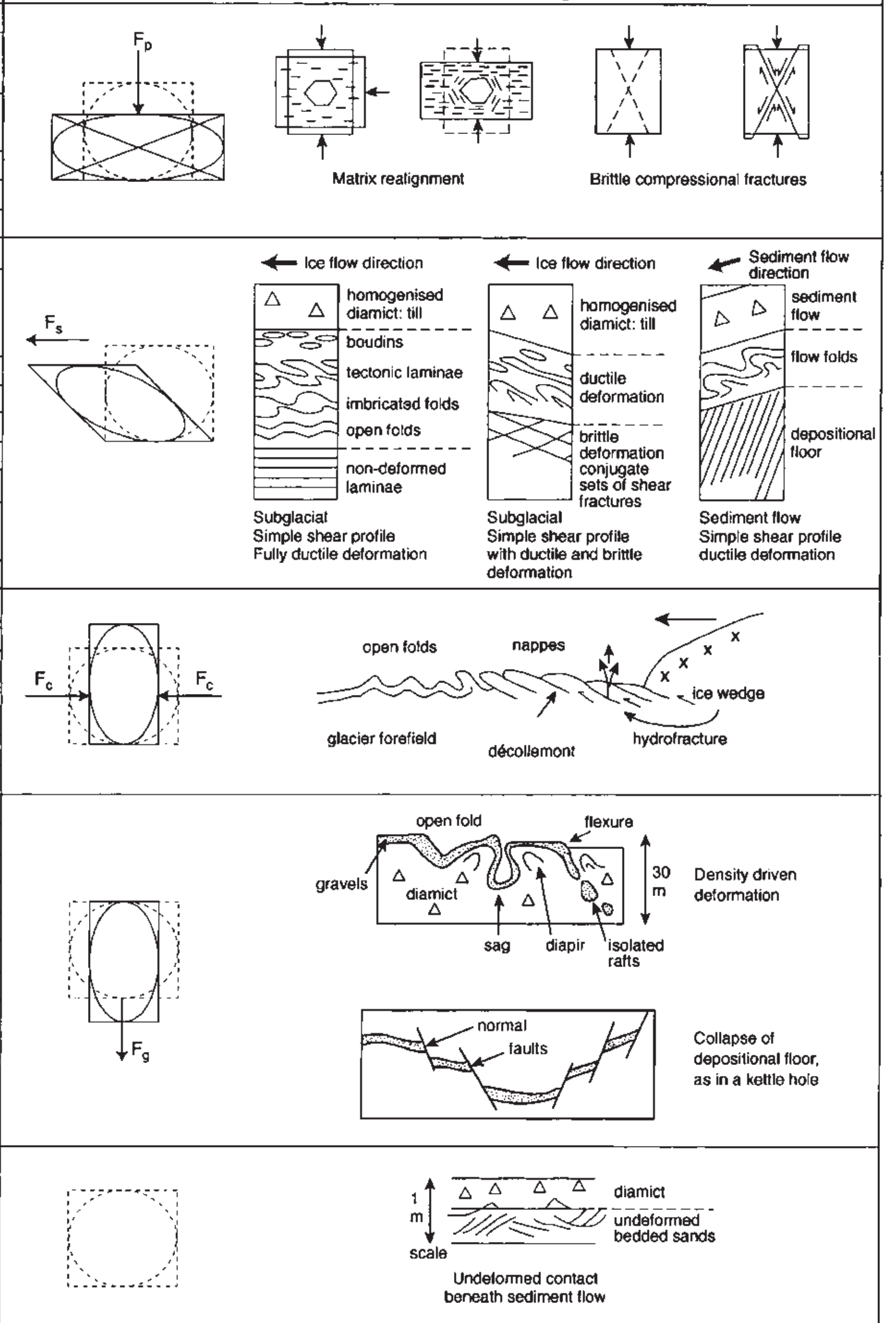

Deformation styles	Subglacial	Ice marginal	Proglacial (terrestrial)	Glaciolacustrine	Glaciomarine
Pure shear deformation	Very common	Common	Absent	Absent	Absent
Simple shear deformation	Dominant	Common (geometry relates to ice flow)	Rare–common (geometry relates to slope)	Absent	Absent
Compressional deformation	Rare	Dominant	Rare	Absent	Absent
Vertical deformation	Absent	Rare	Common	Very common	Rare
No deformation	Absent	Rare	Common	Dominant	Dominant
Iceberg dump and deformation	Absent	Absent	Absent	Common	Common

Fig. 9 Soft sediment deformation structures and codes for description of macroscopic glaciotectonic structures. Strain ellipses indicate deformation style under different stress regimes; forces Fp, Fs, Fc and Fg refer to pure shear, simple shear, compressional and gravitational, respectively. From McCarroll and Rijsdijk (2003). Copyright (2003) John Wiley & Sons, Limited. Reproduced with permission.

indicators, since debrites clasts can also deform and truncate underlying laminae. For Proterozoic sediments, it is worth noting that perennial sea and lake ice would also have been capable of entraining and rafting gravel-sized material (see Smith, 2000). Pebble-sized clasts are generally considered the best proxy for ice-rafted debris (Grobe, 1987; Andrews *et al.*, 1997, Smith & Andrews, 2000).

Other features that are important for palaeoenvironmental discrimination include macroscopic deformation structures, which are often associated with ice-marginal sediment assemblages. These include faults (normal, reverse, low-angle thrust faults and shear zones; Croot, 1988), folds (Hart & Boulton, 1991) and more chaotic structures resulting from subglacial deformation of poorly consolidated deformable substrate (Benn & Evans, 1996; Boulton, 1996), drumlinisation (Hart, 1995a, b), density inversion in saturated depositional sequences (e.g. Rijsdijk, 2001) and injection of clastic dykes (Le Heron & Etienne, 2005). McCarroll and Rijsdijk (2003) have provided a detailed account of macroscopic glacitectonic structures and their relative dominance in different glacially influenced environments (Fig. 9). These features complement glaciclastic debris such as dropstones, striated clasts and till pellets highlighted by Eyles and Januszczak (2004) as key criteria for identifying glacial influences on sedimentation in Neoproterozoic successions, and may provide a means to distinguish primary subglacial facies from sediment redistributed by subaqueous debris flow processes.

THICKNESSES OF GLACIALLY INFLUENCED MARINE SUCCESSIONS

Eyles and Januszczak (2004) argued that less than 100 m of stratigraphic section is deposited over a typical 'glacial cycle,' emphasizing the much thicker preserved successions of Neoproterozoic glacially influenced strata. While this statement may be true for terrestrial successions, or those deposited over short-term glacial/interglacial cycles, sediment yields in basins for glacial epochs spanning tens of millions of years far exceed this.

With the exception of DSDP/ODP (Deep Sea Drilling Programme/Ocean Drilling Programme), CIROS (Cenozoic Investigations of the Ross Sea) and CRP (Cape Roberts Project) recovery, much of what we know about glacimarine sedimentation is limited to short gravity core and geophysical investigations. Nonetheless, AMS (Accelerated Mass Spectrometry) ^{14}C dates provide important constraints on Pleistocene and Holocene sedimentation rates in glacially influenced basins. Predictably, sediment accumulation rates vary both spatially and temporally. For example, sedimentation rates across the North Atlantic region over the past 3 Myrs varied from 0.02 to 0.1 m ka^{-1}, and 0.12 m ka^{-1} on the Norwegian continental margin (Heinrich *et al.*, 2002 and references therein). Similar figures have been presented for shallow, distal areas of the Barents Sea (0.03 m ka^{-1}; Elverhøi *et al.*, 1989). Spatial and temporal variability is exhibited by Quaternary sedimentation rates for the Reykjanes Ridge between Heinrich events 1 and 2 (0.09 to 0.15 m ka^{-1}) and events 3 and 4 (0.12 to 0.22 m ka^{-1}; Moros *et al.*, 2002) and from Pleistocene and Holocene data on Kejser Franz Joseph Fjord (Greenland) and the adjacent continental margin (Evans *et al.*, 2002). Here Evans *et al.*, (2002) reported sedimentation rates of 0.3 m ka^{-1} on the upper continental slope and 0.16 m ka^{-1} on the mid-lower slope during the glacial maxima, with deglacial fluxes in the order of 0.51–0.79 m ka^{-1} (mid-lower slope), and 1.11 m ka^{-1} (in the fjord and inner slope). High sedimentation rates are also known from other fjords in Greenland including Nansen fjord where proximal sedimentation rates are calculated at 1.8 m ka^{-1} and 1.3 m kyr^{-1} in distal areas, and accumulation rates of 0.1 to 0.3 m kyr^{-1} in Scoresby Sund (Dowdeswell *et al.*, 2000). However, these examples are relatively low by comparison with Kongsfjorden in Svalbard, where present-day annual sedimentation rates are ~70 mm yr^{-1} (Elverhøi *et al.*, 1998).

Based on the above examples, if we assume a modest average sedimentation rate of 0.05 m/kyr over a 30 million year period (the upper predicted limit for the duration of a Snowball Earth event; Hoffman *et al.*, 1998a), it is possible to generate ~1.5 km of non-compacted stratigraphy. Given the higher sedimentation rates recorded in ice-proximal regions, and the vast volumes of sediment deposited in grounding zone wedges (*cf*. Shipp *et al.*, 2002), considerably thicker sequences may be preserved in glacially influenced marine basins, particularly those associated with temperate or polythermal ice masses (see Elverhøi *et al.*, 1998). However, it should be noted that in the long-term, the thickness of sedimentary successions is ultimately controlled by tectonically generated accommodation space.

Glacial and non-glacially influenced strata deposited over the past 800,000 years on the south-western part of the Barents Sea Shelf are known to approach 150 m in thickness (Rafaelsen *et al.*, 2002), Miocene to Quaternary strata in the Polar North Atlantic exceed 1 km in thickness (Thiede *et al.*, 1998), Miocene and Pliocene deposits of the Pagodroma Group in Antarctica are ~300 m thick (Hambrey & McKelvey, 2000) and Miocene to Pleistocene deposits of the Yakataga Formation along the southern continental margin of Alaska are ~7 km thick (Zellers & Lagoe, 1992). In the lower part, the Yakataga Formation consists primarily of debrites and turbidites, passing up into glacimarine diamictites, sandstones and mudstones (Eyles & Lagoe, 1990; Zellers & Lagoe, 1992), and in this respect bears similarity to many Neoproterozoic glacially influenced facies associations. For example, 1.5 km of glacially influenced Eocene-Pleistocene strata including mudstones, sandstones, diamictites and conglomerates have been proven in core from the Victoria Land basin in the East Antarctic rift system (Taviani & Beu, 2003; Figs 10, 11b). Cyclical controls on basin sedimentation are

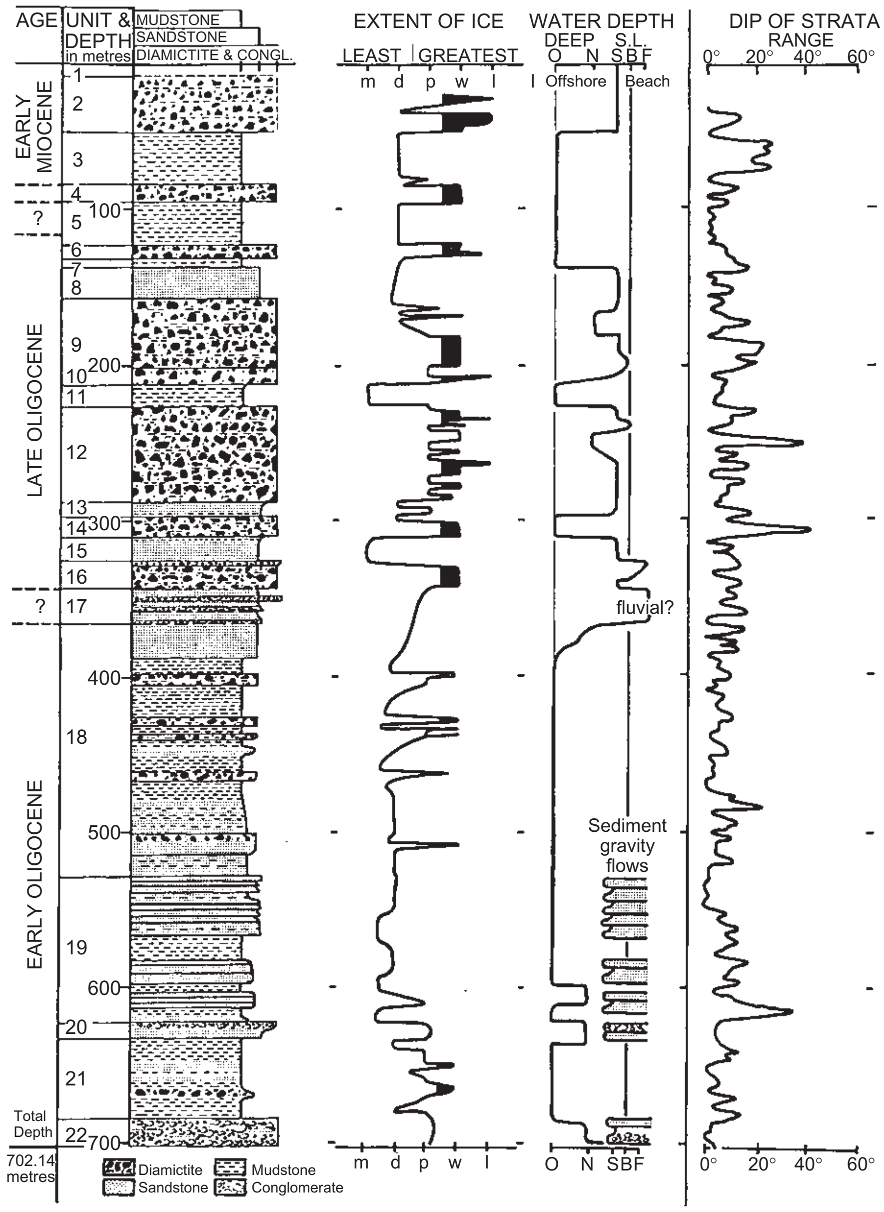

Fig. 10 Lithostratigraphy of the CIROS 1 drillcore, McMurdo Sound, Antarctica. Reproduced with permission from Hambrey *et al.* (1989b).

clear from IRD (ice rafted debris) proxy data and sedimentary facies, while spatial variability in thickness and stratigraphic preservation are evident from condensed sequences preserved over basement highs and extensive disconformities across the basin-fill (Hambrey *et al.*, 2002). These Cenozoic successions show that marine glacially influenced strata can achieve thicknesses comparable to the Neoproterozoic in similar depositional settings over similar timescales. The Victoria Land basin preserves both rift-related volcanics and huge volumes of glacially influenced strata, and in this respect is an excellent analogue for the Neoproterozoic Abu Mahara rift basin in North Oman which contains pillowed basalts of the Saqlah Formation, beneath the c. 1.5 km thick glacially influenced Fiq Member of the Ghadir Manqil Formation (Leather *et al.*, 2002; Allen *et al.*, 2004; Fig. 11a). Some characteristic features regarding the preservation potential of glaciomarine successions across different basin settings (craton, shelf, slope and deep basin environments) are dealt with in Brookfield (1994). For example, the most complete sequences tend to be found in actively subsiding basins in basin slope settings as illustrated in Figure 12.

SEDIMENTARY SEQUENCES

Glacimarine facies assemblages comprise a wide spectrum of stacking patterns, including progradational, aggradational and retrogradational packages (Powell & Cooper, 2002; Fig. 7). Distinct processes associated with advance, maxima and recessional glacial stages permit the construction of sequence stratigraphic models for glacially influenced marine basins which may be applied to Neoproterozoic basin-fill successions (Powell & Cooper, 2002). Although grounding line fan systems can be stratigraphically complex (Powell *et al.*, 2000), sediment accumulations on continental margins are remarkably consistent, with a stratigraphic architecture dominated by prograding clinoforms overlain by well-defined topsets (Eyles *et al.*, 2001). This seismic architecture has been recognised from glaciated continental margins around Antarctica (Fig. 13; Hambrey *et al.*, 1991; Eyles *et al.*, 2001; Escutia *et al.*, 2005), Greenland (Vanneste *et al.*, 1995; Solheim *et al.*, 1998), Norway (Vorren *et al.*, 1984; Saettem *et al.*, 1992), Canada (Hiscott & Aksu, 1994) and Alaska (Powell & Cooper, 2002). Analogous sediment-stacking patterns also characterize many Neoproterozoic successions, including the Chang'an-Nantuo sequence in south China (Jiang *et al.*, 2003), the Umberatana Group in the Adelaide Rift basin in Australia (Young & Gostin, 1991; McKirdy *et al.*, 2001), parts of the Windermere Supergroup in Canada (Eisbacher, 1985) and the Smalfjord Formation in Norway (Fig. 14; Arnaud & Eyles 2002a; but see also Edwards and Føyn, 1981). In the Antarctica Peninsular, upper Miocene to Quaternary strata are dominated by turbidites, diamictites interbedded with lonestone-bearing muds and subglacially cannibalized marine sediments (Eyles *et al.*, 2001). This lithofacies association is characteristic of many Neoproterozoic successions, particularly those where sediment gravity flows comprise a significant component (e.g. Fiq Formation, Oman, Allen *et al.*, 2004; Smalfjord Formation, Arnaud & Eyles, 2002a; Port Askaig Formation, Arnaud & Eyles, 2002b; Mineral Fork Formation, Young, 2002; Table 1).

DURATION AND CYCLICITY OF GLACIAL EPOCHS

It is widely accepted that Cenozoic glacial-interglacial climatic transitions were driven largely as a result of orbital forcing (Milankovitch cycles), although several other factors are known to be important, including changes in atmospheric levels of radiative gases, creation of topography resulting from rift flank uplift or continental collision and changes in oceanic circulation (e.g. Broecker *et al.*, 1988; Haug *et al.*, 2001; Hiscott *et al.*, 2001; Smith & Pickering, 2003; Piotrowski *et al.*, 2005). Yet, the exact nature of the relationship between insolation, ice volume, carbon cycling and thermohaline circulation remains to be firmly established, particularly since some millennial scale climatic oscillations may have been triggered by changes in oceanic circulation (Piotrowski *et al.*, 2005), glaciation may have been initiated by global warming (Kukla & Gavin, 2005), and significant ice volume may actually be required to amplify weak insolation in order for deglaciation to occur (Parrenin & Paillard, 2003). On a simple level, we know that these short-term glacial/interglacial transitions are superimposed on higher order cycles

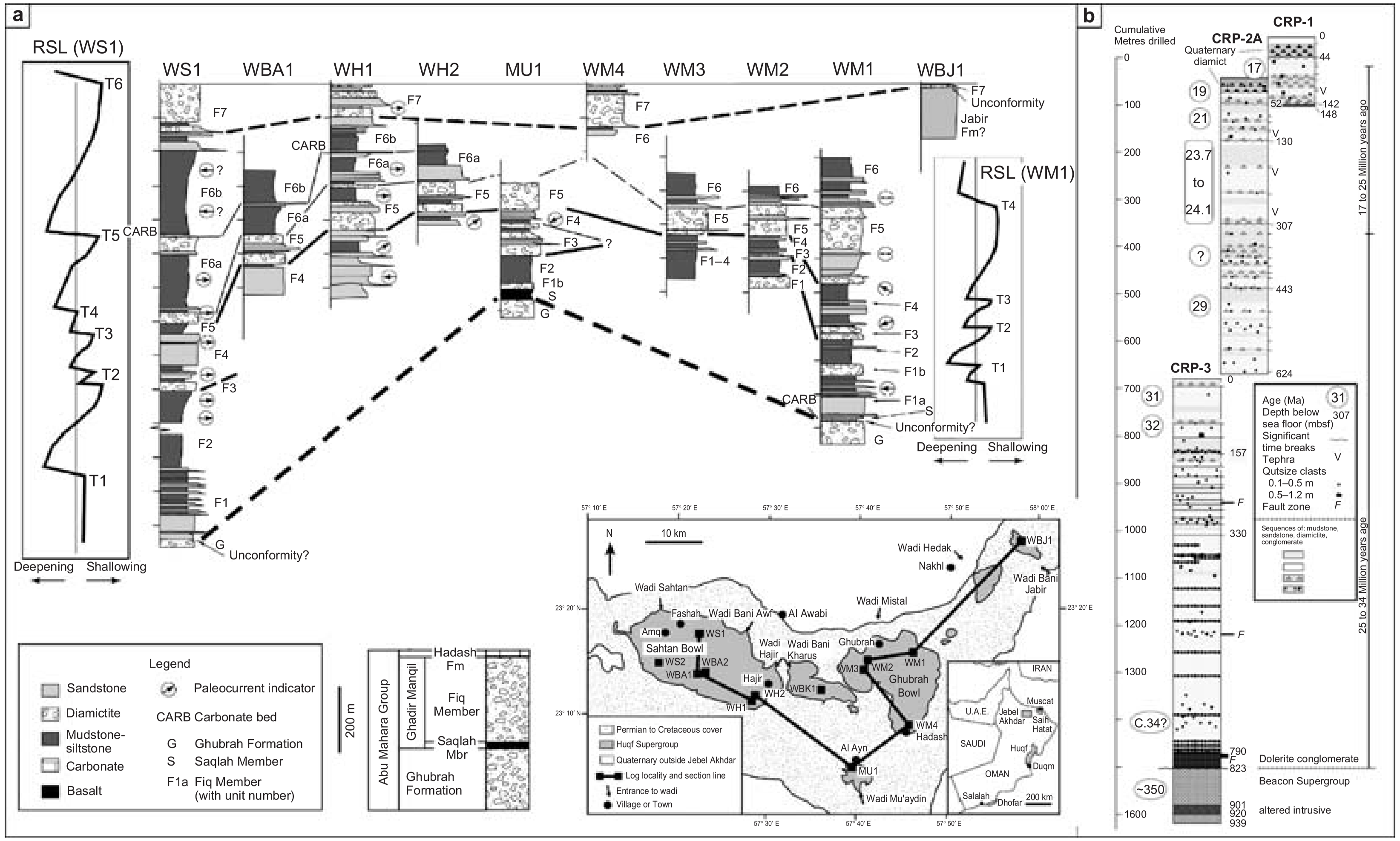

Fig. 11 Glacially influenced rift basin-fill successions (a) the Neoproterozoic Fiq Member of the Ghadir Manqil Formation, Jebel Akhdar, Sultanate of Oman. Reproduced from Leather *et al.* (2002) with permission of the Geological Society of America; (b) Cenozoic CRP (Cape Roberts Project) core stratigraphy for the Victoria Land Basin, Antarctica. Reprinted from Taviani and Beu (2003) with permission from Elsevier.

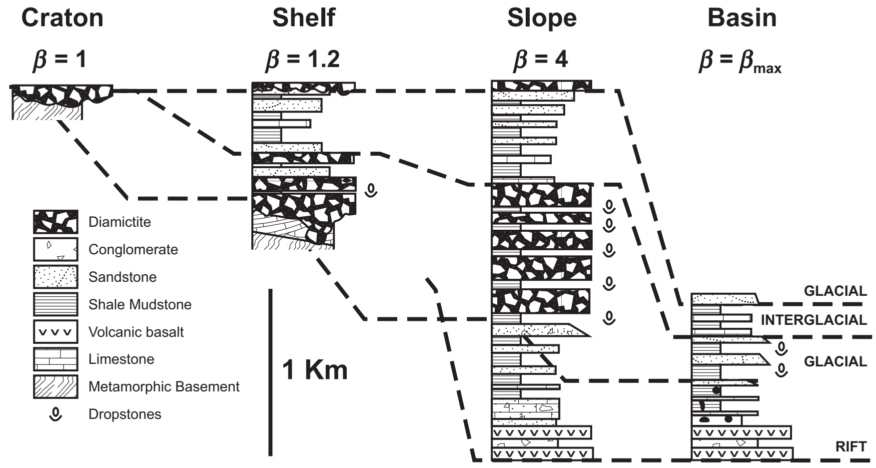

Fig. 12 Simplified facies models for glacial deposits across craton, shelf, slope and deep basin environments. Re-drawn from Brookfield (1994). Reproduced with permission from Elsevier.

of glaciation, represented in the Cenozoic by the onset of southern hemisphere glaciation at least as far back as the latest Eocene (Hambrey *et al.*, 2002; Taviani & Beu, 2003), in high latitude settings during the Miocene and Pliocene, and mid-latitudes during the Quaternary (Ehlers & Gibbard, 2003). It is worth noting the recognition of orbital cycles in glacimarine sediments around the Oligocene-Miocene boundary (Naish *et al.*, 2001). Climate models suggest that ice sheets were also sensitive to orbital changes during the Late Ordovician glaciation of Gondwana (Poussart *et al.*, 1999), but longer term glacial cycles (5–7 Myr) identified from Permo-Carboniferous glacial deposits in the Karoo Basin do not coincide with known orbital cycles, and Scheffler *et al.* (2003) suggested that changes in global temperature gradients or atmospheric-oceanic circulation were important factors.

In contrast to the Phanerozoic glacial record, which is relatively well constrained by radiometric and biostratigraphic markers, the timing of Neoproterozoic glaciations remains poorly understood. Independent attempts to distinguish the number of Neoproterozoic glaciations have involved lithostratigraphic correlation (Zhenjia & Jianxin, 1985), calibration of carbon and strontium isotope curves (Kaufman *et al.*, 1997; Halverson, 2005) and cladistic analysis (Kennedy *et al.*, 1998), with estimations ranging between 2, 3, 4 or possibly 5 glacial episodes. Over the past decade, and particularly in the last five years, a number of new radiometric ages have been published that provide firmer controls on the timing and duration of Neoproterozoic glacial epochs. New U-Pb and Re-Os ages from sections in Africa, the United States and Australia challenge the conventional Sturtian-Marinoan subdivision typically applied to Neoproterozoic glacial successions; however, undisputed evidence for glacial influences on sedimentation is yet to be demonstrated for some of these successions (Tables 1, 4). At the present time, the best constrained diamictite-bearing successions include the Gaskiers Formation (~580 Ma; Bowring *et al.*, 2003), the Squantum Tillite (570–589 Ma; Thompson & Bowring, 2000; Thompson *et al.*, 2000), the Nantuo Formation (635–667 Ma; Condon *et al.*, 2005), the Scout Mountain Member (662–714 Ma; Fanning & Link 2004), the Kaigas Formation (735–777 Ma; Frimmel *et al.*, 1996, 2002) and the Grand Conglomerat of the Kundelungu Basin (730–770 Ma; Key *et al.*, 2001). Syn-depositional ages further constrain sedimentation between 730–735 Ma (Key *et al.*, 2001), 739–713 Ma (Brasier *et al.*, 2000), 702–705 Ma (Tollo & Hutson, 1996), 678–692 Ma (Lund *et al.*, 2003) and 634.3–636.7 Ma (Hoffman *et al.*, 2004). Some details of the sedimentology of these sections can be found in Table 1. Table 4 provides some published radiometric age constraints for different Neoproterozoic diamictite-bearing successions, variably interpreted as glacial in origin. Many of the ages should be approached with caution, particularly where there are conflicts dependent on different dissolution techniques (e.g. the Olympic Formation is constrained by competing ^{187}Re-^{187}Os maximum ages of 592 ± 14 Ma; Schaefer & Burgess (2003) and 658 ± 5.5 Ma; Kendall & Creaser, 2004) or the full details of the isotopic data remain to be published.

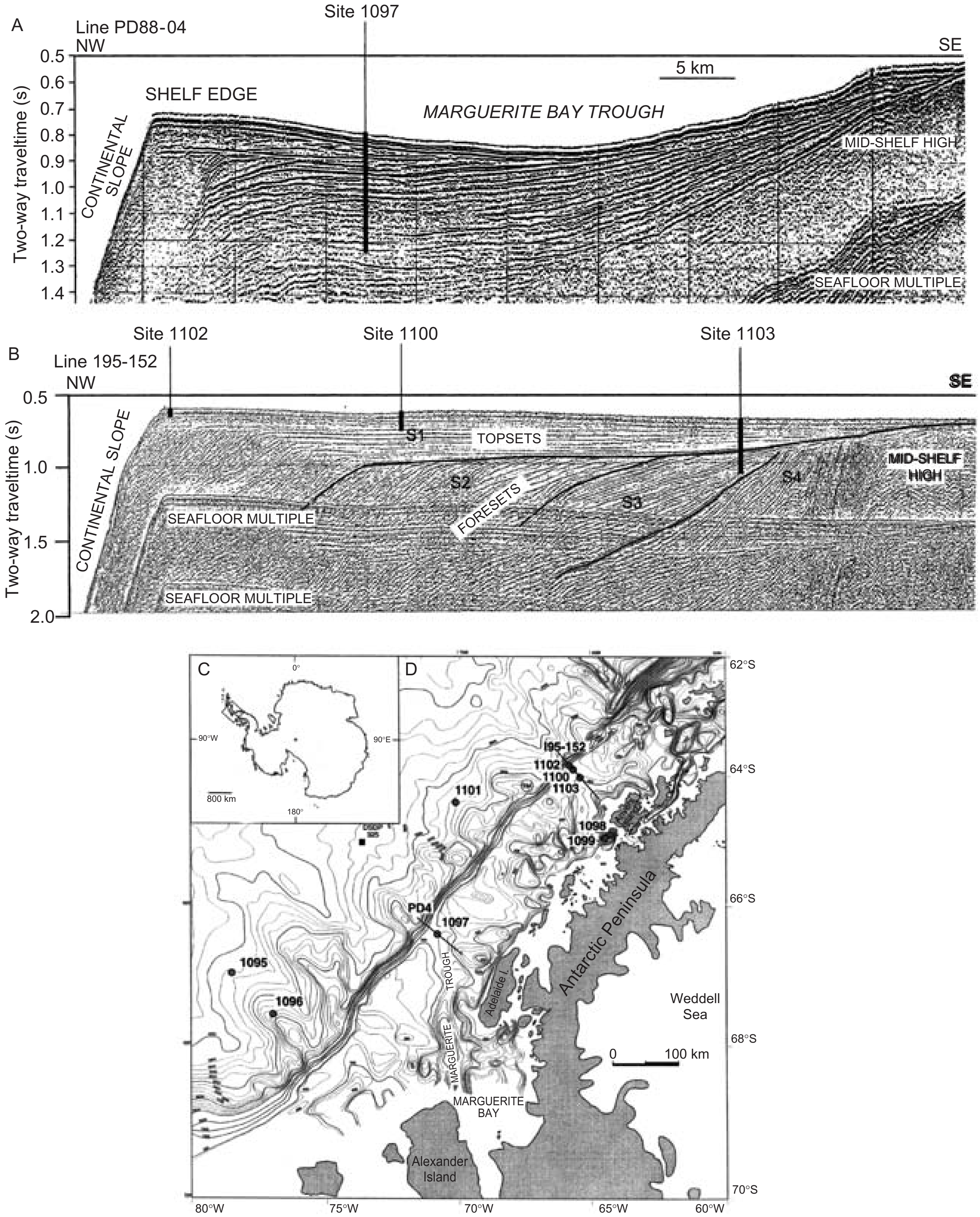

Fig. 13 Acoustic stratigraphy of glacially influenced marine deposits on the Antarctic peninsula; (A) ODP leg 178 site 1097; (B) ODP leg 178 site 1103; (C) location of drill sites. (A) and (B) after Bart and Anderson (1995) and Barker *et al.* (1998). Reprinted from Eyles (2002) with permission from Elsevier.

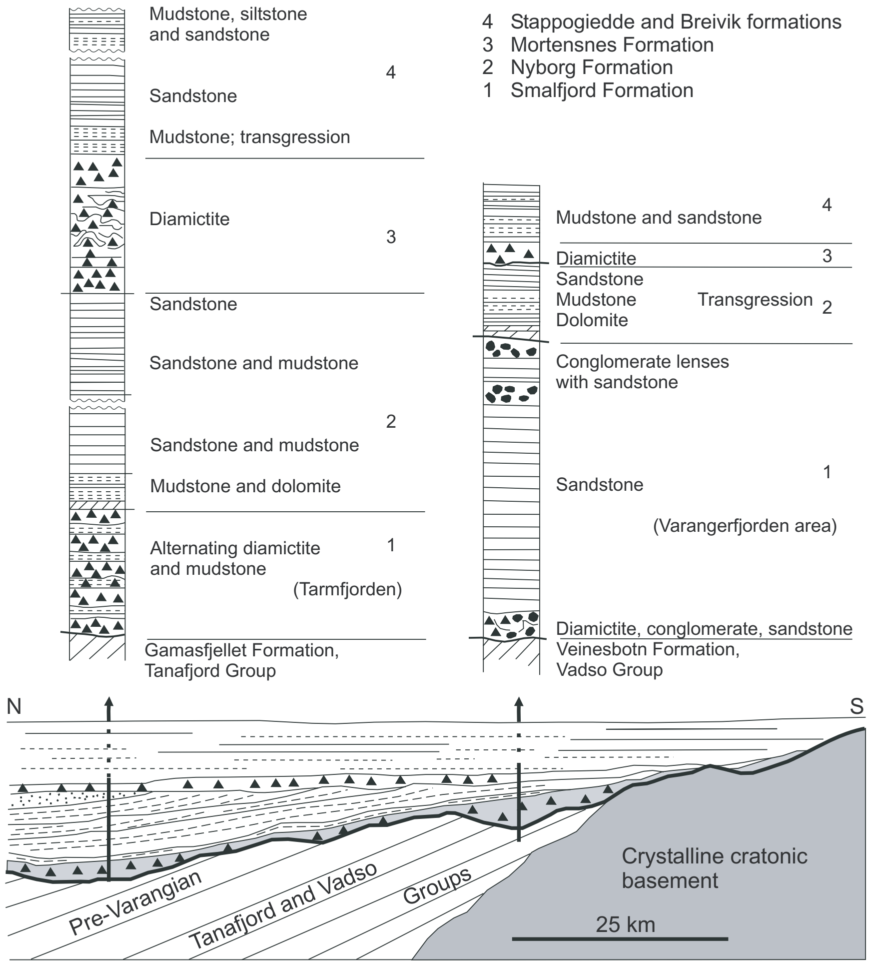

Fig. 14 Stratigraphy and geometry of the Smalfjord Formation in east Finnmark. Redrawn after Arnaud and Eyles (2002a) modification of Banks *et al.* (1971) and Nystuen (1985). Copyright (2002) Blackwell Publishing, reproduced with permission.

Estimations of glacial epoch durations have been derived from palaeomagnetic reversal studies (Sohl *et al.*, 1999), thermal subsidence modeling (Hoffman *et al.*, 1998a) and accumulation rates of inter-planetary dust particles (Bodiselitsch *et al.*, 2005), all of which indicate long-lived glacial activity. While many successions lie within the predicted range of Snowball Earth timescales, none are unusual in their longevity. It is accepted, for example, that the Permo-Carboniferous glacial epoch lasted ~90 Myrs from the Tournaisian (Early Carboniferous) until the Roadian (Mid-Permian; Crowell, 1978), and the Pleistocene (2.6 Ma; Jansen & Sjøholm, 1991; Larsen *et al.*, 1994; Ehlers & Gibbard, 2003) is merely the latest expression of Cenozoic glaciation initiated at least as far back as the late-Eocene (~35 Ma) in Antarctica (e.g. Hambrey *et al.*, 2002; Escutia *et al.*, 2005), and the Miocene in Alaska, the Polar North Atlantic, southern South America and New Zealand (Thiede *et al.*, 1998; Ehlers & Gibbard, 2003). At the present time, geochronological constraints are too poor to constrain any shorter-term cyclicity that may be represented in Precambrian successions. However, depositional cyclicity may be used to infer palaeoclimatic conditions. This approach has been adopted by Leather (2000), Leather *et al.* (2002) and Allen *et al.* (2004), for the Fiq Member of the Ghadir Manqil Formation in North Oman. Seven gross depositional cycles are recognised which are interpreted to reflect glacial-interglacial transitions (Allen *et al.*, 2004). These cycles are also characterized by variations in CIA (Chemical Index of Alteration) values, which are thought to be indicative of climatic changes from cold/arid to warm/wet conditions (Rieu *et al.*, unpublished data). CIA may thus be used as a proxy tool for evaluating Neoproterozoic

Table 19.4 Radiometric age constraints on Neoproterozoic diamictite-bearing successions. We consider the U-Pb zircon ages as most reliable since any open-system behaviour may be evaluated by comparison of the ^{238}U-^{206}Pb and ^{235}U-^{207}Pb parent-daughter isotope systems (see Bowring & Schmitz, 2003). For information on individual radiometric ages and error bars we advise the reader to refer to the original source references

Stratigraphic Unit	Radiometric age (Ma)	Isotope system	Material dated	Significance of date	Source reference
AUSTRALIA					
Wilyerpa Fm.	802 ± 10	SHRIMP ^{238}U-^{206}Pb	Rook Tuff in the Callana Gp.	Max. age for the Elatina Fm.	Fanning *et al.* (1986)
(including	~800	^{147}Sm-^{143}Nd	Mafic dykes intruding the Pandurra Fm. Stuart	Max. age for the Elatina Fm.	Zhao *et al.* (1994)
underlying	777 ± 7	SHRIMP ^{238}U-^{206}Pb	Shelf	Max. age for the Elatina Fm.	Walter *et al.* (2000)
Appila & Pualco	750 ± 53	^{87}Rb-^{87}Sr	Boucat volcanics/Rhynie sandstone rhyolite;	Max. age for the Elatina Fm?	Preiss (1987)
Tillites), Elatina	690 ± 21	^{87}Rb-^{87}Sr	zircon	Max. age for the Elatina Fm?	Jenkins & Cooper (1998)
Fm. & Pepuarta	657 ± 17	^{238}U-^{206}Pb	Tapley Hill Fm.	Max. age for Elatina Fm.	Ireland *et al.* (1998)
Tillite.	601 ± 68	^{87}Rb-^{87}Sr	Enamora Shale and Trezona Fm.	Min. age for Elatina Fm?	Preiss (1987)
	526 ± 4	SHRIMP ^{238}U-^{206}Pb	Marino Arkose underlying Elatina; detrital zircon	Min. age for Elatina Fm.	Cooper *et al.* (1992)
			Brachina Fm. overlying the Nuccaleena Fm. cap dolomite		
			Thin tuff in Early Cambrian Heatherdale Shale; zircon		
Areyonga and Olympic Fm.	897 ± 9	^{87}Rb-^{87}Sr	Stuart Dyke Swarm	Max. age for the Areyonga Fm.	Marjoribanks & Black (1974) Black *et al.* (1980)
	592 ± 14	^{187}Re-^{187}Os	Black shale underlying Olympic Fm., overlies Areyonga Fm.	Min. age for Areyonga Fm.; Max. age for Olympic Fm.	Schaefer & Burgess (2003)
Sturt Diamictite	777 ± 7	^{238}U-^{206}Pb zircon	Boucat volcanics	Possible max. age for Sturt?	Walter *et al.* (2000)
	724 ± 40	^{87}Rb-^{87}Sr	Postglacial Yudnapinna beds	Min. age for the Sturt tillite	Preiss (1987) Drexel *et al.* (1993)
Cottons Breccia	579 ± 16	^{147}Sm-^{143}Nd	Bold Head and Shower Droplet Volcanics overlying the Yarra Creek Shale and Cottons Breccia	Min. age for Cottons Breccia	Calver *et al.* (2004)
	574.7 ± 3	SHRIMP ^{238}U-^{206}Pb zircon	Intermediate sills (Grimes Intrusive Suite) intruded into Cottons Breccia		Meffre *et al.* (2004)
Moonlight Valley and Fargoo Tillites	672 ± 70	^{87}Rb-^{87}Sr	Ranford Fm. shales	Max. age for Moonlight valley and Fargoo tillites	Coats & Preiss (1980)

Croles Hill Diamictite	582.1 ± 4.1	SHRIMP ^{238}U-^{206}Pb zircon	Rhyodacite flow unit underlying partly glacigenic Croles Hill Diamictite	Croles Hill Diamictite interpreted as stratigraphically equivalent to Cottons Breccia	Calver *et al.* (2004)
AFRICA					
Chuos & Ghaub Fms.	758.5 ± 3.5	^{238}U-^{206}Pb zircon	Ombombo Sub-group	Max. ages for Chuos and Ghaub	Hoffmann & Prave (1996) Hoffman *et al.* (1998)
Namibia	756 ± 2	^{238}U-^{206}Pb zircon	Ombombo Sub-group	Max. ages for Chuos and Ghaub	Buchwaldt *et al.* (1999) Hoffman *et al.* (1998)
	746 ± 2	^{238}U-^{206}Pb zircon	Ash in underlying Naawpoort Fm. (Nosib Gp.)	Max. ages for Chuos and Ghaub	Buchwaldt *et al.* (1999) Hoffman *et al.* (1998)
	635.5 ± 1.2	^{238}U-^{206}Pb zircon	Ash in uppermost Ghaub Fm.	Syn-depositional age for Ghaub; Max. age for Chuos	Hoffmann *et al.* (2004)
	538 ± 12	^{40}K-^{40}Ar	Mulden Gp. fines	Min. age constraint for the Ghaub	Clauer & Kröner (1979)
	537 ± 7	^{87}Rb-^{87}Sr	Mulden Gp. fines	Min. age constraint for the Ghaub	Clauer & Kröner (1979)
	534 ± 7	^{238}U-^{206}Pb zircon	Syn-tectonic syenogranites (Damara orogeny)	Min. age constraint for the Ghaub	Briqueu *et al.* (1980)
	508 ± 2	^{238}U-^{206}Pb monazite	Post-tectonic sheeted leucogranites	Min. age constraint for the Ghaub	Briqueu *et al.* (1980)
Blaubeker Fm.	545 ± 1	^{238}U-^{206}Pb zircon	Overlying Spitskopf Fm.	Min. age constraint for the Blaubeker	Grotzinger *et al.* (1995)
Namibia	543.3 ± 1	^{238}U-^{206}Pb zircon	Overlying Spitskopf Fm.	Min. age constraint for the Blaubeker	Grotzinger *et al.* (1995)
	539.4 ± 1	^{238}U-^{206}Pb zircon	Overlying Nomtsas Fm.	Min. age constraint for the Blaubeker	Grotzinger *et al.* (1995)
Kaigas & Numees Fm. **Namibia**	781 + 34/−31	^{87}Rb-^{87}Sr	Lekkersing granite basement	Max. age for Kaigas and Numees	Allsopp *et al.* (1979) recalculated in: Frimmel & Frank (1998)
	771 ± 6	^{238}U-^{206}Pb zircon	Granite of Richtersveld Igneous Complex	Max. age for Kaigas and Numees	Frimmel *et al.* (2001)
	741 ± 6	^{207}Pb-^{206}Pb zircon	Rosh Pinah Rhyolite	Min. age for Kaigas; Max. age for Numees	Frimmel *et al.* (1996) Frimmel *et al.* (2002)
	717 ± 11	^{87}Rb-^{87}Sr	Gannakouriep Suite Mafic Dyke	Min. age for Kaigas; Max. age for Numees	Reid *et al.* (1991)
	542 ± 4	^{40}K-^{40}Ar	Metamorphism of the Gannakouriep mafic dyke	Min. age for Numees	Onstott *et al.* (1986)
	521 + 24/−20	^{238}U-^{206}Pb zircon	Post-tectonic alkaline intrusive Bremen complex	Min. age for Numees	Allsopp *et al.* (1979) recalculated in: Frimmel & Frank (1998)
Grand	765 ± 5	SHRIMP ^{238}U-^{206}Pb	Mwashia Gp. Lavas; zircon	Max. age of Grand Conglomerat	Key *et al.* (2001)
Conglomerat,	763 ± 6	SHRIMP ^{238}U-^{206}Pb	Mwashia Gp. Lavas; zircon	Max. age of Grand Conglomerat	Key *et al.* (2001)
Kundelungu Basin **Zambia**	735 ± 5	SHRIMP ^{238}U-^{206}Pb	Altered volcanic pods in contact with glacial strata; zircon	Min./syn-depositional age of Grand Conglomerat	Key *et al.* (2001)

Table 19.4 (*cont'd*)

Stratigraphic Unit	Radiometric age (Ma)	Isotope system	Material dated	Significance of date	Source reference
Jbéliat Fm. **Mauritania**	632 ± 13	^{87}Rb-^{87}Sr	Detrital smectite grains in Jbéliat Fm. diamictites	Max. age for Jbéliat Fm.	Clauer & Deynoux (1987)
	595 ± 43	^{87}Rb-^{87}Sr	Fine micas	Min. age for Jbéliat Fm.	Clauer (1976) Clauer *et al.* (1982)
	633.8 ± 0.5	^{40}Ar-^{39}Ar	Muscovite in Kara Nappe	Min. age constraint for Jbéliat Fm.	Attoh *et al.* (1997)
	608.1 ± 1.2	^{40}Ar-^{39}Ar	Muscovite in quartz schist of basal Atacora Nappe	Min. age constraint for Jbéliat Fm.	Attoh *et al.* (1997)
Matheos Fm. **Ethiopia**	854 ± 3	^{207}Pb-^{206}Pb zircon	Low-grade metavolcanics	Max. age based on a tentative lithostratigraphic correlation between the Tsaliet Gp. (underlying Tambien Gp.) and a sequence in neighbouring Eritrea.	Teklay (1997) Miller *et al.* (2003)
	~800	^{207}Pb-^{206}Pb zircon	Bizen Domain metavolcanics	Max. age based on correlation between Bizen	Teklay (1997)
	796	^{207}Pb-^{206}Pb zircon	Ghedem Domain paraschists and orthogneisses underlying the Bizen Domain metavolcanics	Domain metavolcanics in Eritrea and Tsaliet metavolcanics in N. Ethiopia.	Beyth *et al.* (2003) Teklay (1997) Beyth *et al.* (2003)
	720–800	^{147}Sm-^{143}Nd and ^{87}Rb-^{87}Sr	Units similar to the Tsaliet Gp in the west, intruded by syn-tectonic granodiorites	Max. age for Matheos Fm.	Tadesse *et al.* (2000)
	~630	^{207}Pb-^{206}Pb zircon	Granitoids in Lehazin, E. Eritrea	Min. age of Matheos	Teklay (1997) Beyth *et al.* (2003)
	613.4 ± 0.9	^{207}Pb-^{206}Pb age	Post-D1 tectonic deformation intrusions	Min. age of Matheos	Miller *et al.* (2003)
	606.0 ± 0.9	^{207}Pb-^{206}Pb age	Post-D1 tectonic deformation intrusions	Min. age of Matheos	Miller *et al.* (2003)
	545 ± 24	Th-U-total Pb on zircon	Post-tectonic granite intrusion	Min. age of Matheos	Tadesse *et al.* (1997) Beyth *et al.* (2003)
NORTH AMERICA					
Toby Fm. **Canada**	762–728	^{238}U-^{206}Pb zircon and ^{147}Sm-^{143}Nd	Granitic and volcanic rocks which unconformably underlie, or are intruded into the base of the succession	Max. age for the Windermere Supergroup	Ross *et al.* (1995) Ross & Villeneuve (1997)
	634 ± 57	^{187}Re-^{187}Os	Post-glacial chlorite-grade black shale of Upper Old Fort	Min. age for Toby Fm.	Kendall *et al.* (2004)
	607.8 ± 4.7	^{187}Re-^{187}Os	Point Fm.	Min. age for Toby Fm.	Kendall *et al.* (2004)
	569.6 ± 5.3	^{238}U-^{206}Pb zircon	Volcanics unconformably overlying Windermere Supergroup	Min. age for Toby Fm.	Colpron *et al.* (2002)

Sayunei, Shezal & Icebrook Fm. **Canada**	755 ± 18	^{238}U-^{206}Pb zircon	Leucogranite dropstone in Sayunei Formation	Max. age for Rapitan Gp.	Ross & Villeneuve (1997)
Gaskiers Fm. **Canada**	631 ± 2	^{238}U-^{206}Pb zircon	Volcanics of the Harbour Main Group	Max. age for Gaskiers	Krogh *et al.* (1988)
	622.6 + 2.3/–2.0	^{238}U-^{206}Pb zircon	Volcanics of the Harbour Main Group	Max. age for Gaskiers	Krogh *et al.* (1988)
	606 + 3.7/–2.9	^{238}U-^{206}Pb zircon	Volcanics of the Harbour Main Group	Max. age for Gaskiers	Krogh *et al.* (1988)
	604 + 4/–3	^{238}U-^{206}Pb zircon	Volcanics of the Harbour Main Group	Max. age for Gaskiers	Myrow & Kaufman (1999)
	580	^{238}U-^{206}Pb zircon	Ash beds lying below, within and above glacigenic deposits	Timing and duration of glaciation to <1 Ma	Bowring *et al.* (2003)
	565 ± 3	^{238}U-^{206}Pb zircon	Uppermost Conception Group	Min. age for Gaskiers	Dunning *pers. comm.* in Benus (1988)
Musgravetown Gp.	620 ± 1	^{238}U-^{206}Pb zircon	Underlying Love Cove Group volcanics	Max. age constraint on Musgravetown Gp.	Dec *et al.* (1992)
Canada	~610	^{238}U-^{206}Pb zircon	Thin ash bed in underlying Connecting Point Group	Max. age constraint on Musgravetown Gp.	O'Brien *et al.* (1992)
Roxbury Conglomerate;	610 ± 2.2	^{238}U-^{206}Pb zircon	Porphyritic granophyre within the diamictite	Max. age of Squantum tillite	Thompson *et al.* (2000a)
Squantum Tillite	606 ± 3.7	^{238}U-^{206}Pb zircon	Welded tuff clast within the diamictite	Max. age of Squantum tillite	Thompson *et al.* (2000a)
Mbr.	601 ± 3.7	^{238}U-^{206}Pb zircon	Crystal-poor tuff	Max. age of Squantum tillite	Thompson *et al.* (2000a)
Massachusetts	595 ± 2	^{238}U-^{206}Pb zircon	Welded tuff clast within the tillite	Max. age of Squantum tillite	Thompson & Bowring (2000)
U.S.A.	587 ± 2	^{207}Pb-^{206}Pb	Vesicular basaltic andesite	Max. age of Squantum tillite	Thompson *et al.* (2000b)
	570	^{238}U-^{206}Pb zircon	Ash bed in overlying Cambridge Argillite.	Min. age of Squantum tillite	Thompson & Bowring (2000)
Edwardsburg Fm. **Idaho, U.S.A.**	685 ± 7	SHRIMP ^{238}U-^{206}Pb	Volcanic rocks interbedded with glacigenic facies of 1st	Approximate age for timing of glaciation, dependant on the likely duration of volcanic activity	Lund *et al.* (2003)
	684 ± 4	SHRIMP ^{238}U-^{206}Pb	Windermere glaciation = Rapitan? Zircon		
Scout Mountain Member,	717 ± 4	SHRIMP ^{238}U-^{206}Pb	Porphyritic rhyolite clast; zircon	Max. age for Scout Mountain Mbr.	Fanning & Link (2004)
Pocatello Fm.	709 ± 5	SHRIMP ^{238}U-^{206}Pb	Epiclastic plagioclase-phyric tuff breccia immediately below	Max. age for Scout Mountain Mbr.	Fanning & Link (2004)
Idaho, U.S.A.	667 ± 5	SHRIMP ^{238}U-^{206}Pb	Scout Mountain Member; zircon simple igneous zircon population from reworked fallout tuff bed 20 m above uppermost diamictite and cap carbonate? and immediately below a second cap carbonate; zircon	Min. age for glacial Scout Mountain Mbr. (lithostratigraphically correlative to Edwardsburg Fm.)	Fanning & Link (2004)
	580 ± 7	^{40}Ar-^{39}Ar	Browns Hole Formation extrusive volcanics	Min. age for Pocatello Fm.	Christie-Blick & Levy (1989)
Mechum River Fm.	729	^{238}U-^{206}Pb zircon	Robertson River granitoid;	Max. age of Mechum River Fm.	Tollo & Aleinikoff (1992) Tollo & Hutson (1996)
Virginia, U.S.A	702–705	^{238}U-^{206}Pb zircon	Robertson River Igneous Suite; 2 Perialkaline units of the Battle Mountain volcanic centre	Syn-depositional age based on interpreted timing of rhyolite eruption of Mechum River	Bailey & Peters (1998)

Table 19.4 *(cont'd)*

Stratigraphic Unit	Radiometric age (Ma)	Isotope system	Material dated	Significance of date	Source reference
Konnarock Fm. (formerly Mount Rogers Fm.) **Virginia, U.S.A**	758 ± 12	^{238}U-^{206}Pb zircon	Mount Rogers volcanics	Max. age of the Konnarock Fm.	Aleinikoff *et al.* (1995)
SOUTH AMERICA					
Jequitai Fm. **Brazil**	900	^{238}U-^{206}Pb zircon	Detrital zircons in Jequitai Fm. diamictites	Max. age of Jequitai Fm.	Buchwaldt *et al.* (1999) Pedrosa-Soares *et al.* (2000) Pimentel & Fuck (1992)
	740 ± 22	^{207}Pb-^{206}Pb	'Cap' carbonates of the Bambuí Group	Min. age of Jequitai Fm.	Babinski & Kaufman (2003)
EUROPE					
Port Askaig Fm. Kinlochlaggan and	806	^{238}U-^{206}Pb monazite	Shear zone truncating the base of the Grampian Group	Max. age for Port Askaig Fm.	Noble *et al.* (1996)
Loch na Cille boulder beds	601 ± 4	^{238}U-^{206}Pb zircon	Tayvallich Volcanic Fm.	Max. age for Loch na Cille; Min. age for Port Askaig	Dempster *et al.* (2002)
Scotland, U.K.	595 ± 4	^{238}U-^{206}Pb zircon	Tayvallich Volcanic Fm.; submarine keratophyre	Min. age for Port Askaig	Halliday *et al.* (1989)
	590 ± 2	^{238}U-^{206}Pb zircon	Ben Vuiruch Granite	Min. age for Dalradian block (and thus glacial successions in Dalradian)	Dempster *et al.* (2002)
	470 ± 9	^{238}U-^{206}Pb zircon	Gabbros of Insch and Morven-Cabrach in Aberdeenshire	Min. age for Dalradian block (and thus glacial successions in Dalradian)	Dempster *et al.* (2002)
Smalfjord &	654 ± 7	^{87}Rb-^{87}Sr	Argillite of the Nyborg Fm.	Min. age for Smalfjord	Roberts *et al.* (1997)
Mortensnes Fm.,	630	^{87}Rb-^{87}Sr	Fine mica; shale	Age of Smalfjord glacial sequence	Gorokhov *et al.* (2001)
Moelv Tillite	560	^{87}Rb-^{87}Sr	Fine mica; shale	Age of 'Mortensnes' glacial sequence	Gorokhov *et al.* (2001)
Norway	807 ± 19	^{87}Rb-^{87}Sr	Underlying Klubbnasen Fm.	Max. age for Smalfjord	Sturt *et al.* (1975) Siedlecka & Roberts (1992)
	612 ± 18	^{87}Rb-^{87}Sr	Ekre Fm.	Min. age for Moelv tillite	Sokolov (1998)
Petrovbreen & Gropbreen Mbrs. **Svalbard**	950	^{238}U-^{206}Pb zircon	Detrital zircons in the Veteranen group in NE Svalbard and zircon in sub-Veteranen Gp. granites in Nordauslandet	Max. ages for Petrovbreen and Gropbreen mbrs.	Larianov *et al.* (1998)
	780	^{87}Rb-^{87}Sr	Middle Grusdievbreen Fm.	Max. ages for Petrovbreen and Gropbreen mbrs.	Jacobsen *pers. comm.* in Halverson *et al.* (2004)

ASIA					
Ghubrah & Fiq Fms. **N. Oman**	~825	^{238}U-^{206}Pb zircon	Halfayn Fm.	Max. age for Ghubrah and Fiq	Leather (2001)
	~800	^{238}U-^{206}Pb zircon	Crystalline basement in the El Jebal El Akdhar mountains, north Oman	Max. age for Ghubrah and Fiq	Leather (2001)
	~780	^{238}U-^{206}Pb zircon	Pan-African crystalline basement	Max. age for Ghubrah and Fiq	Platel *et al.* (1992) Kramers & Frei (1992)
	723 + 16/–10	^{238}U-^{206}Pb zircon	Tuffaceous ash near top of Ghubrah Formation	Syn-depositional age for uppermost Ghubrah	Brasier *et al.* (2000)
	544.5 ± 3.3	^{238}U-^{206}Pb zircon	Ignimbrites in the Fara Fm.	Min. age for underlying Nafun and Abu Mahara Gps.	Brasier *et al.* (2000)
	542 ± 0.6	^{238}U-^{206}Pb zircon	Ash in subsurface lower part of the Ara Gp.	Min. age for underlying Nafun and Abu Mahara Gps.	Amthor *et al.* (2003)
	542.6 ± 0.3	^{238}U-^{206}Pb zircon	Ash in subsurface lower part of the Ara Gp.	Min. age for underlying Nafun and Abu Mahara Gps.	Amthor *et al.* (2003)
Blaini Fm. **N. India**	525 ± 8	^{238}U-^{206}Pb zircon	Detrital zircons from basal Tal Group	Minimum age for Blaini Fm.	Myrow *et al.* (2003)
Chang'an, Tiesiao & Nantuo Fm.	819 ± 7	SHRIMP ^{238}U-^{206}Pb	Granite; zircon	Max. age for Chang'an, Tiesiao and Nantuo successions	Ma *et al.* (1984)
South China	809 ± 16	SHRIMP ^{238}U-^{206}Pb	Tuffaceous bed; zircon	Max. age for Chang'an, Tiesiao and Nantuo successions	Yin *et al.* (2003)
	761 ± 8	^{207}Pb-^{206}Pb	Gabbro intruding Sanmenjie Fm.	Max. age for Chang'an, Tiesiao and Nantuo successions	Ge *et al.* (2001)
	758 ± 23	SHRIMP ^{238}U-^{206}Pb	Dieshuihe Fm; zircon	Max. age for Chang'an, Tiesiao and Nantuo successions	Yin *et al.* (2003)
	748 ± 12	SHRIMP ^{238}U-^{206}Pb	Volcanic ash; zircon	Max. age for Chang'an, Tiesiao and Nantuo successions	Ma *et al.* (1984)
	663 ± 4	^{238}U-^{206}Pb zircon	Tuffaceous bed	Max. age for Nantuo Fm.; Min. age for Chang'an & Tiesiao Fms.	Zhou *et al.* (2004)
	635.4 ± 1.3	^{207}Pb-^{206}Pb	Volcanic ash	Min. age for Nantuo Fm.	Condon *et al.* (2005)
	635.23 ± 0.57	^{238}U-^{206}Pb zircon	Volcanic ash	Min. age for Nantuo Fm.	Condon *et al.* (2005)
	632.50 ± 0.48	^{238}U-^{206}Pb zircon	Volcanic ash	Min. age for Nantuo Fm.	Condon *et al.* (2005)
	632.4 ± 1.3	^{207}Pb-^{206}Pb	Volcanic ash	Min. age for Nantuo Fm.	Condon *et al.* (2005)
	599.3 ± 4.2	^{207}Pb-^{206}Pb	Doushantuo phosphorites	Min. age for Nantuo Fm.	Barfod *et al.* (2002)
	598 ± 26	^{207}Pb-^{206}Pb	Doushantuo phosphorites	Min. age for Nantuo Fm.	Chen *et al.* (2004)
	584 ± 26	^{176}Lu-^{177}Hf	Doushantuo phosphorites	Min. age for Nantuo Fm.	Barfod *et al.* (2002)
	576 ± 14	^{207}Pb-^{206}Pb	Doushantuo phosphorites	Min. age for Nantuo Fm.	Chen *et al.* (2004)
	551.07 ± 0.61	^{238}U-^{206}Pb zircon	Volcanic ash	Min. age for Nantuo Fm.	Condon *et al.* (2005)
	550.55 ± 0.75	^{207}Pb-^{206}Pb	Volcanic ash	Min. age for Nantuo Fm.	Condon *et al.* (2005)
	538.2 ± 1.5	SHRIMP ^{238}U-^{206}Pb	Tuff	Min. age for Nantuo Fm.	Jenkins *et al.* (2002)
Beiyixi, Altungal, Tereeken & Hangelchaok Fm. **North China**	755 ± 15	SHRIMP ^{238}U-^{206}Pb	Volcanics	Max. age for Beiyixi, Altungal, Tereeken & Hangelchaok glacial successions	Xu *et al.* (2005)

climate change (*cf*. Young, 2002), as it has for the Permo-Carboniferous glaciation of Gondwana (Scheffler *et al.*, 2003), although care is required in order to evaluate the effects of diagenesis on pre-burial geochemical composition, sorting effects and changes in sediment provenance over time.

NEOPROTEROZOIC PALAEOGLACIOLOGY

Relatively few detailed sedimentological studies have been undertaken on Neoproterozoic diamictite-bearing successions in the context of Snowball Earth theory, although a wealth of existing literature is available (e.g. Edwards, 1975; Hambrey & Harland, 1981 and references therein; Fairchild & Hambrey, 1984; Spencer, 1985; Hambrey & Spencer, 1987; Moncrieff, 1988; Eyles, 1990; Harland *et al.*, 1993; Arnaud & Eyles, 2002a, b; Allen *et al.*, 2004). Recent investigations have been undertaken on successions in the British Isles (Port Askaig Formation) and in Norway (Smalfjord Formation) which highlight the importance of sediment gravity flow deposits with minor glaciclastic debris components (Arnaud & Eyles, 2002a, b; alternative interpretations of these successions can be found in Edwards (1975), Edwards & Føyn (1981) and Spencer (1985)). Eyles and Januszczak (2004) argued that sediment gravity flow deposits preserved in many Neoproterozoic basins reflect tectonic instability associated with rift-related break-up of the Rodinia supercontinent. However, since sediment gravity flows are a common (if not dominant) process in the accumulation of Quaternary shelf-break fan systems (e.g. Dowdeswell *et al.*, 1996; Powell & Cooper, 2002), distinguishing mass flow diamictites deposited purely as a function of tectonics *versus* glacially transported debris is complicated. Subaqueous mass flow deposits containing a glaciclastic debris component on passive margins are likely to result directly from continental glaciation, but where glaciers were nucleated on uplifted rift basin margins, the picture is less clear, and a combination of both tectonic and climatic controls is likely (*cf*. Allen *et al.*, 2004; Eyles & Januszczak, 2004). Many Neoproterozoic glacial successions fall into the latter category, where a rift to post-rift transition is considered likely, including the Blaini Formation in India (Kumar & Brookfield, 1987), the Chang'an and Nantuo Formations in south China (Jiang *et al.*, 2003), the Fiq in Oman (Allen *et al.*, 2004) and the Rapitan Group in the North American Cordillera (Young, 1995). Sediment redistribution during postglacial eustatic recovery is also problematic, since successions may be significantly reworked during large-scale submarine failures (e.g. Maslin *et al.*, 2004). However, not all glacially influenced successions are dominated by sediment gravity flows. The Ayn Formation (formerly the Lower Member of the Mirbat Sandstone Formation), in Dhofar, south Oman records a terrestrial to marginal marine succession characterized by Gilbert-type glaciofluvial delta systems, which are laterally associated with more distal stratified glacimarine diamictites, containing abundant dropstones and ubiquitous glacially polished and striated clasts, indicative of temperate or polythermal glacial conditions (Figs 1, 15).

Generally speaking, the huge volumes of debris preserved in Neoproterozoic basins comprising a significant glaciclastic debris component in passive margin settings points towards extensive continental ice sheets with either temperate or polythermal basal characteristics. Temperate or polythermal conditions are also indicated from striated and polished clasts, subglacial pavements and plucked bedrock surfaces including roches moutonnées and whaleback forms (Coats & Preiss, 1980; Ojakangas & Matsch, 1980; Deynoux & Trompette, 1981) and welded subglacial breccia deposits which have been used to infer stick-slip basal behaviour (Bestmann *et al.*, 2006). However, the degree of synchroneity between the accumulation of these successions is limited given the current radiometric age constraints (Table 4), and the long-term thermal response of these ice masses to Neoproterozoic climate change is difficult to evaluate. Thus although a demonstrable record of polythermal or temperate glacial systems exists, cold-based ice sheets may also have persisted for considerable periods of time. Suggestions that Ulvesø (Greenland) and Petrovbreen diamictites of Svalbard reflect cold-based glaciation because of ineffective bedrock quarrying (Halverson *et al.*, 2004) are at odds with the volumes of debris associated with these successions (notably the Ulvesø Formation). In the Quaternary record, subglacial debris loads are commonly dominated by local basin lithologies, and the absence of basement

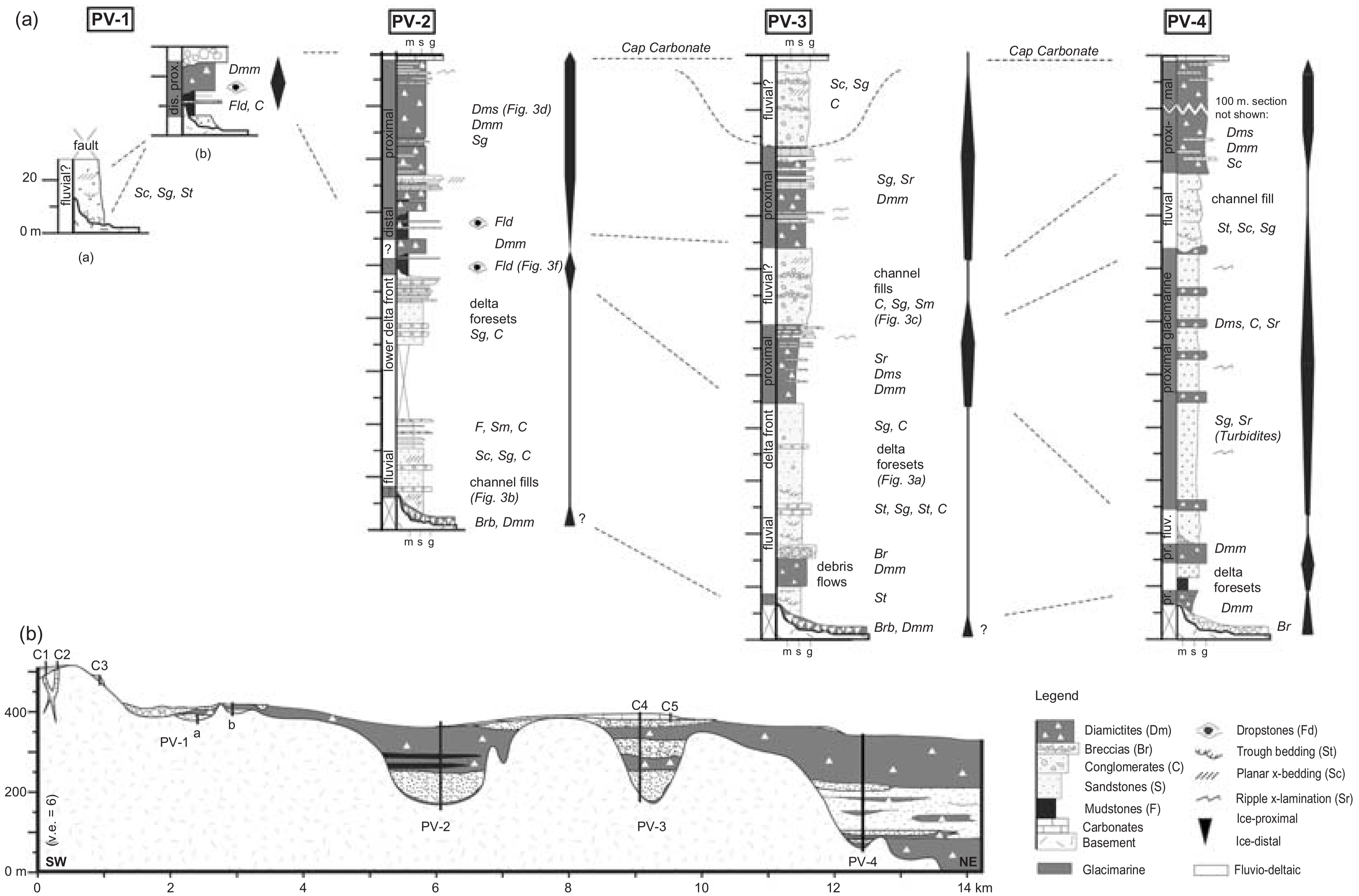

Fig. 15 Lithostratigraphy and interpretive correlation panel of Neoproterozoic valley-fill deposits of the Ayn Fm., Dhofar, south Oman; (a) palaeovalley fills. Section PV-4 modified after Kellerhals & Matter (2003); (b) lateral correlation of palaeovalley fills and elevation of basement, based on logged sections and field mapping. Modified from Rieu *et al.* (*In review*).

clasts does not necessarily negate temperate or polythermal glaciation.

HYDROLOGICAL SHUTDOWN

One of the central tenets of Snowball Earth theory is that decoupling of the ocean and atmosphere, in combination with plummeting surface temperatures would lead to shutdown of the hydrological cycle at the Earth's surface (Hoffman *et al.*, 1998a). Sedimentological investigations have been important in contesting this facet of the Snowball model, with widespread evidence for open marine or even terrestrial conditions, including the occurrence of dropstone horizons (Condon *et al.*, 2002; Fig. 1d), wave-rippled sandstones (Williams, 1996; Allen *et al.*, 2004; Fig. 1e), and periglacial involutions (Hambrey & Spencer, 1987; Moncrieff & Hambrey, 1990). These features are easily explained as a result of Cenozoic-style climate variability over glacial-interglacial transitions, although they could equally be applied to the growth or recessional phases of a Snowball Earth-type glaciation. Nevertheless, the Snowball Earth model has evolved towards one which involves open marine conditions in 'oases' resulting from the early demise of sikussak ice (shorefast multi-annual sea ice; Halverson *et al.*, 2004). In this model, the Arena Formation (Greenland) and MacDonaldryggen Member of the Elbobreen Formation in Svalbard are interpreted by Halverson *et al.*, (2004) to represent the Snowball maxima, when continental ice sheets were effectively landlocked by shorefast sikussak ice and laminites were deposited by density currents resulting from heavy brine formation. This is difficult to defend for the basal part of the Arena Formation where wave-rippled sandstones occur (Hambrey & Spencer, 1987), and is inconsistent with our understanding of laminite sedimentation during the Pleistocene which, as Halverson *et al.*, (2004) acknowledged, occurs predominantly in interglacial periods (Orheim & Elverhøi, 1981; Dowdeswell *et al.*, 1998; but see also Dowdeswell *et al.*, 2000; O'Grady & Syvitski, 2002). Since laminites may be deposited from a range of glacially and non-glacially influenced processes (e.g. as tidal rhythmites, suspension fallout from buoyant plumes and turbidity currents; Stow & Piper, 1984; Pickering *et al.*, 1986; Powell & Molnia, 1989; Cowan & Powell, 1990; Cowan *et al.*, 1997, 1998), and dense brines form a natural component of modern oceanographic circulation, proving the former existence of extensive sea ice may be extremely difficult. In summary, although the Greenland and Svalbard sequences can be interpreted in terms of a Snowball-compatible succession, Phanerozoic analogues are considered more appropriate.

CONCLUSIONS

Neoproterozoic glacigenic and glacially influenced facies associations occur widely throughout the period 780–580 Ma, in passive margin settings and across a range of depositional palaeoenvironments. Definitive sedimentological evidence for a direct glacial influence on sedimentation remains to be presented for many successions. However, for those with a demonstrable glaciclastic debris component, sedimentological data are compatible with Phanerozoic analogues in terms of succession thickness, facies, sedimentological architecture and cyclicity. Widespread evidence for open marine or terrestrial periglacial conditions testifies to a strongly functioning hydrological cycle. Although these features could be attributed to pulsed growth and recessional stages of continental ice sheets during a Snowball-type glaciation, the recently proposed 'oases' model limits the use of sedimentological evidence for testing the hydrological shutdown facet of Snowball Earth theory. Given the current limitations of available radiometric and palaeogeographic databases, it is difficult to demonstrate globally synchronous glaciation, or the extent to which glaciation occurred. On a simple level, the vast volumes of sediment preserved in Neoproterozoic glacially influenced basins are consistent with temperate or polythermal glaciation. Glaciation was nucleated on locally uplifted rift flanks, but passive margin deposits testify to the existence of continental ice sheets which were probably similar in character to those of the Phanerozoic. The relative roles of glaciation and tectonic activity may be inseparable as causes for the accumulation of debrites which are a key component of the glacimarine sedimentary record. Although repeated widespread Neoproterozoic glaciations are envisaged, the evaluation of climate change during this time, particularly in terms of

Snowball Earth theory, requires further enhancement of the existing sedimentological, geochronological and palaeomagnetic datasets.

ACKNOWLEDGEMENTS

J.L. Etienne and P.A. Allen acknowledge financial support from Schweizerischer Nationalfonds Grant 103502. R. Rieu and E. Le Guerroué are supported by ETH postgraduate studentships. We are most grateful to Joachim Amthor and colleagues at PDO, Manuele Faccenda, Matthias Papp, Gion Kuper, Dhiraj Banerjee (Delhi University), Sumit Ghosh and Rafique Islam (Wadia Institute of Himalayan Geology) for logistical support and discussion during fieldwork in Oman and North India. We also thank Paul Hoffman (Harvard), Galen Halverson (University Paul Sabatier, Toulouse), Martin Kennedy (University of California, Riverside) and Andrea Cozzi (ETH-Zürich) for ongoing and insightful discussion. The constructive comments of referees Mike Hambrey and Ian Fairchild are gratefully acknowledged.

REFERENCES

Aalto, R.K. (1971) Glacial marine sedimentation and stratigraphy of the Toby Conglomerate (Upper Proterozoic), southeastern British Columbia, northwestern Idaho and northeastern Washington. *Can. J. Earth Sci.*, **8**, 753–787.

Aalto, K.R. (1981) The Late Precambrian Toby Formation of British Columbia, Idaho and Washington. In: *Earth's Pre-Pleistocene Glacial Record* (Eds M.J. Hambrey and W.B. Harland), pp. 731–735. Cambridge University Press, Cambridge.

Agassiz, L. (1838) On the polished and striated surfaces of the rocks which form the beds of glaciers in the Alps. *Proc. Geol. Soc. London.*, **3**, 321–322.

Aharon, P. (1988) Oxygen, carbon and U-series isotopes of aragonites from Vestfold Hills, Antarctica: Clues to geochemical processes in subglacial environments. *Geochim. Cosmochim. Acta.*, **52**, 2321–2331.

Aitken, J.D. (1991) Two late Proterozoic glaciations, Mackenzie Mountains, northwestern Canada. *Geology*, **19**, 445–448.

Aleinikoff, J.N., Zartman R.E., Walter, M. Rankin D.W., Lyttle P.T. and Burton W.C. (1995) U-Pb ages of metarhyolites of the Catoctin and Mount Rogers Formations, central and southern Appalachians: Evidence for two pulses of Iapetan rifting. *Am. J. Sci.*, **295**, 428–454.

Allen, P., Leather, J. and Brasier, M. (2004) The Neoproterozoic Fiq glaciation and its aftermath, Huqf Supergroup of Oman. *Basin Res.*, **160**, 507–534.

Alley, R.B., Cuffey, K.M., Evenson, E.B., Strasser, J.C., Lawson, D.E. and Larson, G.J. (1997) How glaciers entrain and transport basal sediment: physical constraints. *Quatern. Sci. Rev.*, **16**, 1017–1038.

Allsopp, H.L., Köstlin, E.O., Welke, H.J., Burger, A.J., Kröner, A. and Blignault, H.J. (1979) Rb–Sr and U–Pb geochronology of Late Precambrian–Early Paleozoic igneous activity in the Richtersveld (South Africa) and southern South West Africa. *Trans. Geol. Soc. S. Afr.*, **82**, 185–204.

Alvarenga, C.J.S., Santos, R.V. and Dantas, E.L. (2004) C–O–Sr isotopic stratigraphy of cap carbonates overlying Marinoan-age glacial diamictites in the Paraguay Belt, Brazil. *Precambrian Res.*, **131**, 1–21.

Amthor, J.E., Grotzinger, J.P., Schröder, S., Bowring, S.A., Ramezani, J., Martin, M.W. and Matter, A. (2003) Extinction of Cloudina and Namacalathus at the Precambrian-Cambrian boundary in Oman. *Geology*, **31**, 431–434.

Andrews, J.T., Smith, L.M., Preston, R., Cooper, T. and Jennings, A.E. (1997) Holocene patterns of ice-rafted detritus (IRD) in cores from the East Greenland shelf. *J. Quatern. Sci.*, **12**, 1–13.

Arnaud, E. and Eyles, C.H. (2002a) Glacial influence on Neoproterozoic sedimentation: the Smalfjord Formation, Northern Norway. *Sedimentology*, **49**, 765–788.

Arnaud, E. and Eyles, C.H. (2002b) Catastrophic mass failure of a Neoproterozoic glacially influenced continental margin, the Great Breccia, Port Askaig Formation, Scotland. *Sed. Geol.*, **151**, 313–333.

Atkins, C.B., Barrett, P.J. and Hicock, S.R. (2002) Cold glaciers erode and deposit: evidence from Allan Hills, Antarctica. *Geology*, **30**, 659–662.

Attoh, K. Dallmeyer, R.D. and Affaton, P. (1997) Chronology of nappe assembly in the Pan-African Dahomeyide Orogen, West Africa; evidence from (super 40) Ar/(super 39) Ar mineral ages. *Precambrian Res.*, **82**, 153–171.

Babinski, M. and Kaufman, A.J. (2003) First direct dating of a Neoproterozoic post-glacial cap carbonate. In: *South American Symposium on Isotope Geology **4** Short Papers*, **1**, pp. 321–323.

Bailey, C.M. and Peters, S.E. (1998) Glacially influenced sedimentation in the late Neoproterozoic Mechum River Formation, Blue Ridge province, Virginia. *Geology*, **26**, 623–626.

Banks, N.L., Edwards, M.B., Geddes, W.P., Hobday, D.K. and Reading, H.G. (1971) Late Precambrian and

Cambro-Ordovician sedimentation in East Finnmark. *Nor. Geol. Unders*., **269**, 197–236.

Baode, G., Ruitang, W., Hambrey, M.J. and Wuchen, G. (1986) Glacial sediments and erosional pavements near the Cambrian-Precambrian boundary in western Henan Province, China. *J. Geol. Soc. London*, **143**, 311–323.

Barfod, G.H., Albarède, F., Knoll, A.H., Xiao, S., Télouk, P., Frei, R. and Baker, J. (2002) New Lu–Hf and Pb–Pb age constraints on the earliest animal fossils. *Earth Planet. Sci. Lett*., **201**, 203–212.

Barker, P.F., Camerlenghi, A. and Acton, G.D. (1998) Antarctic glacial history and sea-level change. ODP, Preliminary report No. 78. Ocean Drilling Program, Texas A & M University, College Station, TX 77845–9547, USA.

Bart, P.J. and Anderson, J.B. (1995) Seismic record of glacial events affecting the Pacific margin of the northwestern Antarctic Peninsula. In: *Geology and Seismic Stratigraphy of the Antarctic Margin* (Eds A.K. Cooper, P.F. Barker and G. Brancolini) *Antarct. Res. Ser*., **68**, 75–96.

Benn, D.I. (1995) Fabric signature of till deformation, Breiðamerkurjökull, Iceland. *Sedimentology*, **42**, 735–747.

Benn, D.I. and Ballantyne, C.K. (1993) The description and representation of particle shape. *Earth Surf. Proc. Land*., **18**, 665–672.

Benn, D.I. and Ballantyne, C.K. (1994) Reconstructing the transport history of glacigenic sediments: a new approach based on the co-variance of clast form indices: *Sed. Geol*., **91**, 215–227.

Benn, D.I. and Evans, D.J.A. (1998) Glaciers and Glaciation. Arnold, London, 734 pp.

Benn, D.I. and Owen, L.A. (2002) Himalayan glacial sedimentary environments: a framework for reconstructing and dating the former extent of glaciers in high mountains. *Quatern. Int*., **97–8**, 3–25.

Benn, D.I. and Ringrose, T.J. (2001) Random variation of fabric eigenvalues: Implications for the use of A-axis fabric data to differentiate till facies. *Earth Surf. Proc. Land*., **26**, 295–306.

Benn, D.I., Wiseman, S. and Hands, K.A. (2001) Growth and drainage of supraglacial lakes on debris-mantled Ngozumpa Glacier, Khumbu Himal, Nepal. *J. Glaciol*., **47**, 626–638.

Benn, D.I. and Prave, A. (2006) Subglacial and proglacial glacitectonic deformation in the Neoproterozoic Port Askaig Formation, Scotland. *Geomorphology*, **75**, 266–280.

Bennett, M.R., Hambrey, M.J., Huddart, D. and Ghienne, J.F. (1996a) The formation of a geometrical ridge network by the surge-type glacier Kongsvegen, Svalbard. *J. Quatern. Sci*., **11**, 437–449.

Bennett, M.R., Huddart, D., Hambrey, M.J. and Ghienne, J.F. (1996b) Moraine development at the high-arctic valley glacier Pedersenbreen, Svalbard. *Geogr. Ann*., **78 A**, 209–222.

Bennett, M.R., Hambrey, M.J. and Huddart, D. (1997) Modification of clast shape in high-arctic environments. *J. Sed. Res*., **67**, 550–559.

Bennett, M.R., Hambrey, M.J., Huddart, D. and Glasser, N.F. (1998) Glacial thrusting and moraine-mound formation in Svalbard and Britain: the example of Coire a'Cheud-chnoic (Valley of Hundred Hills), Torridon Scotland. In: Owen, L.A. (Ed.) Mountain Glaciation. *Quatern. Proc*., **6**, 17–34.

Bennett, M.R., Waller, R.I., Glasser, N.F., Hambrey, M.J. and Huddart, D. (1999) Glacigenic clast fabrics: genetic fingerprint or wishful thinking? *J. Quatern. Sci*., **14**, 125–135.

Benus, A.P. (1988) Sedimentological context of a deep-water Ediacaran fauna (Mistaken Point Formation, Avalon Zone, Eastern Newfoundland). In: *Trace Fossils, Small Shelly Fossils, and the Precambrian-Cambrian Boundary* (Eds E. Landing, G. Narbonne and P. Myrow). *N.Y. State Mus. Bull*., **463**, 8–9.

Bestmann, M., Rice, A.H.N., Langenhorst, F., Grasemann, B. and Heidelbach, F. (2006) Subglacial bedrock welding associated with glacial earthquakes. J. Geol. Soc. London, **163** (3), 417–420.

Beyth, M., Avigad, D., Wetzel, H.-U., Matthews, A., and Berhe, S.M. (2003) Crustal exhumation and indications for Snowball Earth in the East African Orogen: north Ethiopia and east Eritrea. *Precambrian Res*., **123**, 187–201.

Bhatia, M.R. and Prasad, A.K. (1981) Evolution of Late Paleozoic glacial marine sedimentation in the Simla Hills, Lesser Himalaya, India. *N. Jb. Geol. Paläeontol. Mh*., **5**, 267–288.

Bhatia, S.B. and Kanwar, R.C. (1975) Blaini and Related Formations. *Indian Geol. Assoc. Spec. Iss*., **8**, 279 pp.

Binda, P.L. and Van Eden, J.G. (1972) Sedimentological evidence on the origin of the Precambrian Great onglomerate (Kundelungu Tillite), Zambia. *Palaeogeogr., Palaeoclimatol., Palaeoecol*., **12**, 151–168.

Bjørlykke, K. (1981) Late Precambrian tillites of the Bunyoro Series, western Uganda. In: *Earth's Pre-Pleistocene Glacial Record* (Eds M.J. Hambrey and W.B. Harland), pp. 151–152. Cambridge University Press, Cambridge.

Bjørlykke, K. and Nystuen, J.P. (1981) Late Precambrian tillites of South Norway. In: *Earth's Pre-Pleistocene Glacial Record* (Eds M.J. Hambrey and W.B. Harland), pp. 624–628. Cambridge University Press, Cambridge.

Black, L.P., Shaw, R.D. and Offe, L.A. (1980) The age of the Stuart Dyke Swarm and its bearing on the onset of Late Precambrian sedimentation in central Australia. *J. Geol. Soc. Aust.*, **27**, 151–155.

Blake, D.H., Tyler, I.M., Griffin, T.J., Sheppard, S., Thorne, A.M. and Warren, R.G. (1998) Geology of the Halls Creek 1:100 000 sheet area (4461), Western Australia, Australian Geological Survey Organisation, 1v, 36 pp.

Blair, T.C. and McPherson, J.G. (1999) Grain-size and textural classification of coarse sedimentary particles. *J. Sed. Res.*, **69**, 6–19.

Bodiselitsch, B., Koeberl, C., Master, S. and Reimold, W.U. (2005) Estimating Duration and Intensity of Neoproterozoic Snowball Glaciations from Ir Anomalies. *Science*, **308**, 239–242.

Bond, G. (1981) A possible Late Precambrian tillite from the Urungwe District, Zimbabwe. In: *Earth's Pre-Pleistocene Glacial Record* (Eds M.J. Hambrey and W.B. Harland), pp. 178–179. Cambridge University Press, Cambridge.

Boulton, G.S. and Hindmarsh, R.C.A. (1987) Sediment deformation beneath glaciers: rheology and sedimentological consequences. *J. Sed. Res.*, **92**, **B9**, 9059–9082.

Boulton, G.S. (1970) On the deposition of subglacial and melt-out tills at the margins of certain Svalbard glaciers. *J. Glaciol.*, **9**, 231–245.

Boulton, G.S. (1972) The role of thermal regime in glacial sedimentation. In: *Polar Geomorphology* (Eds R.J. Price and D.E. Sugden). *Institute of British Geographers, Special Publication*, **4**, 1–19.

Boulton, G.S. (1978) Boulder shapes and grain-size distribution of debris as indicators of transport paths through a glacier and till genesis. *Sedimentology*, **25**, 773–799.

Boulton, G.S. (1979) Processes of glacier erosion on different substrata. *J. Glaciol.*, **23**, 15–38.

Boulton, G.S. (1996) Theory of glacial erosion, transport and deposition as a consequence of subglacial sediment deformation. *J. Glaciol.*, **140**, 43–62.

Bowring, S.A. and Schmitz, M.D. (2003) High-precision U-Pb zircon geochronology and the stratigraphic record. *Rev. Mineral. Geochem.*, **53**, 305–326.

Bowring, S. Myrow, P. Landing, E. Ramezani, and J. Grotzinger, J. (2003) Geochronological constraints on terminal Proterozoic events and the rise of the Metazoans. *Geophys. Res. Abstr.*, **5**, 13219.

Brasier, M.D. and Shields, G. (2000) Neoproterozoic chemostratigraphy and correlation of the Port Askaig glaciation, Dalradian Supergroup of Scotland. *J. Geol. Soc. London*, **157**, 909–914.

Brasier, M.D., McCarron, G., Tucker, R., Leather, J., Allen, P., and Shields, G. (2000) New U-Pb zircon dates for the Neoproterozoic Ghubrah glaciation and for the top of the Huqf Supergroup, Oman. *Geology*, **28**, 175–178.

Briqueu, L., Lancelot, J.R., Valois, J.-P. and Walgenwitz, F. (1980) Géochronologie U-Pb et genèse d'un type de mineralisation uranifère: Les alaskites de Goanikontès (Namibie) et leur encaissant. *Centr. Rech. Explor. Prod. Elf, Aquitaine Bull.*, **4**, 759–811.

Broecker, W.S., Andree, M., Wolfli, W., Oeschger, H., Bonani, G., Kennett, J.P. and Peteet, D. (1988) The chronology of the last deglaciation: Implications to the cause of the Younger Dryas event. *Palaeoceanog.*, **3**, 1–19.

Brookfield, M. (1987) Lithostratigraphic correlation of Blaini Formation (late Proterozoic, Lesser Himalaya, India) with other late Proterozoic tillite sequences. *Geol. Rund.*, **76**, 477–484.

Brookfield, M. (1994) Problems in applying preservation, facies and sequence models to Sinian (Neoproterozoic) glacial sequences in Australia and Asia. *Precambrian Res.*, **70**, 113–143.

Buchwaldt, R., Toulkeridis, T., Babinski, M., Noce, C.M., Martins Neto, M. and Hercos, C.M. (1999) Age determination and age related Provenance Analysis of the Proterozoic glaciation in central eastern Brazil. *An. Acad. Ci.*, **71(3)**, 527–548.

Burns, S.J. and Matter, A. (1993) Carbon isotopic record of the latest Proterozoic from Oman. *Eclogae Geol. Helv.*, **86**, 595–607.

Caby, R. and Fabre, J. (1981) Late Proterozoic to Early Palaeozoic diamictites, tillites and associated glacigenic sediments in the Serie Pourpree of western Hoggar, Algeria. In: *Earth's Pre-Pleistocene Glacial Record* (Eds M.J. Hambrey and W.B. Harland), pp. 140–145. Cambridge University Press, Cambridge.

Cahen, L. (1954) *Geologie du Congo belge*. H. Vaillant-Carmanne, Liege.

Cahen, L. (1963) Glaciations anciennes et dérive des continents. *Annls. Soc. Geol. Bélg.*, **86 B**, 79-B 84.

Cahen, L. and Lepersonne, J. (1976) Les mixtites du Bas-Zaire: mise au point interimaire. *Rapp. a. Dept. Geol. Miner. Mus. R. Afr. Centr.*, 1975. 33–57.

Cahen, L. and Lepersonne, J. (1981) Proterozoic diamictites of Lower Zaire, In: *Earth's Pre-Pleistocene Glacial Record* (Eds M.J. Hambrey and W.B. Harland), pp. 153–157. Cambridge University Press, Cambridge.

Calver, C.R. (2000) Isotope stratigraphy of the Ediacaran (Neoproterozoic III) of the Adelaide Rift Complex, Australia, and the overprint of water column stratification. *Precambrian Res.*, **100**, 121–150.

Calver, C.R. and Walter, M.R. (2000) The late Neoproterozoic Grassy Group of King Island, Tasmania: Correlation and palaeogeographic significance. *Precambrian Res.*, **100**, 299–312.

Calver, C.R., Black, L.P., Everard, J.L. and Seymour, D.B. (2004) U-Pb zircon age constraints on late Neoproterozoic glaciation in Tasmania. *Geology*, **32**, 893–896.

Chamberlin, T.C. (1888) The rock scourings of the great ice invasions. *U.S. Geol. Surv. Ann. Rep.*, **7**, 155–248.

Chen, D.F., Dong, W.Q., Zhu, B.Q. and Chen, X.P. (2004) Pb–Pb ages of Neoproterozoic Doushantuo phosphorites in South China: constraints on early metazoan evolution and glaciation events. *Precambrian Res.*, **132**, 123–132.

Chinn, T.J.H. and Dillon, A. (1987) Observations on a debris-covered polar glacier 'Whisky Glacier' James Ross Island, Antarctic Peninsula, Antarctica. *J. Glaciol.*, **33**, 300–310.

Christie-Blick, N. (1982) Upper Proterozoic (Eocambrian) Mineral Fork Tillite of Utah: A continental glacial and glaciomarine sequence: Discussion. *Geol. Soc. Am. Bull.*, **93**, 184–186.

Christie-Blick, N. and Levy, M. (1989) Stratigraphic and tectonic framework of Upper Proterozoic and Cambrian rocks in the western United States. In: *Late Proterozoic and Cambrian Tectonics, Sedimentation, and Record of Metazoan Radiation in the Western United States, Fieldtrip Guidebook T331* (Eds N. Christie-Blick and M. Levy), pp. 7–23. 28th International Geological Congress. American Geophysical Union.

Christoffersen, P. (2003) *Thermodynamics of basal freeze-on: subglacial property changes and ice sheet response*. Ph.D. thesis, Technical University of Denmark, pp. 92.

Christoffersen, P. and Tulaczyk, S. (2003) Response of subglacial sediments to basal freeze-on: I. Theory and comparison to observations from beneath the West Antarctic Ice Sheet. *J. Geophys. Res., B*, **108**, 4.

Chumakov, N.M. (1981a) Late Precambrian tilloids of the Rybachiy Peninsula, U.S.S.R. In: *Earth's Pre-Pleistocene Glacial Record* (Eds M.J. Hambrey and W.B. Harland), pp. 602–605. Cambridge University Press, Cambridge.

Chumakov, N.M. (1981b) Late Precambrian glacial deposits of the Vilchitsy Formation of western regions of the U.S.S.R. In: *Earth's Pre-Pleistocene Glacial Record* (Eds M.J. Hambrey and W.B. Harland), pp. 655–659. Cambridge University Press, Cambridge.

Chumakov, N.M. (1981c) Late Precambrian Churochnya tillites of the Polyudov Ridge, U.S.S.R. In: *Earth's Pre-Pleistocene Glacial Record* (Eds M.J. Hambrey and W.B. Harland), pp. 666–669. Cambridge University Press, Cambridge.

Chumakov, N.M. (1996) Tillites and Tilloids on the Western Slope of the Middle Urals (Upper Riphean and Vendian–Early Paleozoic Sections: Guidebook of Geological Trips, All-Russia Conference on the Vendian–Early Paleozoic Paleogeography), Ekaterinburg: *Inst. Geol. Geofiz., Ural. Otd., Ross. Akad. Nauk*, 74–82.

Chumakov, N.M. (1998) Reference Section of Vendian Glacial Deposits in the Southern Urals (Kurgashlya Formation of the Krivoi Luk Graben), (The Urals: Fundamental Problems of the Geodynamics and Stratigraphy), pp. 138–153. Moscow: Nauka.

Clauer, N. (1976) Géochimie isotopique du strontium des milieux sédimentaires. Application à la geochronologie de la couverture du craton ouest-africain. *Mém. Sci. Géol. Strasbourg*, **45**, 256.

Clauer, N. and Deynoux, M. (1987) New Information on the Probable Isotopic Age of the Late Proterozoic Glaciation in West Africa. *Precambrian Res.*, **37**, 89–94.

Clauer, N. and Kröner, A. (1979) Strontium and Argon Isotopic Homogenization of Pelitic Sediments during Low-Grade Regional Metamorphism: The Pan-African Upper Damara Sequence of Northern Namibia (South West Africa). *Earth Planet. Sci. Lett.*, **43**, 117–131.

Clauer, N., Caby, R., Jeannette, D. and Trompette, R. (1982) Geochronology of sedimentary and meta-sedimentary Precambrian rocks of the West African Craton. *Precambrian Res.*, **18**, 53–71.

Coats, R.P. (1973) Copley, South Australia, 1:250 000 explanatory notes. Sheet SH/54–09, 1st edition. *Geol. Surv. S. Aust.*, 1v, 38 pp.

Coats, R.P. (1981) Late Proterozoic (Adelaidean) tillites of the Adelaide Geosyncline. In: *Earth's Pre-Pleistocene Glacial Record* (Eds M.J. Hambrey and W.B. Harland), pp. 537–548. Cambridge University Press, Cambridge.

Coats, R.P. and Preiss, W.V. (1980) Stratigraphic and geochronological reinterpretation of late Proterozoic glaciogenic sequences in the Kimberley region, Western Australia. *Precambrian Res.*, **13**, 181–208.

Colpron, M., Logan, J.M. and Mortensen, J.K. (2002) U–Pb zircon age constraint for late Neoproterozoic rifting and initiation of the lower Paleozoic passive margin of western Laurentia, *Can. J. Earth Sci.*, **39**, 133–143.

Condon, D.J. and Prave, A.R. (2000) Two from Donegal: Neoproterozoic glacial episodes on the northeast margin of Laurentia. *Geology*, **28**, 951–954.

Condon, D.J., Prave, A.R., and Benn, D.I. (2002) Neoproterozoic glacial rain-out intervals: Observations and Implications. *Geology*, **30**, 35–38.

Condon, D. Zhu, M., Bowring, S., Wang, W., Yang, A. and Jin, Y. (2005) U-Pb Ages from the Neoproterozoic Doushantuo Formation, China. *Science*, **308**, 95–98.

Cooper, J.A., Jenkins, R.J.F., Compston, W. and Williams, I.S. (1992) Ion-probe zircon dating of a mid-Early Cambrian tuff in South Australia. *J. Geol. Soc. London.*, **149**, 185–192.

Corkeron, M.L. and George, A.D. (2001) Glacial incursion on a Neoproterozoic carbonate platform in the Kimberley region, Australia. *Geol. Soc. Am. Bull.*, **113**, 1121–1132.

Corsetti, F.A. and Kaufman, A.J. (2003) Stratigraphic investigations of carbon isotope anomalies and Neoproterozoic ice ages in Death Valley, California. *Geol. Soc. Am. Bull*., **115**, 916–932.

Cowan, E.A. and Powell, R.D. (1990) Suspended sediment transport and deposition of cyclically interlaminated sediment in a temperate glacial fjord, Alaska, U.S.A. In: *Glacimarine Environments: Processes and Sediments* (Eds J.A. Dowdeswell and J.D. Scourse) pp. 75–89. *Geol. Soc. Spec. Publ*., **53**.

Cowan, E.A., Cai, J., Powell, R.D., Clark, J.D. and Pitcher, J.N. (1997) Temperate Glacimarine Varves: an example from Disenchantment Bay, Southern Alaska. *J. Sed. Res*., **67**, 536–549.

Cowan, E.A., Cai, J., Powell, R.D., Seramur, K.C. and Spurgeon, V.L. (1998) Modern tidal rhythmites deposited in a deep-water estuary. *Geo-Marine Letters*, **18**, 40–48.

Cozzi, A. and Al-Siyabi, H.A. (2004) Sedimentology and play potential of the late Neoproterozoic Buah Carbonates of Oman. *GeoArabia*, **9**, 11–36.

Croot, D.G. (1988) Morphological, structural and mechanical analysis of neoglacial ice-pushed ridges in Iceland. In: *Glaciotectonics, Forms and Processes* (Ed. D.G. Croot), pp. 33–47. A.A. Balkema, Rotterdam.

Crowell, J.C. (1978) Gondwana glaciation, cyclothems, continental positioning, and climate change. *Am. J. Sci*., **278**, 1345–1372.

Cuffey, K.M., Conway, H., Gades, A.M., Hallet, B., Lorrain, R., Severinghaus, J.P., Steig, E.J., Vaughn, B. and White, J.W.C. (2000) Entrainment at cold glacier beds. *Geology*, **28**, 351–354.

Curry, A.M. and Ballantyne, C.K. (1999) Paraglacial modification of glacigenic sediment. *Geogr. Ann*., **81A**, 409–419.

Daily, B. and Forbes, B.G. (1969) Notes on the Proterozoic and Cambrian, southern and central Flinders Ranges, South Australia. In: *Geological Excursions Handbook* (Ed. B. Daily), 23–30. ANZAAS, Section 3.

Dalgarno, C.D. and Johnson, J.E. (1964) Glacials of the Marinoan Series. *Quart. Geol. Notes geol. Surv. S. Austr*., **11**, 3–4.

Davies, K.A. (1939) The glacial sediments of Bunyoro, N.W. Uganda. *Bull. Geol. Surv. Uganda*, **3**, 20–37.

de Almeida, F.F.M. (1964a) Geologia do centro-oeste matogrossense. *Brazil Minist. Minas Energ. Dep. Nac. Prod. Miner. Bol. Div. Geol. Mineral*., **215**, 1–137.

de Almeida, F.F.M. (1964b) Glaciação Eocambriana em Mato Grosso. *Brazil Minist. Minas Energ. Dep. Nac. Prod. Mineral Notas Prelim. Est*., **117**, 1–10.

Dec, T., O'Brien, S.J. and Knight, I. (1992) Late Precambrian volcanoclastic deposits of the Avalonian Eastport Basin (Newfoundland Appalachians): petrofacies, detrital clinopyroxene geochemistry and plate tectonic implications. *Precambrian Res*., **59**, 243–262.

Dempster, T.J., Rogers, G., Tanner, P.W.G., Bluck, B.J., Muir, R.J., Redwood, S.D., Ireland, T.R. and Paterson, B.A. (2002) Timing of deposition, orogenesis and glaciation within the Dalradian rocks of Scotland: constraints from U–Pb zircon ages. *J. Geol. Soc. London*., **159**, 83–94.

Dewez, V. and Geurts, M.A. (1996) Multivariate mineralogical analysis of sediments from the Upper Wisconsinan of the southwestern Yukon Territory. *Can. J. Earth Sci*., **33**, 42–45.

Deynoux, M. (1982) Periglacial polygonal structures and sand wedges in the late Precambrian glacial formations of the Taoudeni Basin in Adrar of Mauretania (West Africa). *Palaeogeogr., Palaeoclimatol., Palaeoecol*., **39**, 55–70.

Deynoux, M. (1985) Terrestrial of waterlain glacial diamictites? Three case studies from the late Precambrian and Late Ordovician glacial drifts in West Africa. *Palaeogeogr., Palaeoclimatol., Palaeoecol*., **51**, 97–141.

Deynoux, M. and Trompette, R. (1981) Late Precambrian tillites of the Taoudeni Basin, West Africa. In: *Earth's Pre-Pleistocene Glacial Record* (Eds M.J. Hambrey and W.B. Harland), pp. 89–96. Cambridge University Press, Cambridge.

Dobkins, J.E. and Folk, R.L. (1970) Shape development on Tahiti-Nui. *J. Sed. Petrol*., **40**, 1167–1203.

Dobrzinski, N. and Bahlburg, H. (*In Press*). Sedimentology and environmental significance of the Cryogenian successions of the Yangtze platform, South China block. *Palaeogeogr., Palaeoclimatol., Palaeoecol*.,

Dobrzinski, N., Bahlburg, H., Strauss, H. and Zhang, Q. (2004) Geochemical climate proxies applied to the Neoproterozoic glacial succession on the Yangtze Platform, South China. In: *The extreme Proterozoic: Geology, Geochemistry and Climate* (Eds Jenkins, G.S., McMenamin, M.A.S., McKay, C.P. and Sohl, L.). – *AGU monograph series*, **146**, 13–32.

Domack, E.W. and Lawson, D.E. (1985) Pebble fabric in an ice rafted diamicton. *J. Geol*., **93**, 577–591.

Dott, R.H. (1961) Squantum 'Tillite', Massachusetts; evidence of glaciation or subaqueous mass movements? *Geol. Soc. Am. Bull*., **72**, 1289–1306.

Dow, D.B. and Gemuts, I. (1967) Dixon Range, W.A., 1:250 000. *Geol. Set., Bur. Miner. Resour. Geol. Geophys., Anst., Explan. Notes*, SE/52–6.

Dowdeswell, J.A., and Sharp, M. (1986) Characterization of pebble fabrics in modern terrestrial glacigenic sediments. *Sedimentology*, **33**, 699–710.

Dowdeswell, J.A., Hambrey, M.J. and Wu, R. (1985) A comparison of clast fabric and shape in late Precambrian and modern glacigenic sediments. *J. Sed. Petrol*., **55**, 691–704.

GSP_4_C19.qxd 9/18/07 17:11 Page 388

Dowdeswell, J.A., Uenzelmann-Neben, G., Whittington, R.J. and Marienfeld, P. (1994) The Late Quaternary sedimentary record in Scoresby Sund, East Greenland. *Boreas*, **23**, 294–310.

Dowdeswell, J.A., Kenyon, N.H., Elverhøi, A., Laberg, J.S., Hollender, F-J, Mienert, J. and Siegert, M.J. (1996) Large-scale sedimentation on the glacier-influenced Polar North Atlantic margins: Long-range side-scan sonar evidence. *Geophys. Res. Lett*., **23**, 3535–3538.

Dowdeswell, J.A., Elverhøi, A. and Spielhagen, R. (1998) Glacimarine sedimentary processes and facies on the polar North Atlantic Margins. *Quatern. Sci. Rev.*, **17**, 243–272.

Dowdeswell, J.A., Whittington, R.J., Jennings, A.E., Andrews, J.T., Mackensen, A. and Marienfeld, P. (2000) An origin for laminiated glacimarine sediments through sea-ice build-up and suppressed iceberg rafting. *Sedimentology*, **47**, 557–576.

Dreimanis, A. (1988) Tills: Their genetic terminology and classification. In: *Genetic Classification of Glacigenic Deposits* (Eds R.P. Goldthwait and C.L. Matsch), pp. 17–84. A.A. Balkema, Rotterdam.

Drexel, J.F., Preiss, W.V. and Parker, A.J. (1993) *The Geology of South Australia, Vol. 1. The Precambrian. Geol. Surv. S. Aust. Bull.*, **54**, 242 pp.

Dunn, P.R., Thomson, B.P. and Rankama, K. (1971) Late Precambrian glaciation in Australia as a stratigraphic boundary. *Nature*, **231**, 498–502.

Dunster, J.N., Beier, P.R., Burgess, J.M. and Cutovinos, A. (2000) Auvergne, Northern Territory, 1:250 000 geological Map Series, Sheet SD 52–15 – Explanatory Notes, Northern Territory Geological Survey. 1:250 000 geological map series. Explanatory notes., 1v, 34 pp.

Echelmeyer, K. and Wang, Z. (1987) Direct observation of basal sliding and deformation of basal drift at sub-freezing temperatures. *J. Glaciol.*, **33**, 83–98.

Edwards, M.B. and Føyn, S. (1981) Late Precambrian tillites in Finnmark, North Norway. In: *Earth's Pre-Pleistocene Glacial Record* (Eds M.J. Hambrey and W.B. Harland), pp. 606–609. Cambridge University Press, Cambridge.

Ehlers, J. and Gibbard, P.L. (2003) Extent and chronology of glaciations. *Quatern. Sci. Rev*., **22**, 1561–1568.

Eisbacher, G.E. (1981) Sedimentary tectonics and glacial record in the Windermere Supergroup, Mackenzie Mountains, Northwest Territories. *Geol. Surv. Can., Pap*., 80–27, 40 pp.

Eisbacher, G.H. (1985) Late Proterozoic rifting, glacial sedimentation, and sedimentary cycles in the light of Windermere deposition, Western Canada. *Palaeogeogr., Palaeoclimatol., Palaeoecol.*, **51**, 231–254.

Elverhøi, A., Pfirman, S.L., Solheim, A. and Larssen, B.B. (1989) Glaciomarine sedimentation in epicontinental seas exemplified by the Northern Barents Sea. *Mar. Geol.*, **85**, 225–250.

Elverhøi, A., Hooke, R. LeB. and Solheim, A. (1998) Late Cenozoic erosion and sediment yield from the Svalbard-Barents Sea region: implications for understanding erosion of glacierised basins. *Quatern. Sci. Rev*., **17**, 209–241.

Elverhøi, A., de Blasio, F.V., Butt, F.A., Issler, D., Harbitz, C., Engvik, L., Solheim, A. and Marr, J. (2002) Submarine mass-wasting on glacially-influenced continental slopes: processes and dynamics. In: *Glacier-Influenced Sedimentation on High-Latitude Continental Margins* (Eds J.A. Dowdeswell and C.O. Cofaigh), Geol. *Soc. London Spec. Publ*., **203**, 73–87.

Escutia, C., De Santis, L., Donda, F., Dunbar, R.B., Cooper, A.K., Brancolini, G. and Eittreim, S.L. (2005) Cenozoic ice sheet history from East Antarctic Wilkes Land continental margin sediments. *Glob. Planet. Change*., **45**, 51–81.

Etienne, J.L. (2004) *Quaternary glacigenic sedimentation along the Welsh margin of the Irish Sea basin*. Unpublished Ph.D. thesis, University of Wales, Aberystwyth.

Evans, D.A.D. (2000) Stratigraphic, geochronological, and paleomagnetic constraints upon the Neoproterozoic climatic paradoxes. *Am. J. Sci*., **300**, 347–443.

Evans, J. and Ó Cofaigh C. (2003) Supraglacial debris along the front of the Larsen-A Ice Shelf, Antarctic Peninsula. *Antarctic Sci.*, **15(4)**, 503–506.

Evans, J., Dowdeswell, J.A., Grobe, H., Niessen, F., Stein, R., Hubberten, H.-W. and Whittington, R.J. (2002) Late Quaternary sedimentation in Kejser Franz Joseph Fjord and the continental margin of East Greenland. In: *Glacier-Influenced Sedimentation on High-Latitude Continental Margins* (Eds J.A. Dowdeswell and C.O. Cofaigh), Geol. *Soc. London Spec. Publ*., **203**, 149–179.

Eyles, C.H. and Lagoe, M.B. (1998) Slump-generated megachannels in the Pliocene-Pleistocene glaciomarine Yakataga Formation, Gulf of Alaska. *Geol. Soc. Am. Bull.*, **110**, 395–408.

Eyles, N. (1990) Marine debris flows: Late Precambrian 'tillites' of the Avalonian-Cadomian orogenic belt. *Palaeogeogr., Palaeoclimatol., Palaeoecol*., **79**, 73–98.

Eyles, N., Daniels, J., Osterman, L.E. and Januszczak, N. (2001) Ocean Drilling Program Leg 178 (Antarctic Peninsula): sedimentology of glacially influenced continental margin topsets and foresets. *Mar. Geol*., **178**, 135–156.

Eyles, N. and Januszczak, N. (2004) 'Zipper-Rift': a tectonic model for Neoproterozoic glaciations during the breakup of Rodinia after 750 Ma. *Earth Sci. Rev*., **65**, 1–73.

Fairchild, I.J. and Hambrey, M.J. (1984) The Vendian succession of north-eastern Spitsbergen: petrogenesis of a dolomite-tillite association. *Precambrian Res*., **26**, 111–167.

Fairchild, I.J., Hambrey, M.J., Spiro, B. and Jefferson, T.H. (1989) Late Proterozoic glacial carbonates in north-east Spitsbergen: new insights into the carbonate-tillite association. *Geol. Mag.*, **126**, 469–490.

Fairchild, I.J. and Hambrey, M.J. (1995) Vendian basin evolution in East Greenland and NE Svalbard. *Precambrian Res.*, **73**, 217–233.

Fanning, C.M. and Link, P.K. (2004) U-Pb SHRIMP ages of Neoproterozoic (Sturtian) glaciogenic Pocatello Formation, southeastern Idaho. *Geology*, **32**, 881–884.

Fanning, C.M., Ludwig, K.R., Forbes, B.G. and Preiss, W.V. (1986) Single and multiple grain U–Pb zircon analysis for the early Adelaidean Rook Tuff, Willouran Ranges. *S. Aust. Abstr. Geol. Soc. Aust.*, **15**, 71–72.

Fitzsimons, S.J., McManus, K.J., and Lorrain R.D. (1999) Structure and strength of basal ice and substrate of a dry based glacier: evidence for substrate deformation at subfreezing temperatures. *Ann. Glaciol.*, **28**, 236–240.

Freeman, M.J., Oaks, R.Q. Jr. and Shaw, R.D. (1991) Stratigraphy of the Late Proterozoic Gaylad Sandstone, northeastern Amadeus Basin, and recognition of an underlying regional unconformity. In: *Geological and geophysical studies in the Amadeus Basin, central Australia* (Eds Korsch and Kennard). *Bur. Mineral Resour., Aust., Bull.*, **236**, 137–154.

Frimmel, H.E., Foelling, P.G. and Eriksson, P.G. (2002) Neoproterozoic tectonic and climatic evolution recorded in the Gariep Belt, Namibia and South Africa. *Basin Res.*, **14**, 55–67.

Frimmel, H.E. and Frank, W. (1998) Neoproterozoic tectono-thermal evolution of the Gariep Belt and its basement, Namibia and South Africa. *Precambrian Res.*, **90**, 1–28.

Frimmel, H.E., Kloetzli, U.S. and Siegfried, P.R. (1996) New Pb-Pb single zircon age constraints on the timing of Neoproterozoic glaciation and continental break-up in Namibia. *J. Geol.*, **104**, 459–469.

Frimmel, H.E., Zartman, R.E. and Späth, A. (2001) Dating Neoproterozoic continental break-up in the Richtersveld Igneous complex, South Africa. *J. Geol.*, **109**, 493–508.

Gale, S.J. (1990) The shape of beach gravels. *J. Sed. Petrol.*, **60**, 787–789.

Gaucher, C., Boggiani, P.C., Sprechmann, P., Sial, A.N. and Fairchild, T. (2003) Integrated correlation of the Vendian to Cambrian Arroyo del Soldado and Corumbá Groups (Uruguay and Brazil): palaeogeographic, palaeoclimatic and palaeobiologic implications. *Precambrian Res.*, **120**, 241–278.

Ge, W.C., Li, X.H., Li, Z.X. and Zhou, H.W. (2001) Mafic intrusions in Longsheng area: age and its geological implications. *Chin. J. Geol.*, **36**, 112–118.

Glasser, N.F. and Hambrey, M.J. (2001) Styles of sedimentation beneath Svalbard valley glaciers under changing dynamic and thermal regimes. *J. Geol. Soc.*, **158**, 697–707.

Goodman, J.C. and Pierrehumbert, R.T. (2003) Glacial flow of floating marine ice in 'Snowball Earth'. *J. Geophys. Res.*, **108** (C10), 3308.

Gorokhov, I.M., Siedlecka, A., Roberts, D., Melnikov, N.N. and Turchenko, T.L. (2001) Rb–Sr dating of diagenetic illite in Neoproterozoic shales, Varanger Peninsula, northern Norway. *Geol. Mag.*, **138**, 541–562.

Gower, P.J. (1977) The Dalradian rocks of the west coast of the Tayvallich peninsula. *Scottish Journal of Geology*, **13**, 125–33.

Gray, A. (1930) The correlation of the ore-bearing sediments of the Katanga and Rhodesian Copperbelt. *Econ. Geol.*, **25**, 783–801.

Griffin, T.J., Tyler, I.M., Orth, K. and Sheppard, S. (1998) *Geology of the Angelo* 1:100 000 Sheet. *Geol. Surv. W. Aust.* Explanatory Notes., 1v, 27 pp.

Grobe, H. (1987) A simple method for the determination of ice-rafted debris in sediment cores. *Polarforschung*, **57**, 123–126.

Grotzinger, J.P., Bowring, S.A., Saylor, B.Z. and Kaufman, A.J. (1995) Biostratigraphic and geochronologic constraints on early animal evolution. *Science*, **270**, 598–604.

Hallet, B. (1979) Subglacial regelation water film. *J. Glaciol.*, **23**, 321–334.

Halliday, A.N., Graham, C.M., Aftalion, M. and Dymoke, P. (1989) The depositional age of the Dalradian Supergroup: U-Pb and Sm-Nd isotopic studies of the Tayvallich Volcanics, Scotland. *J. Geol. Soc. London.*, **146**, 3–6.

Halverson, G.P. (2005) A Neoproterozoic chronology. In: S. Xiao (Editor), Neoproterozoic Geobiology. *Kluwer Academic Publishers, Delft, Netherlands*.

Halverson, G.P., Hoffman, P.F., Schrag, D.P. and Kaufman, A.J. (2002) A major perturbation of the carbon cycle before the Ghaub glaciation (Neoproterozoic) in Namibia: prelude to snowball Earth? *Geochem., Geophys., Geosyst.*, **3**.

Halverson, G.P., Maloof, A.C. and Hoffman, P.F. (2004) The Marinoan glaciation (Neoproterozoic) in north-east Svalbard. *Basin Res.*, **16**, 297–324.

Halverson, G.P., Hoffman, P.F., Schrag, D.P., Maloof, A.C. and Rice, A.H.N. (2005) Towards a Neoproterozoic composite carbon isotope record. *Geol. Soc. Am. Bull.*, **117**, 1181–1207.

Ham, N.R. and Mickelson, D.M. (1994) Basal till fabric and deposition at Burroughs Glacier, Glacier Bay, Alaska. *Geol. Soc. Am. Bull.*, **106**, 1552–1559.

Hambrey, M.J. (1983) Correlation of Late Proterozoic tillites in the North Atlantic region and Europe. *Geol. Mag.*, **120**, 209–232.

GSP_4_C19.qxd 9/18/07 17:11 Page 390

Hambrey, M.J. (1988) Late Proterozoic Stratigraphy of the Barents Shelf. In: *Geological Evolution of the Barents Shelf Region* (Eds W.B. Harland and E.K. Dowdeswell), pp. 49–72. Graham & Trotman, London, U.K.

Hambrey, M.J. (1989) The Late Proterozoic sedimentary record of East Greenland: its place in understanding the evolution of the Caledonide Orogen. In: *The Caledonide Geology of Scandinavia* (Ed. R.A. Gayer), pp. 257–262. Graham & Trotman, London, U.K.

Hambrey, M.J. (1994) *Glacial Environments*. UCL Press, London. viii, 296 pp.

Hambrey, M.J. and Glasser, N.F. (2003) Glacial sediments: processes, environments and facies. In: *Encyclopedia of Sediments and Sedimentary Rocks* (Ed. G.V. Middleton). Dordrecht: Kluwer, 316–331.

Hambrey, M.J. and Harland, W.B. (1981) *Earth's Pre-Pleistocene Glacial Record.* Cambridge University Press, Cambridge, 1004 pp.

Hambrey, M.J., Harland, W.B. and Waddams, P. (1981) Late Precambrian tillite of Svalbard. In: *Earth's Pre-Pleistocene Glacial Record* (Eds M.J. Hambrey and W.B. Harland), pp. 592–601. Cambridge University Press, Cambridge.

Hambrey, M.J. and Spencer, A.M. (1987) *Late Precambrian glaciation of central East Greenland*. Meddelelser om Grønland, *Geoscience*, **19**, 50 pp.

Hambrey, M.J., Peel, J.S. and Smith, M.P. (1989a) Upper Proterozoic and Lower Palaeozoic strata in northern East Greenland. *Grønlands Geologiske Undersøgelse Rapport*., **145**, 103–108.

Hambrey, M.J., Barrett, P.J., Hall, K.J. and Robinson, P.H. (1989b) Stratigraphy. In: *Antarctic Cenozoic history from the CIROS-1 drillhole, McMurdo Sound, Antarctica* (Ed. P.J. Barrett). DSIR Bulletin 245, 23–48, Wellington, New Zealand.

Hambrey, M.J. and Huddart, D. (1995) Englacial and proglacial glaciotectonic processes at the snout of a thermally complex glacier in Svalbard. *J. Quatern. Sci*., **10**, 313–326.

Hambrey, M.J., Huddart, D., Bennett, M.R. and Glasser, N.F. (1997) Genesis of 'hummocky moraines' by thrusting in glacier ice: evidence from Svalbard and Britain. *J. Geol. Soc. London*, **154**, 623–632.

Hambrey, M.J. and McKelvey, B. (2000) Neogene fjordal sedimentation on the western margin of the Lambert Graben, East Antarctica. *Sedimentology*, **47**, 577–607.

Hambrey, M.J., Barrett, P.J. and Powell, R.D. (2002) Late Oligocene and early Miocene glaciomarine sedimentation in the SW Ross Sea, Antarctica: the record from offshore drilling. In: *Glacier-Influenced Sedimentation on High-Latitude Continental Margins* (Eds J.A. Dowdeswell and C. O Cofaigh), *Geol. Soc. Lond. Spec. Publ*., **203**, 105–128.

Harland, W.B., Hambrey, M.J. and Waddams, P. (1993) Vendian Geology of Svalbard. *Nor. Polarinst. Skr.*, **193**, Oslo. 150 pp.

Harland, W.B. (1997) The Geology of Svalbard. *Geol. Soc. London Mem*., **17**, 521 pp.

Harris, C. (1998) The micromorphology of paraglacial and periglacial slope deposits: a case study from Morfa Bychan, west Wales, UK. *J. Quatern. Sci*., **13**, 73–84.

Harris, C. and Bothamley, K. (1984) Englacial deltaic sediments as evidence for basal freezing and marginal shearing, Leirbreen, southern Norway. *J. Glaciol*., **30**, 30–34.

Hart, J.K. (1995a) Drumlin formation in southern Anglesey and Arvon, northwest Wales. *J. Quatern. Sci*., **10**, 3–14.

Hart, J.K. (1995b) Drumlin formation in southern Anglesey and Arvon, northwest Wales – Reply. *J. Quatern. Sci*., **10**, p. 399.

Hart, J.K. and Boulton, G.S. (1991) The interrelation of glaciotectonic and glaciodepositional processes within the glacial environment. *Quatern. Sci. Rev*., **10**, 335–350.

Haug, G.H., Tiedemann, R., Zahn, R. and Ravelo, A.C. (2001) Role of Panama uplift on oceanic freshwater balance. *Geology*, **29**, 207–210.

Hein, F.J. and McMechan, M.E. (1994) Proterozoic-Lower Cambrian strata of the Western Canada Sedimentary Basin. In: *Geological Atlas of the western Canada Sedimentary Basin* (Eds G.D. Mossop and I. Shetsen), pp. 57–68. Canadian Soc. Petrol. Geol. Calgary.

Heinrich, R., Baumann, K.-H., Huber, R. and Meggers, H. (2002) Carbonate preservation records of the past 3 Myr in the Norwegian-Greenland Sea and the northern North Atlantic: implications for the history of NADW production. *Mar. Geol*., **184**, 17–39.

Hiemstra, J.F. and van der Meer, J.J.M. (1997) Pore-water controlled grain fracturing as an indicator for subglacial shearing in tills. *J. Glaciol*, **43**, 446–454.

Hiscott, R.N. and Aksu, A.E. (1994) Submarine debris flows and continental slope evolution in the front of Quaternary ice sheets. *Bull. Am. Assoc. Petrol. Geol.*, **78**, 445–460.

Hiscott, R.N., Aksu, A.E., Mudie, P.J. and Parsons, D.F. (2001) A 340,000 year record of ice rafting, palaeoclimatic fluctuations, and slef-crossing glacial advances in the southwestern Labrador Sea. *Glob. Planet. Change*, **28**, 227–240.

Hoffman, P.F. (2005) 28th DeBeers Alex. Du Toit Memorial Lecture, 2004. On Cryogenian (Neoproterozoic) ice-sheet dynamics and the limitations of the glacial sedimentary record. *S. Afr. J. Geol.*, **108**, 557–578

Hoffman, P.F. and Schrag, D.P. (2002) The snowball Earth hypothesis: testing the limits of global change. *Terra Nova*, **14**, 129–155.

Hoffman, P.F., Kaufman, A.J., Halverson, G.P. and Schrag, D.P. (1998a) A Neoproterozoic snowball Earth. *Science*, **281**, 1342–1346.

Hoffman, P.F., Kaufman, A.J. and Halverson, G.P. (1998b) Comings and goings of global glaciations in a Neoproterozoic tropical platform in Namibia. *Geol. Soc. Am. Today*, **8**, 1–9.

Hoffmann, K.-H. and Prave, A.R. (1996) A preliminary note on a revised subdivision and regional correlation of the Otavi Group based on glaciogenic diamictites and associated cap dolostones. *Commun. Geol. Surv. Namibia*, **11**, 81–86.

Hoffmann, K.-H., Condon, D.J. Bowring, S.A. and Crowley, J.L. (2004) U-Pb zircon date from the Neoproterozoic Ghaub Formation, Namibia: Constraints on Marinoan glaciation. *Geology*, **32**, 817–820.

Holdsworth, G. (1974) Meserve Glacier, Wright Valley, Antarctica: Part 1. Basal Processes. *Ohio State University, Institute of Polar Studies Report*, **37**, 104 pp.

Hubbard, B. (1991) Freezing-rate effects on the physical characteristics of basal ice formed by net adfreezing. *J. Glaciol.*, **37**, 339–347.

Hubbard, B. and Sharp, M.J. (1989) Basal ice formation and deformation: a review. *Progress in Physical Geography*, **13**, 529–558.

Hubbard, B. and Sharp, M. (1993) Weertman regelation, multiple refreezing events and the isotopic evolution of the basal ice layer. *J. Glaciol.*, **39**, 275–291.

Hutter, K. and Olunloyo, V.O.S. (1981) Basal stress condition due to abrupt changes in boundary conditions: A cause for high till concentration at the bottom of a glacier. *Ann. Glaciol.*, **2**, 29–33.

Ireland, T.R., Flöttmann, T., Fanning, C.M., Gibson, G.M. and Preiss, W.V. (1998) Development of the Early Paleozoic Pacific Margin of Gondwana from detrital zircon ages across the Delamerian Orogen. *Geology*, **26**, 243–246.

Isotta, C.A.L., Rocha-Campos, A.C. and Yoshida, R. (1969) Striated pavement of the the Upper-Precambrian glaciation in Brazil. *Nature*, **222**, 467–468.

Iverson, N.R. (2000) Sediment entrainment by a soft-bedded glacier: a model based on regelation into the bed. *Earth Surf. Proc. Land.*, **25**, 881–893.

Jago, J.B. (1974) The origin of the Cottons Breccia, King Island, Tasmania. *R. Soc. South Austr. Trans.*, **98**, 13–28.

Jain, A.K. and Varadaraj, N. (1978) Stratigraphy and provenance of Late Palaeozoic diamictites in parts of Garhwal Lesser Himalaya, India. *Geol. Rund.*, **67**, 49–72.

Jansen, E. and Sjøholm, J. (1991) Reconstruction of glaciation over the past 6 Myr from ice-borne deposits in the Norwegian Sea. *Nature*, **349**, 600–603.

Jenkins, R.J.F., Cooper, J.A. and Compston, W. (2002) Age and biostratigraphy of Early Cambrian tuffs from SE Australia and southern China. *J. Geol. Soc. Lond.*, **159**, 645–658.

Jenkins, R.J.F. and Cooper, J.A. (1998) Rb–Sr whole-rock dating of the transition between the Bunyeroo and Wonoka Formations. In: *The Ediacaran in South Australia: Proposal and Field Guide supporting GSSP Position 'C' at Wearing Dolomite, Flinders Ranges* (Eds R.J.F. Jenkins, D.M. McKirdy and C. Nedin), pp. 11–15. IUGS Working Group on the Terminal Proterozoic System, University of Adelaide.

Jiang, G., Christie-Blick, N., Kaufman, A.J., Banerjee, D.M. and Rai, V. (2002) Sequence stratigraphy of the Neoproterozoic Infra Krol Formation and Krol Group, Lesser Himalaya, India. *J. Sed. Res.*, **72**, 524–542.

Jiang, G., Kennedy, M.J. and Christie-Blick, N. (2003a) Stable isotopic evidence for methane seeps in Neoproterozoic postglacial cap carbonates. *Nature*, **426**, 822–826.

Jiang, G., Sohl, L.E. and Christie-Blick, N. (2003b) Neoproterozoic stratigraphic comparison of the Lesser Himalaya (India) and Yangtze block (south China): Paleogeographic implications. *Geology*, **31**, 917–920.

Kasemann, S.A., Hawkesworth, C.J., Prave, A.R., Fallick, A.E. and Pearson, P.N. (2005) Boron and calcium isotope composition in Neoproterozoic carbonate rocks from Namibia: evidence for extreme environmental change. *Earth Planet. Sci. Lett.*, **231**, 73–86.

Kaufman, A.J., Knoll, A.H. and Narbonne, G.M. (1997) Isotopes, ice ages, and terminal Proterozoic earth history. *Proc. Natl. Acad. Sci. USA*, **94**, 6600–6605.

Kellerhals, P. and Matter, A. (2003) Facies analysis of a glaciomarine sequence, the Neoproterozoic Mirbat Sandstone formation, Sultanate of Oman. *Eclog. Geolog. Helvet.*, **96**, 49–50.

Kendall, B.S., Creaser, R.A., Ross, G.M. and Selby, D. (2004) Constraints on the timing of Marinoan 'Snowball Earth' glaciation by ^{187}Re–^{187}Os dating of a Neoproterozoic, post-glacial black shale in Western Canada. *Earth Planet. Sci. Lett.*, **222**, 729–740.

Kendall, B.S. and Creaser, R.A. (2004) Re-Os depositional age of Neoproterozoic Aralka Formation (Amadeus basin, Australia) revisited. *Geol. Soc. Am. Abstr. Prog.*, **36**, 459.

Kennedy, M.J., Runneger, B., Prave, A.R., Hoffman, K.-H. and Arthur, M.A. (1998) Two or four Neoproterozoic glaciations? *Geology*, **26**, 1059–1063.

Kennedy, M.J., Christie-Blick, N. and Sohl, L.E. (2001) Are Proterozoic cap carbonates and isotopic excursions a record of gas hydrate destabilization following Earth's coldest intervals? *Geology*, **29**, 443–446.

Kent, D.V. and Smethurst, M.A. (1998) Shallow bias of paleomagnetic inclinations in the Paleozoic and Precambrian. *Earth Planet. Sci. Lett.*, **160**, 391–402.

Key, R.M., Liyungu, A.K., Njamu, F.M., Somwe, V., Banda, J., Mosley, P.N. and Armstrong, R.A. (2001) The western arm of the Lufilian Arc in NW Zambia and its potential for copper mineralization. *J. Afr. Earth Sci.*, **33**, 503–528.

Khatwa, A. and Tulaczyk, S. (2001) Microstructural interpretations of modern and Pleistocene subglacially deformed sediments: the relative role of parent material and subglacial processes. *J. Quatern. Sci.*, **16**, 507–517.

Kirkbride, M.P. (1995) Processes of transportation. In: *Modern Glacial Environments, Processes, Dynamics and Sediments (Glacial Environments: Volume I)* (Ed. J. Menzies), pp. 261–292. Butterworth-Heinemann, Oxford.

Kirschvink, J.L. (1992) Late Proterozoic low latitude glaciation: the Snowball Earth. In: *The Proterozoic Biosphere: A Multidisciplinary Study* (Eds J.W. Schopf and C. Klein), pp. 51–52. Cambridge University Press, Cambridge.

Kjaer, K.H., Kruger, J. and van der Meer, J.J.M. (2003) What causes till thickness to change over distance? Answers from MΩrdalsjökull, Iceland. *Quatern. Sci. Rev.*, **22**, 1687–1700.

Kleman, J. and Hättestrand, C. (1999) Frozen-bed Fennoscandian and Laurentide ice sheets during the Last Glacial Maximum. *Nature*, **402**, 63–66.

Kleman, J., Hättestrand, C., Borgström, I. and Stroeven, A. (1997) Fennoscandian palaeoglaciology reconstructed using a glacial geological inversion model. *J. Glaciol.*, **43**, 283–300.

Kluiving, S.J., Bartek, L.R. and van der Wateren, F.M. (1999) Multi-scale analyses of subglacial and glaciomarine deposits from the Ross Sea continental shelf, Antarctica. *Ann. Glaciol.*, **28**, 90–96.

Koerner, R.M. and Fisher, D.A. (1979) Discontinuous flow, ice texture, and dirt content in the basal debris layers of the Devon Island ice cap. *J. Glaciol.*, **23**, 209–221.

Kramers, J.D. and Frei, R. (1992) Report on age determination carried out on rocks from the Mirbat region, south Oman. Unpublished Report, Mineralogy-Petrography Institute, University of Bern.

Krieg, G.W., Rogers, P.A., Callen, R.A., Freeman, P.J., Alley, N.F. and Forbes, B.G. (1991) *Curdimurka, South Australia, 1:250 000 Sheet Explanatory Notes*. *Geol. Surv. S. Aust.*, 1v, 60 pp.

Krogh, T.E., Strong, D.F., O'Brien, S.J. and Papezik, V.S. (1988) Precise U-Pb zircon dates from the Avalon Terrane in Newfoundland. *Can. J. Earth Sci.*, **25**, 442–453.

Kröner, A. (1981) Late Precambrian diamictites of South Africa and Namibia. In: *Earth's Pre-Pleistocene Glacial Record* (Eds M.J. Hambrey and W.B. Harland), pp. 167–177. Cambridge University Press, Cambridge.

Kröner, A. and Correia, H. (1973) Further evidence for glaciogenic origin of Late Precambrian mixtites in Angola. *Nature*, **246**, 115–117.

Krüger, J. (1994) Glacial processes, sediments, landforms, and stratigraphy in the terminus region of Myrdalsjökull, Iceland. *Folia Geographica Danica*, **21**, 1–233.

Kruse, P.D., Brakel, A.T., Dunster, J.N. and Duffett, M.L. (2002) Tobermory, Northern Territory 1:250 000 geological map series. Explanatory Notes Sheet SF 53–12, Northern Territory Geological Survey, 58 pp.

Kukla, G. and Gavin, J. (2005) Did glacials start with global warming? *Quatern. Sci, Rev.*, **24**, 1547–1557.

Kumar, R. and Brookfield, M.E. (1987) Sedimentary environments of the Simla Group (Upper Precambrian), Lesser Himalaya, and their palaeotectonic significance. *Sed. Geol.*, **52**, 27–43.

Kumpulainen, R. (1981) The Late Precambrian Lillfjället Formation in the southern Swedish Caledonides. In: *Earth's Pre-Pleistocene Glacial Record* (Eds M.J. Hambrey and W.B. Harland), pp. 620–623. Cambridge University Press, Cambridge.

Laberg, J.S. and Vorren, T.O. (2000) Flow behaviour of the submarine glacigenic debris flows on the Bear Island Trough Mouth Fan, western Barents Sea. *Sedimentology*, **47**, 1105–1117.

Lachniet, M.S., Larson, G.J., Lawson, D.E., Evenson, E.B. and Alley, R.B. (2001) Microstructures of sediment flow deposits and subglacial sediments: a comparison. *Boreas*, **30**, 254–262.

Larianov, A., Gee, D.G., Tebenkov, A.M. and Witt-Nillson, P. (1998) Detrital zircon ages from the Planetfjella Group of the Mosselhalvøya Nappe, NE Spitsbergen, Svalbard. In: *International Conference on Arctic Margins, III, Celle, Germany, Abstr.*, 109–110.

Larsen, H.C., Saunders, A.D., Clift, P.D., Beget, J., Wei, W., Spezzaferri, S. and ODP Leg 152 Scientific Party. (1994) Seven million years of glaciation in Greenland. *Science*, **264**, 952–955.

Lawson, D.E., Evenson, E.B., Strasser, J.C., Alley, R.B. and Larson, G.J. (1996) Subglacial supercooling, ice accretion, and sediment entrainment at the Matanuska Glacier, Alaska. *Geol. Soc. Am. Abstr. Prog.*, **28**.

Le Guerroué, E., Allen, P.A., Cozzi, A. and Fanning, M. (2006) 50 Million Year Duration negative carbon isotopic excursion in the Ediacaran ocean. *Terra Nova*, **18**, 147–153.

Le Heron, D.P. and Etienne, J.L. (2005) A complex subglacial clastic dyke swarm, Sólheimajökull, southern Iceland. *Sed. Geol.*, **181** (1–2), 25–37.

Le Heron, D.P., Sutcliffe, O.E., Whittington, R.J. and Craig, J. (2005) The origins of glacially related soft-sediment deformation structures in Upper Ordovician glaciogenic rocks: implication for ice-sheet dynamics. *Palaeogeogr., Palaeoclimatol., Palaeoecol.*, **218**, 75–103.

Leather, J. (2001) *Sedimentology, chemostratigraphy and geochronology of the lower Huqf Supergroup, Oman.* Unpublished PhD Thesis, Trinity College, Dublin. 227 pp.

Leather, J., Allen, P.A., Brasier, M.D. and Cozzi, A. (2002) Neoproterozoic snowball earth under scrutiny: evidence from the Fiq glaciation of Oman. *Geology*, **30**, 891–894.

Leblanc, M. (1981) The Late Precambrian Tiddiline Tilloid of the Anti-Atlas, Morocco. In: *Earth's Pre-Pleistocene Glacial Record* (Eds M.J. Hambrey and W.B. Harland), pp. 120–122. Cambridge University Press, Cambridge.

Lee, J.R., Rose, J., Riding, J.B., Moorlock, B.S.P. and Hamblin, R.J.O. (2002) Testing the case for a Middle Pleistocene Scandinavian glaciation in Eastern England: evidence for a Scottish ice source for tills within the Corton Formation of East Anglia, U.K. *Boreas*, **31**, 345–355.

Lemon, N.M. and Reid, P.W. (1998) The Yaltipena Formation of the central Flinders Ranges. *MESA J.*, **8**, 37–39.

Lemon, N.M. and Williams, G.E. (1998) Flinders Ranges field trip, 16–22 June 1998. *Adjunct Field Guide. IUGS Working Group on the Terminal Proterozoic System*. The University of Adelaide (unpublished).

Lewis, J.P., Weaver, A.J., Johnston, S.T. and Eby, M. (2003) The Neoproterozoic 'Snowball Earth': dynamic sea ice over a quiescent ocean. *Paleoceanography*, **18** (4).

Lindsay, J.F. (1989) Depositional controls on glacial facies associations in a basinal setting, Late Proterozoic, Amadeus Basin, Central Australia. *Palaeogeogr., Palaeoclimatol., Palaeoecol.*, **73**, 205–232.

Link, P.K., Miller, J.M.G. and Christie-Blick, N. (1994) Glacial-marine facies in a continental rift environment: Neoproterozoic rocks of the western United States Cordillera. In: *International Geological Correlation Project 260: Earth's glacial record* (Eds M. Deynoux, J.M.B. Miller, E.W. Domack, N. Eyles, I.J. Fairchild and G.M. Young), pp. 29–46. Cambridge University Press, London.

Lønne, I. (1995) Sedimentary facies and depositional architecture of ice-contact glaciomarine systems. *Sed. Geol.*, **98**, 13–43.

Lowe, J.J., McCarroll, D., Knight, J. & Rijsdijk, K. (2001) The glaciation of the Irish Sea basin. *J. Quatern. Sci.*, **16** (5).

Lund, K., Aleinikoff, J.N., Evans, K.V. and Fanning, C.M. (2003) SHRIMP U-Pb geochronology of Neoproterozoic Windermere Supergroup, central Idaho: Implications for rifting of western Laurentia and synchroneity of Sturtian glacial deposits. *Geol. Soc. Am. Bull.*, **115**, 349–372.

Ma, G.G., Lee, H. and Zhang, Z. (1984) An investigation of the age limits of the Sinian System in South China. Bull. *Yichang Inst. Geol. Miner. Res., Chinese Acad. Geol. Sci.*, **8**, 1–29.

Maltman, A.J., Hubbard, B. and Hambrey, M.J. (2000) Deformation *of Glacial Materials*. *Geol. Soc. London, Spec. Publ.*, **176**, pp. 344.

Marjoribanks, R.W. and Black, L.P. (1974) Geology and geochronology of the Arunta Complex, north of Ormiston George, central Australia. *J. Geol. Soc. Aust.*, **21**, 291–300.

Martin, H. (1965) The Precambrian geology of South West Africa and Namaqualand. *Precambrian Res. Unit, Univ. Cape Town, Bull.*, **4**, 1–177.

Martin, H., Porada, H. and Walliser, O.H. (1985) Mixtite deposits of the Damara sequence, Namibia: problem of interpretation. *Palaeogeogr. Palaeoclimatol. Palaeoecol.*, **51**, 159–196.

Maslin, M., Owen, M., Day, S. and Long, D. (2004) Linking continental-slope failures and climate change: Testing the clathrate gun hypothesis. *Geology*, **32**, 53–56.

Maslov, A.V. (2000) Some Specific Features of Early Vendian Sedimentation in the Southern and Middle Urals. *Lithology and Mineral Resources*, **35**, 556–570. (Translated from Russian).

Mawson, E. (1949) The Elatina Glaciation. A third recurrence of glaciation evidenced in the Adelaide System. *Trans. R. Soc. S. Austr.*, **73**, 117–121.

McCarroll, D. and Rijsdijk, K.F. (2003) Deformation styles as a key for interpreting glacial depositional environments. *J. Quatern. Sci.*, **18**, 473–489.

McCarron, G.M.E. (2000) *The sedimentology and chemostratigraphy of the Nafun Group, Huqf Supergroup, Oman.* Unpublished Ph.D. thesis, Oxford University, 175 pp.

McKirdy, D.M., Burgess, J.M., Lemon, N.M., Yu, X., Cooper, A.M., Gostin,V.A., Jenkins, R.J.F. and Both, R.A. (2001) A chemostratigraphic overview of the late Cryogenian interglacial sequence in the Adelaide Fold-Thrust Belt, South Australia. *Precambrian Res.*, **106**, 149–186.

Meert, J.G. and Powell, C. McA. (2001) Introduction to the special volume on the assembly and breakup of Rodinia. *Precambrian Res.*, **110**, 1–8.

Meert, J.G. and Torsvik, T.H. (2004) Paleomagnetic Constraints on Neoproterozoic 'Snowball Earth' Continental Reconstructions. In: *The Extreme Proterozoic: Geology, Geochemistry, and Climate* (Eds G.S., Jenkins, M.A.S. McMenamin, C.P. McKay and L. Sohl), pp. 5–11. Geophysical Monograph Series 146, A.G.U.

Meffre, S., Direen, N.G., Crawford, A.J. and Kamenetsky, V. (2004) Mafic volcanics on King Island, Tasmania: Evidence for plume-triggered breakup in East Gondwana at around 579 Ma. *Precambrian Res.*, **135**, 177–191.

Menzies, J. (1981) Freezing fronts and their possible influence upon processes of subglacial erosion and deposition. *Ann. Glaciol.*, **2**, 52–56.

Menzies, J. (1988) Microstructures within subglacial diamictons. In: *Relief and Deposits of Present-day and Pleistocene Glaciation of the Northern Hemisphere – Selected problems* (Ed. A. Kostrzewski), pp. 153–166. Adam Mickiewicz University Press, Geography Series no. 58. Poznan, Poland.

Menzies, J. (2000) Micromorphological analyses of microfabrics and microstructures indicative of deformation processes in glacial sediments. In: *Deformation of Glacial Materials* (Eds A.J. Maltman, B. Hubbard and M.J. Hambrey), *Geol. Soc. London, Spec. Publ.*, **176**, 245–258.

Menzies, J. and Maltman, A.J. (1992) Microstructures in diamictons – evidence of subglacial bed conditions. *Geomorphology*, **6**, 27–40.

Menzies, J. and Shilts, W.W. (1996) Subglacial Environments. In: *Past Glacial Environments: Sediments, Forms and Techniques* (Ed. J. Menzies), pp. 15–136. Butterworth-Heinemann, Oxford.

Menzies, J., Zaniewski, K. and Dreger, D. (1997) Evidence, from microstructures, of deformable bed conditions within drumlins, Chimney Bluffs, New York State. *Sed. Geol.*, **111**, 161–175.

Mickelson, D.M., Ham N.R. and Ronnert, L. (1992) Striated Clast Pavements – Products Of Deforming Subglacial Sediment – Comment. *Geology*, **20**, 285–285.

Miller, J.M.G. (1996) Glacial Sediments. In: *Sedimentary Environments: Processes, Facies and Stratigraphy* (Ed. H.G. Reading), pp. 454–484. Oxford; Blackwell Science.

Miller, J.M.G., Wright, L.A. and Troxel, B.W. (1981) The Late Precambrian Kingston Peak Formation, Death Valley region, Cailfornia. In: *Earth's Pre-Pleistocene Glacial Record* (Eds M.J. Hambrey and W.B. Harland), pp. 45–748. Cambridge University Press, Cambridge.

Miller, N.R., Alene, M., Sacchi, R., Stern, R.J., Conti, A., Kröner, A. and Zuppi, G. (2003) Significance of the Tambien Group (Tigrai, N. Ethiopia) for Snowball Earth events in the Arabian–Nubian Shield. *Precambrian Res.*, **121**, 263–283.

Moncrieff, A.C.M. (1988) *The Vendian Stratigraphy and Sedimentology of East Greenland*. Unpublished Ph.D. thesis, Cambridge University.

Moncrieff, A.C.M. (1989a) Classification of poorly sorted sedimentary rocks. *Sed. Geol.*, **65**, 191–194.

Moncrieff, A.M. (1989b) The Tillite Group and related rocks of East Greenland: implications for Late Proterozoic palaeogeography. In: *The Caledonide Geology of Scandinavia* (Ed. R.A. Gayer). Graham and Trotman, London, 285–297.

Moncrieff, A.C.M. and Hambrey, M.J. (1988) Glacial erosional pavements in the Late Precambrian Tillite Group, central East Greenland. *Palaeogeog., Palaeoclimatol. Palaeoecol.*, **65**, 183–200.

Moncrieff, A.C.M. and Hambrey, M.J. (1990) Marginal-marine glacial sedimentation in the late Precambrian succession of East Greenland. In: *Glacimarine environments: processes and sediments* (Eds J.A. Dowdeswell and J.D. Scourse), *Geol. Soc. London Spec. Publ.*, **53**, 387–410.

Moros, M., Kuijpers, A., Snowball, I., Lassen, S., Bäckstöm, D., Gingele, F. and McManus, J. (2002) Were glacial iceberg surges in the North Atlantic triggered by climate warming? *Mar. Geol.*, **192**, 393–417.

Myrow, P.M. and Kaufman, A.J. (1999) A newly discovered cap carbonate above Varanger-age glacial deposits in Newfoundland. *J. Sed. Res.*, **69**, 784–793.

Myrow, P.M., Hughes, N.C., Paulsen, T.S., Williams, I.S., Parcha, S.K., Thompson, K.R., Bowring, S.A., Peng, S.-C. and Ahluwalia, A.D. (2003) Integrated tectonostratigraphic analysis of the Himalaya and implications for its tectonic reconstruction. *Earth Planet. Sci. Lett.*, **212**, 433–441.

Naish T.R., Woolfe, K.J., Barrett, P.J., Wilson, G.S., Atkins, C., Bohaty, S.M., Bucker, C.J., Claps, M., Davey, F.J., Dunbar, G.B., Dunn, A.G., Fielding, C.R., Florindo, F., Hannah, M.J., Harwood, D.M., Henrys, S.A., Krissek, L.A., Lavelle, M., van Der Meer, J., McIntosh, W.C., Niessen, F., Passchier, S., Powell, R.D., Roberts, A.P., Sagnotti, L., Scherer, R.P., Strong, C.P., Talarico, F., Verosub, K.L., Villa, G., Watkins, D.K., Webb, P.N. and Wonik, T. (2001) Orbitally induced oscillations in the East Antarctic Ice Sheet at the Oligocene-Miocene boundary. *Nature*, **413**, 719–723.

Narbonne, G.M., Kaufman, A.J. and Knoll, A.H. (1994) Integrated chemostratigraphy and biostratigraphy of the Windermere Supergroup, northwestern Canada: Implications for Neoproterozoic correlations and the early evolution of animals. *Geol. Soc. Am. Bull.*, **106**, 1281–1292.

Noble, S.R., Hyslop, E.K. and Highton, A.J. (1996) High-precision U-Pb monazite geochronology of the c. 806 Ma Grampian shear zone and the implications for the evolution of the Central Highlands of Scotland. *J. Geol. Soc. Lond.*, **153**, 511–514.

Nogueira, A.C.R., Riccomini, C., Sial, A.N., Moura, C.A.V. and Fairchild, T.R. (2003) Soft-sediment deformation at the base of the Neoproterozoic Puga cap carbonate (southwestern Amazon craton, Brazil): Confirmation of rapid icehouse to greenhouse transition in snowball Earth. *Geology*, **31**, 613–616.

Nygård, A., Sejrup, H.P., Haflidason, H. and King, E.L. (2002) Geometry and genesis of glacigenic debris flows on the North Sea Fan: TOBI imagery and deep-tow boomer evidence. *Mar. Geol.*, **188**, 15–33.

Nygård, A., Sejrup, H.P., Haflidason, H. and Bryn, P. (2005) The glacial North Sea Fan, southern Norwegian Margin: architecture and evolution from the upper continental slope to the deep-sea basin. *Mar. Petrol. Geol.*, **22**, 71–84.

Nystuen, J.P. (1985) Facies and preservation of glaciogenic sequences from the Varanger ice age in Scandinavia and other parts of the North Atlantic Region. *Palaeogeogr. Palaeoclimatol. Palaeoecol.*, **51**, 209–229.

Ó Cofaigh, C., Dowdeswell, J.A., Evans, J., Kenyon, N.H., Taylor, J., Mienert, J. and Wilken, M. (2004) Timing and significance of glacially influenced mass-wasting in the submarine channels of the Greenland Basin. *Mar. Geol.*, **207**, 39–54.

O'Brien, S.J., Tucker, R.D., Dunning, G.R. and O'Driscoll, C.F. (1992) Four-fold subdivision of the late Precambrian magmatic record of the Avalon Zone area (east Newfoundland): nature and significance. *Geol. Assoc. Can. Abstr. Prog.*, **17**, A85.

O'Grady, D.B. and Syvitski, J.P.M. (2002) Large-scale morphology of Arctic continental slopes: the influence of sediment delivery on slope form. In: *Glacier-Influenced Sedimentation on High-Latitude Continental Margins* (Eds J.A. Dowdeswell and C.O. Cofaigh), Geol. *Soc. London Spec. Publ.*, **203**, 11–31.

Ojakangas, R.W. and Matsch, C.L. (1980) Upper Precambrian (Eocambrian) Mineral Fork Tillite of Utah: A continental glacial and glaciomarine sequence. *Geol. Soc. Am. Bull.*, **91**, 495–501.

Onstott, T.C., Hargraves, R.B. and Reid, D.L. (1986) Constraints on the tectonic evolution of the Namaqua Province; III, Palaeomagnetic and (super 40úAr/ (super 39úAr results from the Gannakouriep dyke swarm. *Trans. Geol. Soc. S. Afr.*, **89**, 171–183.

Orheim, O. and Elverhøi, A. (1981) Model for submarine glacial deposition. *Ann. Glaciol.*, **2**, 123–128.

Parkin, L.W. (1969) Handbook of South Australian Geology. *Geol. Surv. S. Austr.* 268 pp.

Parrenin, F. and Paillard, D. (2003) Amplitude and phase of glacial cycles from a conceptual model. *Earth Planet. Sci. Lett.*, **214**, 243–250.

Paterson, W.S.B. (1994) *The Physics of Glaciers*. Pergamon Press, Oxford, 480 pp.

Pedrosa-Soares, A.C., Cordani, U.G. and Nutman, A. (2000) Constraining the age of Neoproterozoic glaciation in eastern Brazil: first U–Pb (SHRIMP) data of detrital zircons. *Rev. Bras. Geoc.*, **30**, 58–61.

Pickering, K.T., Stow, D.A.V., Watson, M.P. and Hiscott, R.N. (1986) Deep water facies, processes and models: a review and classification scheme for modern and ancient sediments. *Earth-Sci. Rev.*, **23**, 75–174.

Pimentel, M.M. and Fuck, R.A. (1992) Neoproterozoic crustal accretion in central Brazil. *Geology*, **20**, 375–379.

Piotrowski, A.M., Goldstein, S.L., Hemming, S.R. and Fairbanks, R.G. (2005) Temporal Relationships of Carbon Cycling and Ocean Circulation at Glacial Boundaries, *Science*, **307**, no. 5717, 1933–1938.

Platel, J.P., Roger, J., Peters, T., Mercolli, I., Kramers, J.D. and Le Metour, J. (1992) Geological map of Salalah NE 40–09 1:250,000 with explanatory notes. Directorate General of Minerals, Oman Ministry of Petroleum and Minerals.

Poussart, P.F., Weaver, A.J. and Barnes, C.R. (1999) Late Ordovician glaciation under high atmospheric CO_2: A coupled model analysis: *Paleoceanography*, **14**, 542–558.

Powell, R.D. and Molnia, B.F. (1989) Glacimarine sedimentary processes, facies and morphology of the south-southeast Alaska shelf and fjords. *Mar. Geol.*, **85**, 359–390.

Powell R.D. and Cooper, J.M. (2002) A glacial sequence stratigraphic model for temperate, glaciated continental shelves. In: *Glacier-Influenced Sedimentation on High-Latitude Continental Margins* (Eds J.A. Dowdeswell and C.O. Cofaigh), Geol. *Soc. London Spec. Publ.*, **203**, 215–244.

Powell, R.D., Krissek, L.A. and van der Meer, J.J.M. (2000) Preliminary depositional environmental analysis of CRP-2/2A, Victoria Land Basin, Antarctica: Palaeogeographical and palaeoclimatic inferences. *Terra Antarctica*, **7**, 313–322.

Powers, M.C. (1953) A new roundness scale for sedimentary particles. *J. Sed. Petrol.*, **23**, 117–119.

Prave, A.R. (1999a) Two diamictites, two cap carbonates, two $\delta^{13}C$ excursions, two rifts: Te Neoproterozoic Kingstone Peak Formation, Death Valley, Cailfornia. *Geology*, **27**, 339–342.

Prave, A.R. (1999b) The Neoproterozoic Dalradian Supergroup of Scotland: an alternative hypothesis. *Geol. Mag.*, **136**, 609–617.

Preiss, W.V. (1987) The Adelaide Geosyncline—late Proterozoic stratigraphy, sedimentation, palaeontology and tectonics. *S. Australian Geol. Surv. Bull.*, **53**, 438 pp.

Preiss, W.V. (2000) The Adelaide Geosyncline of South Australia and its significance in Neoproterozoic continental reconstruction. *Precambrian Res.*, **100**, 21–63.

Preiss, W.V., Dyson, I.A., Reid, P.W. and Cowley, W.M. (1998) Revision of lithostratigraphic classification of the Umberatana Group. *MESA J.*, **9**, 36–42.

Prichard, C.E. and Quinlan, T. (1962) The geology of the southern half of the Hermannsburg 1:250 000 Sheet. *Bur. Mineral. Resour. Geol. Geophys. Rep.*, **61**.

Rabu, D. (1988) Géologie de l'autochtone des montagnes d'Oman, la fenêtre du Jabal Akhdar. Thèse Doct. ès-Sciences de l'Université Pierre et Marie Curie, Paris 6, and documents BRGM, **130**.

Rafaelsen, B., Andreassen, K., Kuilman, L.W., Lebesbye, E., Hogstad, K. and Midtbø, M. (2002) Geomorphology of buried glacigenic horizons in the Barents Sea from three-dimensional seismic data. In: *Glacier-Influenced Sedimentation on High-Latitude Continental Margins* (Eds J.A. Dowdeswell and C.O. Cofaigh), Geol. *Soc. London Spec. Publ*., **203**, 259–275.

Rehmer, J. (1981) The Squantum tilloids member of the Roxbury Conglomerate of Boston, Massachusetts. In: *Earth's Pre-Pleistocene Glacial Record* (Eds M.J. Hambrey and W.B. Harland), pp. 756–759. Cambridge University Press, Cambridge.

Reid, D.L., Ransome, I.G.D., Onstott, T.C. and Adams, C.J. (1991) Time of Emplacement and Metamorphism Of Late Precambrian Mafic Dykes Associated with the Pan-African Gariep Orogeny, Southern Africa: Implications for the Age of the Nama Group. *J. Afr. Earth Sci.*, **13**, 531–541.

Rijsdijk, K., Owen, G., Warren, W.P., McCarroll, D., and van der Meer, J.J.M. (1999) Clastic dykes in consolidated tills: evidence from Killiney Bay, eastern Ireland. *Sed. Geol.*, **129**, 111–126.

Rijsdijk, K.F. (2001) Density-driven deformation structures in glacigenic consolidated diamicts: examples from Traeth y Mwnt, Cardiganshire, Wales, UK. *J. Sed. Res*., **71**, 122–135.

Robert, M. (1956) *Géologie et Géographie du Katanga.* Hayez, Bruxelles, 620 pp.

Roberts, D. *et al.* (1998) Rb-Sr dating of illite fractions from Neoproterozoic shales on Varanger Peninsula, North Norway. *Nor. Geol. Unders. Bull.*, **433**, 24–25.

Roberts, H.G., Gemuts, I. and Halligan, R. (1972) Adalaidean and Cambrian stratigraphy of the Mount Ramsay, 1:250 000 sheet area, Limberley Region, Western Australia. *Rep. Bur. Miner. Resour. Geol. Geophys., Aust.*, **150**.

Rocha-Campos, A.C. and Hasui, Y. (1981a) Tillites of the Macaúbas Group (Proterozoic) in central Minas Gerais and southern Bahia, Brazil. In: *Earth's Pre-Pleistocene Glacial Record* (Eds M.J. Hambrey and W.B. Harland), pp. 933–938. Cambridge University Press, Cambridge.

Rocha-Campos, A.C. and Hasui, Y. (1981b) Late Precambrian Jangada Group and Puga Formation of central western Brazil. In: *Earth's Pre-Pleistocene Glacial Record* (Eds M.J. Hambrey and W.B. Harland), pp. 916–919. Cambridge University Press, Cambridge.

Rogers, A.W. (1916) The geology of part of Namaqualand. *Trans. Geol. Soc. S. Afr*., **18**, 72–101.

Ronnert, L. and Mickelson, D.M. 1992. High porosity of basal till at Burroughs glacier, southeastern Alaska. *Geology*, **20**, 849–852.

Ross, G.M. and Villeneuve, M.E. (1997) U–Pb geochronology of stranger stones in Neoproterozoic diamictites, Canadian Cordillera: implications for provenance and ages of deposition. *Radiogenic Age and Isotopic Studies: Report* **10**, *Geol. Surv. Can. Curr. Res. 1997-F*, 141–155.

Ross, G.M., Bloch, J.D. and Krouse, H.R. (1995) Neoproterozoic strata of the southern Canadian Cordillera and the isotopic evolution of seawater sulfate. *Precambrian Res.*, **73**, 71–99.

Saettem, J., Pool, D.A.R., Eilingsen, L. and Sejrup, H.P. (1992) Glacial geology of outer Björnöyrenna, Southwestern Barents Sea. *Mar. Geol.*, **103**, 15–51.

Schaefer, B.F. and Burgess, J.M. (2003) Re-Os isotopic age constraints on deposition in the Neoproterozoic Amadeus Basin: implications for the 'Snowball Earth' *J. Geol. Soc. Lond.*, **160**, 825–828.

Scheffler K., Hoernes, S. and Schwark, L. (2003) Global changes during Carboniferous-Permian glaciation of Gondwana; linking polar and equatorial climate evolution by geochemical proxies. *Geology*., **31**, 605–608.

Schermerhorn, L.J.G. (1974) Late Precambrian mixtites: glacial and/or nonglacial? *Am. J. Sci*., **274**, 673–824.

Schermerhorn, L.J.G. (1975) Tectonic framework of Late Precambrian supposed glacials. In: *Ice Ages: Ancient and Modern* (Eds A.E. Wright and F. Moseley), pp. 241–274. Geol. J. Spec. Publ.

Schermerhorn, L.J.G. (1981) Late Precambrian tilloids of northwest Angola. In: *Earth's Pre-Pleistocene Glacial Record* (Eds M.J. Hambrey and W.B. Harland), pp. 158–161. Cambridge University Press, Cambridge.

Schermerhorn, L.J.G. and Stanton, W.I. (1963) Tilloids in the west Congo geosyncline. *Q. Jl. Geol. Soc. Lond*., **119**, 201–241.

Schmidt, P.W. and Williams, G.E. (1995) The Neoproterozoic climatic paradox: equatorial paleolatitude for Marinoan glaciation near sea level in South Australia. *Earth Planet. Sci. Lett.*, **134**, 107–124.

Schmidt, P.W., Williams, G.E. and Embleton, B.J.J. (1991) Low palaeolatitudes of Late Proterozoic glaciation: early timing of remanence in haematite of the Elatina Formation, South Australia. *Earth Planet. Sci. Lett.*, **105**, 355–367.

Schrag, D.P., Berner, R.A., Hoffman, P.F. and Halverson, G.P. (2002) On the initiation of a snowball Earth. *Geochem., Geophys., Geosyst*., **3**, No. 6.

Schwab, F.L. (1981) Late Precambrian tillites of the Appalachians. In: *Earth's Pre-Pleistocene Glacial Record* (Eds M.J. Hambrey and W.B. Harland), pp. 751–755. Cambridge University Press, Cambridge.

Sejrup, H.P., Haflidasona, H., Hjelstuena, B.O., Nygård, A., Brynb, P. and Lienb, R. (2004) Pleistocene development of the SE Nordic Seas margin. *Mar. Geol*., **213**, 169–200.

Shipp, S.S., Wellner, J.S. and Anderson, J.B. (2002) Retreat signature of a polar ice stream: sub-glacial geomorphic features and sediments from the Ross Sea, Antarctica. In: *Glacier-Influenced Sedimentation on High-Latitude Continental Margins* (Eds J.A. Dowdeswell and C.O. Cofaigh), Geol. *Soc. London Spec. Publ*., **203**, 277–303.

Siedlecka, A. and Roberts, D. (1992) The bedrock geology of Varanger Peninsula, Finnmark, north Norway: an excursion guide. *Nor. Geol. Unders. Spec. Publ.*, **5**, 45 pp.

Smith, A.G. and Pickering, K.T. (2003) Oceanic gateways as a critical factor to initiate icehouse Earth. *J. Geol. Soc. Lond*., **160**, 337–340.

Smith, I.R. (2000) Diamictic sediments within high Arctic lake sediment cores: evidence for lake ice rafting along the lateral glacial margin. *Sedimentology*, **47**, 1157–1179.

Smith, L.M. and Andrews, J.T. (2000) Sediment characteristics in iceberg dominated fjords, Kangerlussuaq region, East Greenland. *Sed. Geol*., **130**, 11–25.

Sohl, L.E., Christie-Blick, N. and Kent, D.V. (1999) Paleomagnetic polarity reversals in Marinoan (ca. 600 Ma) glacial deposits of Australia: implications for the duration of low-latitude glaciations in Neoproterozoic time. *Geol. Soc. Am. Bull*., **111**, 1120–1139.

Sokolov, B.S. (1998) Ocherki stanovleniya venda. KMK Ltd., Moscow.

Solheim, A., Faleide, J.I., Andersen, E.S., Elverhøi, A., Forsberg, C.F., Vanneste, K., Uenzelmann-Neben, G. and Channell, J.E.T. 1998. Late Cenozoic seismic stratigraphy and glacial geological development of the East Greenland and Svalbard-Barents Sea continental margins. *Quatern. Sci. Rev*., **17**, 155–184.

Songnian, L., Guogan, M., Zhenjia, G. and Weixing, L. (1985) Sinian ice ages and glacial sedimentary facies-areas in China. *Precambrian Res*., **29**, 53–63.

Songnian, L. and Zhenjia, G. (1987) Characteristics of the Sinian glaciogenic rocks of the Shennongjia region, Hubei Province, China. *Precambrian Res*., **36**, 127–142.

Souchez, R.A. and Lemmens, M. (1985) Subglacial carbonate deposition: an isotopic study of a present-day case. *Palaeogeogr., Palaeoclimatol., Palaeoecol*., **51**, 357–364.

Spencer, A.M. (1985) Mechanisms and environments of deposition of Late Precambrian geosynclinal tillites: Scotland and East Greenland. *Palaeogeogr., Palaeoclimatol., Palaeoecol*., **51**, 143–157.

Sprigg, R.C. (1942) Geology of the Eden-Moana Fault Block. *Trans. R. Soc. S. Austr*., **66**, 185–214.

Stow, D.A.V. and Piper, D.J.W. (1984) Deep-water fine-grained sediment: facies models. In: *Fine-grained sediment: deep water processes and facies* (Eds D.A.V. Stow and D.J.W. Piper), pp. 611–646. Blackwell Scientific, Oxford.

Strasser, J.C., Lawson, D.E., Larson, G.C., Evenson, E.B. and Alley, R.B. (1996) Preliminary results of tritium analyses in basal ice, Matanuska Glacier, Alaska, USA: evidence for subglacial ice accretion. *Ann. Glaciol*., **22**, 126–133.

Stratten, T. (1974) Notes on the application of shape parameters to differentiate between beach and river deposits in southern Africa. *Trans. Geol. Soc. S. Afr*., **77**, 59–64.

Strømberg, A.G.B. (1981) The Late Precambrian Sito tillite and the Vakkejokk breccia in the northern Swedish Caledonides. In: *Earth's Pre-Pleistocene Glacial Record* (Eds M.J. Hambrey and W.B. Harland), pp. 611–614. Cambridge University Press, Cambridge.

Sturt, B.A., Pringle, I.R. and Roberts, D. (1975) Caledonian nappe sequence of Finnmark, northern Norway, and the timing of the orogenic deformation and metamorphism. *Geol. Soc. Am. Bull*., **86**, 710–718.

Sugden, D.E. (1978) Glacial erosion by the Laurentide Ice Sheet. *J. Glaciol*., **20**, 367–391.

Sumner, D.Y., Kirschvink, J.L. and Runnegar, B.N. (1987) Soft-sediment paleomagnetic fold tests of late Precambrian glaciogenic sediments. *Eos*, **68**, 1251.

Tadesse, T., Hoshino, M., Suzuki, K. and Iisumi, S. (2000) Sm–Nd, Rb–Sr and Th–U–Pb zircon ages of syn- and post-tectonic granitoids from the Axum area of northern Ethiopia. *J. Afr. Earth Sci*., **30**, 313–327.

Tadesse, T., Suzuki, K. and Hoshino, M. (1997) Chemical Th–U total Pb isochron age of zircon from the Mareb Granite in northern Ethiopia. *J. Earth Planet. Sci. Negoya Univ*., **44**, 21–27.

Taviani, M. and Beu, A.G. (2003) The palaeoclimatic significance of Cenozoic marine macrofossil assemblages from Cape Roberts Project drillholes, McMurdo Sound, Victoria Land Basin, East Antarctica. *Palaeogeogr., Palaeoclimatol., Palaeoecol*., **198**, 131–143.

Taylor, J., Dowdeswell, J.A., Kenyon, N.H. and Ó Cofaigh, C. (2002) Late Quaternary architecture of trough-mouth fans: debris flows and suspended sediments on the Norwegian margin. In: *Glacier-Influenced Sedimentation on High-Latitude Continental Margins* (Eds J.A. Dowdeswell and C.O. Cofaigh), *Geol. Soc. London Spec. Publ*., **203**, 55–71.

Teklay, M. (1997) Petrology, geochemistry and geochronology of Neoproterozoic magmatic arc rocks from Eritrea: implications for crustal evolution in the southern Nubian Shield, Eritrea. *Dept. Mines Mem.* **1**, 125 pp.

Thelander, T. (1981) Late Precambrian (?) Långmarkberg Formation in the central Swedish Caledonides. In: *Earth's Pre-Pleistocene Glacial Record* (Eds M.J. Hambrey and W.B. Harland), pp. 615–619. Cambridge University Press, Cambridge.

Thiede, J., Winkler, A., Wolf-Welling, T., Eldholm, O., Myhre, A.M., Baumann, K.-H., Henrich, R. and Stein, R. (1998) Late Cenozoic history of the polar North Atlantic: results from ocean drilling. *Quatern. Sci. Rev.*, **17**, 185–208.

Thompson, M.D. and Bowring, S.A. (2000) Age of the Squantum 'tillite', Boston Basin, Massachusetts: U–Pb zircon constraints on terminal Neoproterozoic glaciation. *Am. J. Sci.*, **300**, 630–655.

Thompson, M.D., Keefe, K.L.D., Martin, M.W. and Bowring, S.A. (2000) Refined U-P zircon age of terminal Neoproterozoic Varanger (?) glaciation in the Boston Basin, eastern Massachusetts. *Geol. Soc. Am. Abstr. Prog.*, **32**, 375–376.

Thompson, M.D., Keefe, K.L.D., Martin, M.W. and Bowring, S.A. (2000) Maximum depositional age of the Neoproterozoic Squantum 'Tillite', Boston Basin, Massachusetts; new U-Pb zircon age constraint on Varanger glaciation. *Geol. Soc. Am. Abstr. Prog.*, **32**, 78.

Tollo, R.P. and Aleinikoff, J.M. (1992) Age and compositional relations of the Robertson River Igneous Suite, Blue Ridge Province, Virginia: Implications for the nature of Laurentian rifting. *Geol. Soc. Am. Abstr. Prog.*, **24**, A365.

Tollo, R.P. and Hutson, F.E. (1996) 700 Ma age for the Mechum River Formation, Blue Ridge province, Virginia: A unique time constraint on pre-Iapetan rifting of Laurentia. *Geology*, **24**, 59–62.

Treagus, J.E. (1981) The Lower Dalradian Kinlochlaggan Boulder Bed, central Scotland. In: *Earth's Pre-Pleistocene Glacial Record* (Eds M.J. Hambrey and W.B. Harland), pp. 637–639. Cambridge University Press, Cambridge.

Trompette, R. (1973) Le Precambrien supérieur et le Paléozoi'que inférieur de l'Adrar de Mauritanie (bordure oceidentale du basin de Taoudeni, Afrique de l'Ouest). Un exemple de sédimentation de craton. Etude stratigraphique et sédimentologique. *Tray. Lab. Sci. Terre St-Jr.*, Marseille, B, **7**, 702 pp.

Tucker, M.E. and Reid, P.C. (1981) Late Precambrian glacial sediments, Sierra Leone. In: *Earth's Pre-Pleistocene Glacial Record* (Eds M.J. Hambrey and W.B. Harland), pp. 132–133. Cambridge University Press, Cambridge.

van der Meer, J.J.M., Menzies, J. and Rose, J. (2003) Subglacial till: the deforming glacier bed. *Quatern. Sci. Rev.*, **22**, 1659–1685.

van der Wateren, F.M., Kluiving, S.J. and Bartek, L.R. (2000) Kinematic indicators of subglacial shearing. In: Maltman, A.J., Hubbard, B. and Hambrey, M.J. (eds). *Deformation of Glacial Materials*. *Geol. Soc. London Spec. Publ.*, **176**, 259–278.

Vanneste, K., Uenzelmann, G. and Miller, H. (1995) Seismic evidence for long-term history of glaciation on central East Greenland shelf south of Scoresby Sund. *Geo-Marine Letters*, **15**, 63–70.

Vidal, B. and Bylund, G. (1981) Late Precambrian boulder beds in the Visingsö Beds, southern Sweden. In: *Earth's Pre-Pleistocene Glacial Record* (Eds M.J. Hambrey and W.B. Harland), pp. 629–631. Cambridge University Press, Cambridge.

Von Veh, M.W. (1993) The stratigraphy and structural evolution of the Late Proterozoic Gariep Belt in the Sendelingsdrif-Annisfontein area, northwestern Cape Province. *Precambrian Res. Unit, Univ. Cape Town, Bull.*, **38**, 1–174.

Vorren, T.O., Hald, M. and Thomsen, E. (1984) Quaternary sediments and environments on the continental shelf off northern Norway. *Mar. Geol.*, **57**, 229–257.

Walter, M.R. (1981) Late Proterozoic tillites of the southwestern Georgina Basin, Australia. In: *Earth's Pre-Pleistocene Glacial Record* (Eds M.J. Hambrey and W.B. Harland), pp. 525–527. Cambridge University Press, Cambridge.

Walter, M.R., Veevers, J.J., Calver, C.R., Gorjan, P. and Hill, A.C. (2000) Dating the 840–544 Ma Neoproterozoic interval by isotopes of strontium, carbon, and sulfur in seawater, and some interpretive models. *Precambrian Res.*, **100**, 371–433.

Warren, S.G., Brandt, R.E., Grenfell, T.C. and McKay, C.P. (2002) Snowball Earth: ice thickness on the tropical ocean. *J. Geophys. Res.*, **107**(C10), 3167.

Weertman, J. (1957) On the sliding of glaciers. *J. Glaciol.*, **3**, 33–38.

Weertman, J. (1961) Mechanism for the formation of inner moraines found near the edge of cold ice caps and ice sheets. *J. Glaciol.*, **3**, 965–978.

Weertman, J. (1964) The theory of glacier sliding. *J. Glaciol.*, **5**, 287–303.

Wells, A.T. (1976) Ngalia Basin. In: *Economic Geology of Australia and Papua New Guinea 3. Petroleum* (Eds R.B. Leslie, H.J. Evans, and C.L. Knight, C.L.), pp. 226–230. Aus. IMM. Monograph Series, **7**.

Wells, A.T. (1981) Late Proterozoic diamictites of the Amadeus and Ngalia Basins, central Australia. In: *Earth's Pre-Pleistocene Glacial Record* (Eds M.J. Hambrey and W.B. Harland), pp. 515–524. Cambridge University Press, Cambridge.

Wells, A.T., Ranford, L.C., Stewart, A.J., Cook, P.J. and Shaw, R.D. (1967) The geology of the north-eastern part of the Amadeus Basin, Northern Territory. *Bur. Miner. Resour. Geol. Geophys., Rep.*, **113**, 97 pp.

Williams, G.E. (1996) Soft-sediment deformation structures from the Marinoan glacial succession, Adelaide foldbelt: implications for the paleolatitude of late Neoproterozoic glaciation. *Sediment. Geol.*, **106**, 165–175.

Williams, G.E. and Schmidt, P.W. (2004) Neoproterozoic Glaciation: Reconciling Low Paleolatitudes and the Geologic Record. In: *The Extreme Proterozoic: Geology, Geochemistry, and Climate. Geophysical Monograph Series*, **146**. A.G.U. 145–159.

Xu, B., Jian, P. Zheng, H., Zou, H., Zhang, L. and Liu, D. (2005) U–Pb zircon geochronology and geochemistry of Neoproterozoic volcanic rocks in the Tarim Block of northwest China: implications for the breakup of Rodinia supercontinent and Neoproterozoic glaciations. *Precambrian Res.*, **136**, 107–123.

Yeates, A.N. and Muhling, P.C. (1977) Explanatory Notes on the Mount Bannerman 1:250 000 Geological Sheet. *Bur. Miner. Resour. Geol. Geophys. and Geol. Surv. W. Austr. Rep.*, 24 pp.

Yeo, G.M. (1981) The Late Proterozoic Rapitan glaciation in the northern Cordillera. In: *Proterozoic basins of Canada* (Ed. F.H.A. Campbell). *Geol. Surv. Canada Paper*, 81–10, 25–46.

Yin, C., Liu, D., Gao, L., Wang, Z., Xing, Y., Jian, P. and Shi, Y. (2003) Lower boundary age of the Nanhua System and the Gucheng glacial stage; evidence from SHRIMP II dating. *Chinese Sci. Bull.*, **48**, 1657–1662.

Young, G.M. (1995) Are Neoproterozoic glacial deposits preserved on the margins of Laurentia related to the fragmentation of two supercontinents? *Geology*, **23**, 153–156.

Young, G.M. (2002) Geochemical investigation of a Neoproterozoic glacial unit: The Mineral Fork Formation in the Wasatch Range, Utah. *Geol. Soc. Am. Bull.*, **114**, 387–399.

Young, G.M. and Gostin, V.A. (1991) Late Proterozoic (Sturtian) succession of the North Flinders Basin, South Australia: an example of temperate glaciation in an active rift setting. In: Glacial Marine Sedimentation: Paleoclimatic Significance (Eds J.B. Anderson and G. Ashley), pp. 207–223. *Geol. Soc. Am. Spec. Publ. Pap.*, **261**.

Yuelun, W., Songnian, L., Zhengjia, G., Weixing, L. and Guogan, M. (1981) Sinian tillites of China. In: *Earth's Pre-Pleistocene Glacial Record* (Eds M.J. Hambrey and W.B. Harland), pp. 386–401. Cambridge University Press, Cambridge.

Zellers, S.D. and Lagoe, M.B. (1992) Stratigraphic and seismic analyses of offshore Yakataga Formation sections, northeastern Gulf of Alaska. In: *Proceedings of the International Conference on Arctic Margins, Anchorage.* OCS Study. MMS 94–0040, 111–116.

Zhao, J., McCulloch, M.T. and Korsch, R.J. (1994) Characterisation of a plume-related approximately 800 Ma magmatic event and its implications for basin formation in central-southern Australia. *Earth Planet. Sci. Lett.*, **121**, 349–367.

Zhenjia, G. and Jianxin, Q. (1985) Sinian glacial deposits in Xinjiang, Northwest China. *Precambrian Res.*, **29**, 143–147.

Zhou, C., Tucker, R., Xiao, S., Peng, Z., Yuan, X. and Chen, Z. (2004) New constraints on the ages of Neoproterozoic glaciations in south China. *Geology*, **32**, 437–440.